NWC TP 6386

(12)

AD A122803

Naval Weapons Center Plume Radar Frequency Interference Code

by
Blaine E. Pearce
Robert W. McCullough
Aeronautical Research Associates of Princeton, Inc.
for
Ordnance Systems Department

OCTOBER 1982

NAVAL WEAPONS CENTER
CHINA LAKE, CALIFORNIA 93555

A

Approved for public release; distribution unlimited.

DTIC FILE COPY

82 12 28 073

Naval Weapons Center

AN ACTIVITY OF THE NAVAL MATERIAL COMMAND

FOREWORD

This report presents results of a study to develop a computer code for predicting the interactions of radio frequency electromagnetic radiation with gaseous rocket exhaust plumes. The work reported herein was conducted from 8 May 1981 through 24 June 1982 by Aeronautical Research Associates of Princeton, Inc., under Contract No. N60530-81-C-0254 to the Naval Weapons Center.

The effort described herein was supported by the Naval Air Systems Command under the Missile Propulsion Technology Block Program (AIRTASK A03W3300/008B/0F31300000). Mr. Lee N. Gilbert is the NWC technology manager for this program.

Mr. A. C. Victor, the technical coordinator for this contract, has reviewed this report for technical accuracy. This report is released for information at the working level and does not necessarily reflect the views of NWC.

Approved by
C. L. SCHANIEL, *Head*
Ordnance Systems Department
31 October 1982

Under authority of
J. J. LAHR
Capt., U.S. Navy
Commander

Released for publication by
B. W. HAYS
Technical Director

NWC Technical Publication 6386

Published by ..... Technical Information Department
Collation ..... Cover, 77 leaves
First printing ..... 305 unnumbered copies

UNCLASSIFIED

SECURITY CLASSIFICATION OF THIS PAGE (When Data Entered)

REPORT DOCUMENTATION PAGE		READ INSTRUCTIONS BEFORE COMPLETING FORM
1. REPORT NUMBER NWC TP 6386	2. GOVT ACCESSION NO. AD. 4122 803	3. RECIPIENT'S CATALOG NUMBER
4. TITLE (and Subtitle) NAVAL WEAPONS CENTER PLUME RADAR FREQUENCY INTERFERENCE CODE, FINAL REPORT		5. TYPE OF REPORT & PERIOD COVERED Final Report 8 May 1981 - 24 June 1982
		6. PERFORMING ORG. REPORT NUMBER A.R.A.P. Report No. 467
7. AUTHOR(s) Blaine E. Pearce Robert W. McCullough		8. CONTRACT OR GRANT NUMBER(s) N60530-81-C-0254
9. PERFORMING ORGANIZATION NAME AND ADDRESS Aeronautical Research Associates of Princeton, Inc. 50 Washington Road, P.O. Box 2229 Princeton, New Jersey 08540		10. PROGRAM ELEMENT, PROJECT, TASK AREA & WORK UNIT NUMBERS AirTask A03W3300-008B-0F31300000
11. CONTROLLING OFFICE NAME AND ADDRESS Naval Weapons Center China Lake, California 93555		12. REPORT DATE October 1982
		13. NUMBER OF PAGES 152
14. MONITORING AGENCY NAME & ADDRESS (if different from Controlling Office)		15. SECURITY CLASS. (of this report) UNCLASSIFIED
		15a. DECLASSIFICATION DOWNGRADING SCHEDULE

16. DISTRIBUTION STATEMENT (of this Report)

Approved for public release, distribution unlimited.

17. DISTRIBUTION STATEMENT (of the abstract entered in Block 20, if different from Report)

18. SUPPLEMENTARY NOTES

19. KEY WORDS (Continue on reverse side if necessary and identify by block number)

Plume RF Interference	RF Scattering
Reacting Turbulent Flows	Rocket Exhaust Plumes
RF Absorption	Turbulent Fluctuations

20. ABSTRACT (Continue on reverse side if necessary and identify by block number)

See back of form.

DD FORM 1 JAN 73 1473 EDITION OF 1 NOV 65 IS OBSOLETE
S/N 0102-LF-014-6601

UNCLASSIFIED

SECURITY CLASSIFICATION OF THIS PAGE (When Data Entered)

(U) *Naval Weapons Center Plume Radar Frequency Interference Code. Final Report*, by Blaine E. Pearce and Robert W. McCullough, Aeronautical Research Associates of Princeton, Inc. China Lake, Calif., Naval Weapons Center, October 1982, 152 pp. (NWC TP 6386, publication UNCLASSIFIED.)

(U) A description of the Naval Weapons Center Plume Radar Frequency Interference Code (PRFIC) is given. The methods used to predict the attenuation and phase shifts contributed by the mean plume flowfield, and the scattering and Doppler shift due to turbulent fluctuations, are defined. Examples of the predictions of the plume RF interference using the flowfield predictions of a modified JANNAF Standard Plume Flowfield code are given. The capabilities and limitations of PRFIC are listed and improvements are proposed. A code user's manual and software description are included.

CONTENTS

Introduction. 3

Propagation of an EM Wave in a Weakly Ionized Plasma. 4

Attenuation and Phase 5

Scattering by Turbulence. 16

Differential Cross Section 16

Attenuation due to Scattering. 19

Radar Cross Section. 20

Doppler Shift 21

Shift of Directly Transmitted Wave 21

Turbulence Broadened Spectrum. 21

Applications of PRFIC 22

Transverse Attenuation 22

Diagonal Attenuation 31

Scattering 31

Doppler Shift. 36

Summary of Capabilities and Limitations 42

Suggested Improvements. 43

Summary and Conclusions 44

References. 46

Appendices:

A - User's Manual 47

B - Software Documentation. 88

C - Derivation of the Ray Trace Equation. 138

D - Index of Refraction Fluctuations. 142

E - Doppler Spectrum of Scattered Power 145

Nomenclature. 150

INTRODUCTION

Practical, mass-produced rocket propellants usually contain trace amounts of impurities such as potassium, sodium, or calcium. Even with very low concentrations (~ 100 ppm), these low ionization potential species are sufficiently ionized to contribute a substantial number of free electrons to the exhaust. In the presence of these impurities or additives, the rocket motor exhaust flow becomes a weakly ionized plasma. The exhaust plume becomes electrically active and affects the propagation of those electromagnetic (EM) waves with wavelengths in the microwave range or longer. The exhaust plume can act to attenuate and scatter incident waves which are intended to carry information to or from the missile. The exhaust plume reflects and scatters waves which contribute to a radar cross section in addition to the contribution of the missile body. This class of interactions is the exhaust plume radar frequency (RF) interference problem.

Plume RF interference has an extensive history because it is a potential problem for nearly every missile system. Past problems have been resolved by a judicious combination of experiments and analysis. A comprehensive summary of this work has been published.[1-3] This earlier work identifies the importance of two major components of the problem: (1) the exhaust plume flowfield and composition, and (2) the interaction of the EM wave with the flow. There has recently been a step forward in our capability to deal with the first issue. The first version of the JANNAF Standard Plume Flowfield (SPF/1) Model has been released to industry.[4] This code allows an improved description of the exhaust plume that can account for both the inertially dominated region of the plume (initial expansion) and the turbulent mixing with the

---

[1]Victor, A.C., "Plume-Signal Interference, Part 1. Radar Attenuation," Naval Weapons Center, China Lake, Calif., June 1975. (NWC TP 5319, publication UNCLASSIFIED.)

[2]------. "Plume-Signal Interference, Part 2. Plume-Induced Noise," Naval Weapons Center, China Lake, Calif., May 1972. (NWC TP 5319, publication formerly CONFIDENTIAL, declassified 5 April 1977.)

[3]JANNAF Handbook, Rocket Exhaust Plume Technology, Chapter 4. Plume Electromagnetic Interactions, April 1977. (CPIA Pub. 263, publication UNCLASSIFIED.)

[4]Dash, S.M. and Pergament, H.S., "The JANNAF Standard Plume Flowfield Model (SPF)," Aeronautical Research Associates of Princeton, Inc., N.J., April 1981. (A.R.A.P. Report No. 448, publication UNCLASSIFIED.)

ambient air. Very general chemical kinetics are included.* Moreover, there is a potential to provide some initial predictions of turbulence quantities of importance to scattering of RF waves by extension of the SPF to include equations for the evolution of the second-order correlations of passive scalar quantities (i.e., the g-equation).[5]

This report describes a step forward in dealing with the second category of the interaction of the EM wave with the flow. It describes the Naval Weapons Center Plume Radar Frequency Interference Code (PRFIC) which is intended to unify the calculations performed by previous, separate codes and to utilize the flowfield as predicted by the JANNAF SPF. The combination of these two codes offers the potential for improved predictions of RF plume interference.

This report contains a physical description of plume RF phenomena and includes examples of both the flowfield calculation and EM interaction predictions. The PRFIC user's manual is provided in Appendix A, and the software documentation, in Appendix B.

PROPAGATION OF AN EM WAVE IN A WEAKLY IONIZED PLASMA

Propagation of an electromagnetic wave through an exhaust plume is modeled by a plane, periodic wave of the form[6]

$$E \sim e^{ikx} e^{-i\omega t} \tag{1}$$

The wavenumber k is complex in general. We express it as $k = \beta + i\alpha$, where β is a phase constant, and α, the imaginary part, is an attenuation constant. If this form of the wave is substituted into Maxwell's equations, the resulting dispersion relation is obtained.

*In the laminar limit, i.e., there is no effect of turbulence on reaction rates other than the influence of the mean flow.

[5]Khalil, E.E., Spalding, D.B., and Whitelaw, J.H., "The Calculation of Local Flow Properties in Two-Dimensional Furnaces," Int. J. Heat Mass Transfer, Vol. 18, 1975, pp. 775-791.

[6]Mitchner, M. and Kruger, C. H., Partially Ionized Gases, John Wiley and Sons, N.Y., 1973, pp. 156-61.

$$\left(\frac{kc}{\omega}\right)^2 = 1 - \frac{\left(\frac{\omega_p}{\omega}\right)^2}{1 + \left(\frac{\nu_{en}}{\omega}\right)^2} + i\,\frac{\left(\frac{\omega_p}{\omega}\right)^2\left(\frac{\nu_{en}}{\omega}\right)}{1 + \left(\frac{\nu_{en}}{\omega}\right)^2} \tag{2}$$

where

$$\omega_p = (n_e e^2/\varepsilon_o m_e)^{1/2} \tag{3}$$

is the plasma frequency ($\nu_p = \omega_p/2\pi = 8.97\ n_e^{1/2}$ Hz, n_e in m^{-3}). ν_{en} is the electron-neutral collision frequency

$$\nu_{en} = v_e n \sum_{i=1}^{N} x_i Q_i \tag{4}$$

where v_e is the electron thermal velocity $(3kT/m_e)^{1/2}$, n is the total particle number density p/kT, and x_i is the mole fraction of species i. Q_i is the collision cross section, which can depend on the colliding molecule and temperature (or equivalently, electron velocity). The summation is over the total number of species i = 1...,N. For the calculation given here, we used Q_i = const = $1.5\times10^{-19}\ m^2$. It is useful to note that $\nu_{en} \sim p\ T^{-1/2}$.

ATTENUATION AND PHASE

The plasma frequency is the natural frequency of oscillation of electrons if displaced from their equilibrium positions in the force field of the heavier ions. In the absence of collisions, the attenuation of a wave depends discontinuously on whether this natural frequency is greater or less than the wave frequency. For the special case of no collisions, if $\omega_p > \omega$, the electrons can respond sufficiently rapidly to neutralize the incident wave. k is purely imaginary,

$$k = i\,\frac{\omega}{c}\sqrt{\left(\frac{\omega_p}{\omega}\right)^2 - 1} \tag{5}$$

and no wave of the form of Eq. (1) can propagate into the plasma. This is the "overdense" case in which the electrons can adjust rapidly to a disturbance to reflect the incident energy. Again, for the special case of few collisions, the electrons cannot respond quickly to cancel the incident wave if $\omega_p < \omega$; then k is purely real,

$$k = \frac{\omega}{c}\left(1 - \frac{\omega_p^2}{\omega^2}\right) \tag{6}$$

and there is no attenuation of the wave. This is the "underdense" case. With finite collision frequency, the electron oscillations are damped and the discontinuous nature of the propagation at $\omega = \omega_p$ is smoothed. There is propagation and attenuation throughout the entire range of ω.

The attenuation and phase constants are given explicitly if we let

$$\left(\frac{kc}{\omega}\right)^2 = K_R + i\,K_I \tag{7}$$

$$K_R = 1 - \frac{\left(\frac{\omega_p}{\omega}\right)^2}{1 + \left(\frac{\nu_{en}}{\omega}\right)^2} \tag{8}$$

$$K_I = \frac{\left(\frac{\omega_p}{\omega}\right)^2\left(\frac{\nu_{en}}{\omega}\right)}{1 + \left(\frac{\nu_{en}}{\omega}\right)^2} \tag{9}$$

$$\alpha = \frac{\omega}{c}\left[\frac{|K| - K_R}{2}\right]^{1/2} \tag{10}$$

$$\beta = \frac{\omega}{c}\left[\frac{|K| + K_R}{2}\right]^{1/2} \tag{11}$$

Normalized values of the attenuation and phase constants ($\alpha c/\omega$ and $\beta c/\omega$) are given in Figures 1 and 2, respectively, for a range of ω_p/ω with collision frequency (ν_{en}/ω) as a parameter. As the collision frequency increases, the transition through the critical electron number density at which $\omega = \omega_p$ becomes less abrupt, and the notion of overdense and underdense becomes less meaningful. It is important to note that the maximum attenuation at a given frequency ratio (ω_p/ω) occurs for ν_{en}/ω of order unity.

Magnitudes of the plasma frequency ($\nu_p = \omega_p/2\pi$), the collision frequency ν_{en}, and the attenuation constant α(in m^{-1}) are shown in contour plots for a typical exhaust plume in Figures 3, 4, and 5. These predictions are for 76 percent solids, 12 percent aluminum propellant, in a 20,000 lb_f thrust motor flying at a sonic speed at 2 km altitude. This plume is underdense to all radar frequencies greater than 2.5 GHz. However, the ratio of collision frequency to wave frequency is large ($\nu_{en}/\omega > 1$). Figure 5 suggests that diagonal attenuation through this plume will be severe.

It is useful to consider the limiting behavior of the attenuation and phase for the extremes of electron number density and collision frequency. These limits are defined in Table 1. Low altitude, solid propellant motor exhaust plumes correspond to $\nu_{en}/\omega >> 1$ and $\omega_p/\omega < 1$. Liquid propellant exhaust plumes usually have lower impurity levels such that $\omega_p/\omega << 1$. The attenuation and phase shift of wave propagation through the plumes of missiles therefore depend strongly on the class of propellant and altitude.

TABLE 1. Limiting Forms for the Attenuation and Phase Constants

	$\omega_p/\omega << 1$	$\omega_p/\omega >> 1$
attenuation, α:	$\dfrac{\frac{\omega}{c}\left(\frac{\omega_p}{\omega}\right)^2 \frac{\nu}{\omega}}{2\left[1+\left(\frac{\nu}{\omega}\right)^2\right]}$	$\dfrac{\frac{\omega}{c}\left(\frac{\omega_p}{\omega}\right)\left[1+\sqrt{1+\left(\frac{\nu}{\omega}\right)^2}\right]^{1/2}}{\left\{2\left[1+\left(\frac{\nu}{\omega}\right)^2\right]\right\}^{1/2}}$
phase, β:	$\dfrac{\frac{\omega}{c}\left[1-\left(\frac{\omega_p}{\omega}\right)^2\right]}{1+\left(\frac{\nu}{\omega}\right)^2}$	$\dfrac{\frac{\omega}{c}\left(\frac{\omega_p}{\omega}\right)\left[\sqrt{1+\left(\frac{\nu}{\omega}\right)^2}-1\right]^{1/2}}{\left\{2\left[1+\left(\frac{\nu}{\omega}\right)^2\right]\right\}^{1/2}}$

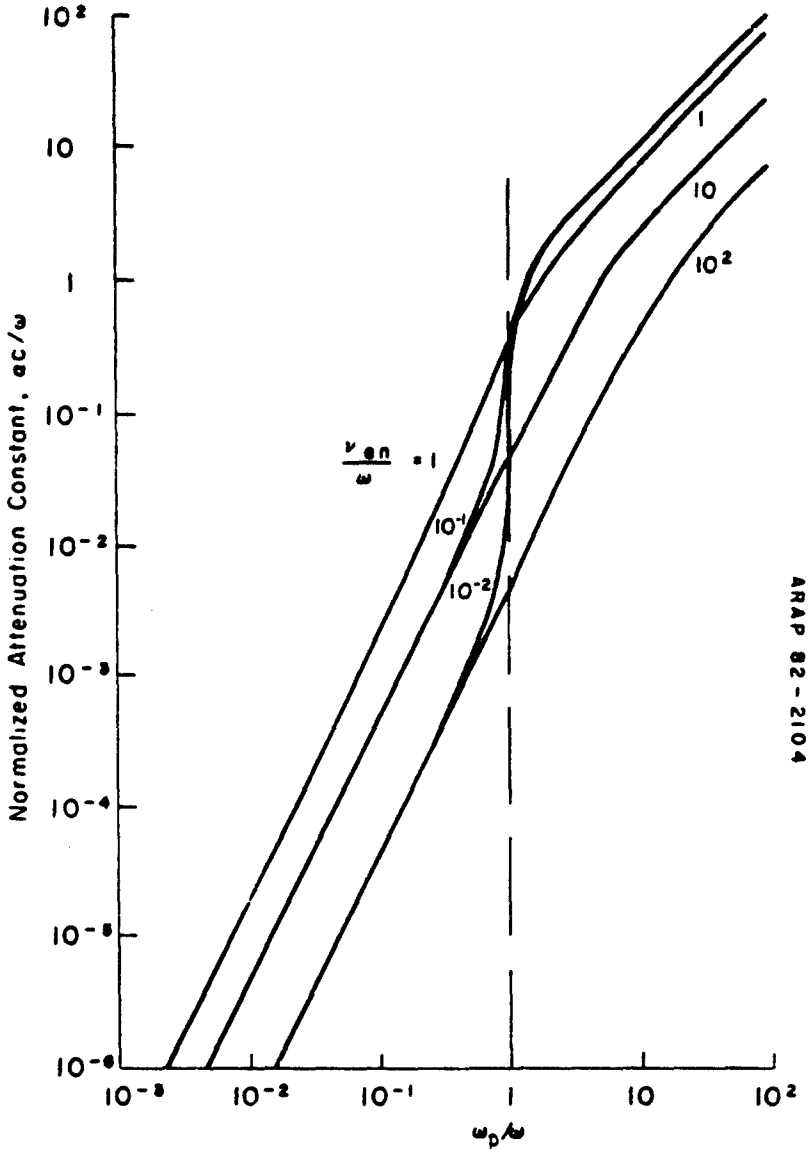

FIGURE 1. Attenuation Constant in an Ionized Gas with Collisions.

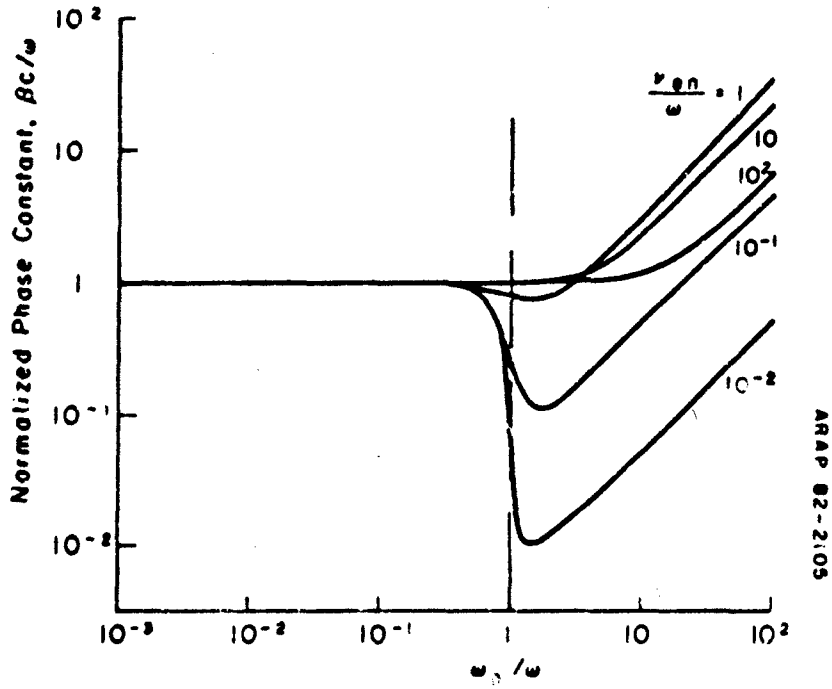

FIGURE 2. Phase Constant in an Ionized Gas with Collisions.

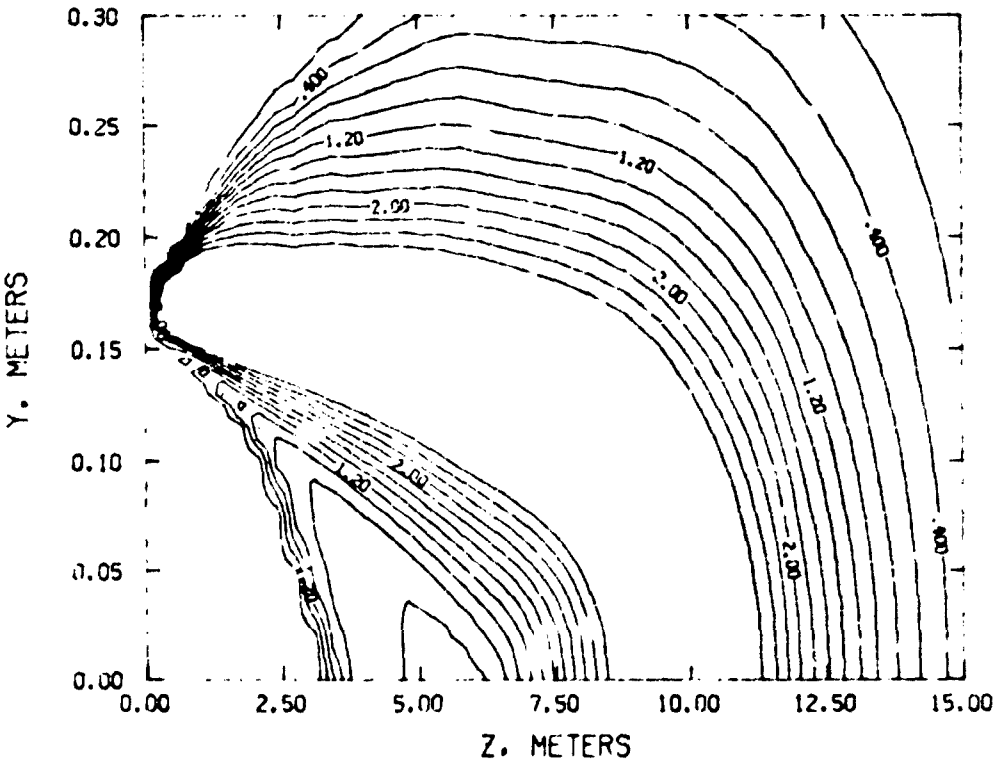

FIGURE 3. Plasma Frequency Distribution in a Solid Rocket Motor Plume ($_p$ in GHz). 20,000 lb_f motor, 76 solids, 12 aluminum, 2 km altitude, M_∞ = 1.

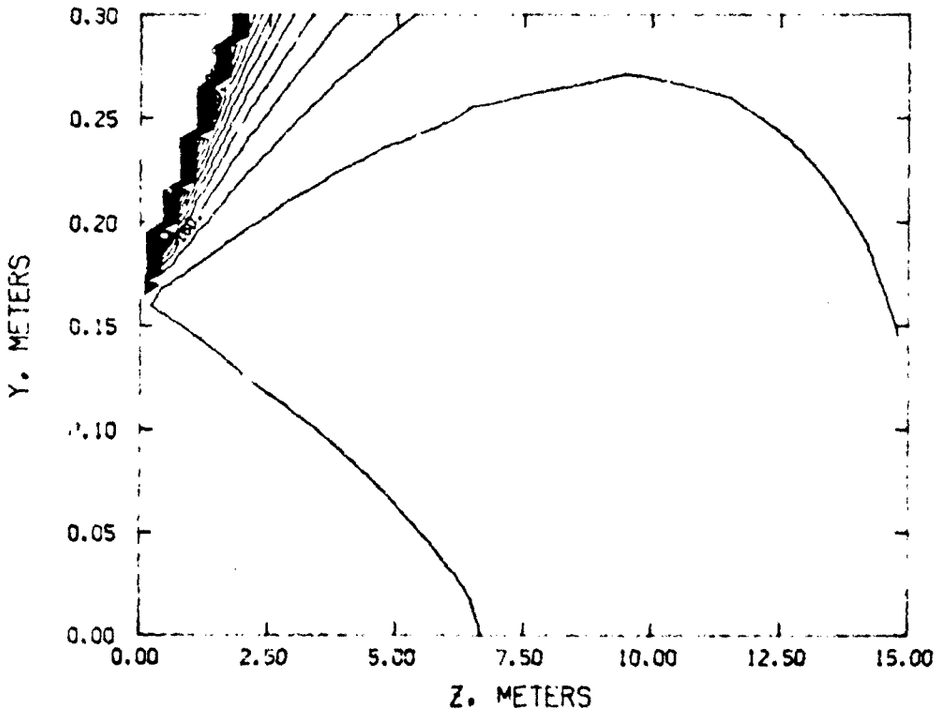

FIGURE 4. Collision Frequency Distribution in a Solid Rocket Motor Plume (ν_{en} in GHz). 20,000 lb_f motor, 76 solids, 12 aluminum, 2 km altitude, M_∞ = 1.

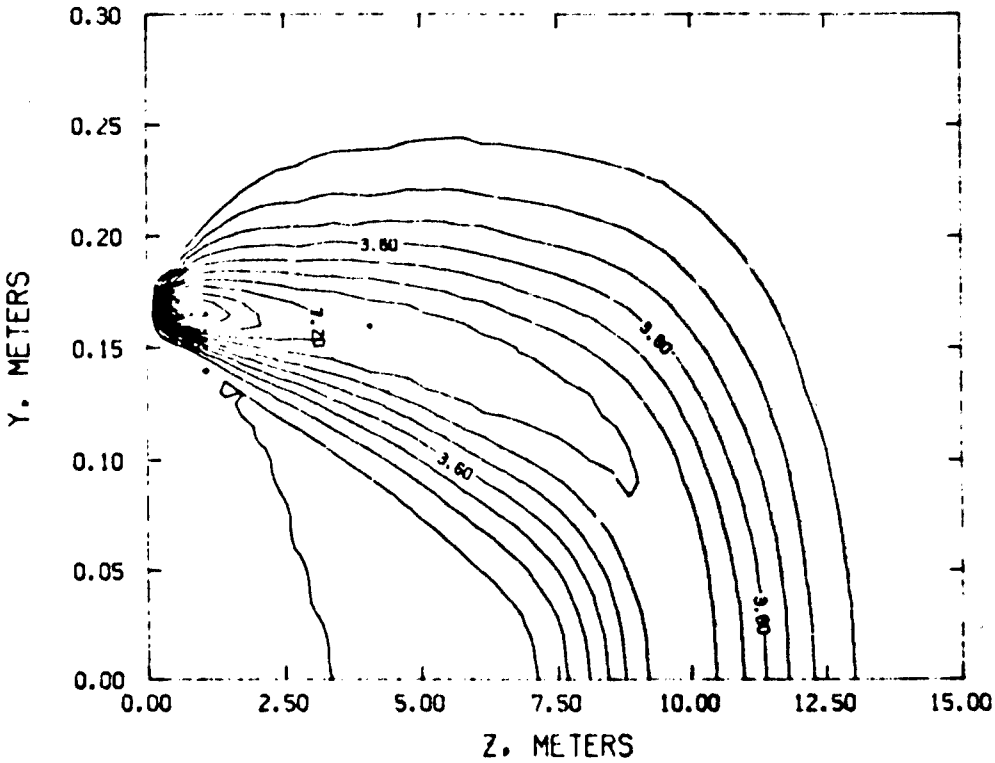

FIGURE 5. Attenuation Constant in a Solid Rocket Motor Plume (in m^{-1}). 20,000 lb_f motor, 76 solids, 12 aluminum, 2 km altitude, M_{∞} = 1.

The definition of the attenuation constant in Eq. (1) applies to the reduction of the electric field. In RF interference problems, the usual measurement is of the power, which depends on E^2. The attenuation used in the remainder of this report is therefore 2α, and the attenuation is given in dB.*

Attenuation and the phase change along an optical path through the plume involve an integral of α and β along the optical path s,

---

*

$$\frac{P}{P_o} \sim e^{-2\alpha x}$$

$$\frac{P}{P_o}, \text{ dB} = 10 \log_{10} \frac{P}{P_o} = 20\alpha x \log_{10} e = 8.659\alpha x$$

$$\text{attenuation} = \int_0^s \alpha \, ds \tag{12}$$

$$\text{phase} = \int_0^s \beta \, ds \quad . \tag{13}$$

In general, this optical path is curved. The propagation is through a medium with variable refractive index, and the plume acts as a lens at these wavelengths. In the geometric optics limit, the ray path is described by[7]

$$\frac{d}{ds}(n\vec{t}) = \nabla n \tag{14}$$

$\vec{t}$ is the unit vector tangent to the ray path, and s is the arc length along the path. This path is curved if there is a component of ∇n normal to the direction of propagation. Eq. (14) is equivalent to three ordinary differential equations for the coordinate of the ray path x(s), y(s), z(s). In the case of an axisymmetric exhaust plume, there are only two components of ∇n: in the radial and axial directions. The complete system to be solved is (see Appendix C for the derivation from Eq. (14)).

$$\frac{d^2x}{ds^2} = \frac{1}{n}\left[\cos\theta \frac{\partial n}{\partial r} - \frac{dx}{ds}\left(\cos\theta \frac{dx}{ds}\frac{\partial n}{\partial r} + \sin\theta \frac{dy}{ds}\frac{\partial n}{\partial r} + \frac{dz}{ds}\frac{\partial n}{\partial z}\right)\right] \tag{15}$$

$$\frac{d^2y}{ds^2} = \frac{1}{n}\left[\sin\theta \frac{\partial n}{\partial r} - \frac{dy}{ds}\left(\cos\theta \frac{dx}{ds}\frac{\partial n}{\partial r} + \sin\theta \frac{dy}{ds}\frac{\partial n}{\partial r} + \frac{dz}{ds}\frac{\partial n}{\partial z}\right)\right] \tag{16}$$

$$\frac{d^2z}{ds^2} = \left[\frac{1}{n}\frac{\partial n}{\partial z} - \frac{dz}{ds}\left(\cos\theta \frac{dx}{ds}\frac{\partial n}{\partial r} + \sin\theta \frac{dy}{ds}\frac{\partial n}{\partial r} + \frac{dz}{ds}\frac{\partial n}{\partial z}\right)\right] \tag{17}$$

In general, we know the initial point x(0), y(0), z(0), and the initial direction of the ray dx/ds, dy/ds, dz/ds at s = 0. The solution provides the final location and direction after traversing the region

---

[7]Marchand, E. W. , Gradient Index Optics, Academic Press, N.Y., 1978, p. 108.

of variable index of refraction. The index of refraction at any point is

$$n = c\beta/\omega \quad . \tag{18}$$

In free space, $n = 1$, and $\beta = 2\pi/\lambda$. In the limit of small gradients in n, or for paths along which $\vec{t} \cdot \nabla n = 0$, the ray trajectory is a straight line-of-sight (LOS).

In our numerical evaluation of this path, the differential equations are solved by finite differences.

$$x(s + \Delta s) = x(s) + \left.\frac{dx}{ds}\right|_s \Delta s + \frac{1}{2}\left.\frac{d^2x}{ds^2}\right|_s \Delta s^2 \tag{19}$$

$$y(s + \Delta s) = y(s) + \left.\frac{dy}{ds}\right|_s \Delta s + \frac{1}{2}\left.\frac{d^2y}{ds^2}\right|_s \Delta s^2 \tag{20}$$

$$z(s + \Delta s) = z(s) + \left.\frac{dz}{ds}\right|_s \Delta s + \frac{1}{2}\left.\frac{d^2z}{ds^2}\right|_s \Delta s^2 \tag{21}$$

A solution proceeds from the known initial location x(0), y(0), z(0) with known direction [dx(0)/ds], [dy(0)/ds], [dz(0)/dx] in a stepwise manner to the final point x(s), y(s), z(s). However, this final point is known in advance (the receiver location), but the initial direction of the refracted ray required to intercept the final point is unknown. This is a two-point boundary value problem in which the initial direction which allows the trajectory to intercept the end point is to be found. The numerical solution proceeds by choosing an initial value for the direction at the transmitter (the direction of the line-of-sight), and then iterating until the final location is within a prescribed distance of the receiver location. Each integration requires a new guess of the direction, which we have taken to be

$$(\cos \alpha_i)^{(n+1)} = (\cos \alpha_i)^{(n)} + RC \cdot \varepsilon_i/s \tag{22}$$

where α_i is the direction cosine with respect to the ith direction, ε_i is the component of the error vector from the end point of the nth integration, and s is the ray path length to that point. RC is an overrelaxation factor ($0 < RC \leq 1$). The end of each integration is taken to be the point at which $|\vec{\varepsilon}|$, the error between the nth integration and the actual end point, is a minimum (i.e., the error is computed at each Δs, and the integration stops when $|\varepsilon|$ begins to increase). When the actual path is obtained, $|\varepsilon| \leq \varepsilon_A$, and the attenuation and phase are evaluated along the curved path, s, according to Eqs. (12) and (13).

SCATTERING BY TURBULENCE

The SPF accounts for turbulence in the exhaust plume flow. The primary emphasis is on mixing and specification of the mean flowfield properties, but predictions of turbulence quantities are also performed. For example, a dynamical equation for the evolution of the turbulence kinetic energy ($k = 1/2\ \overline{q'^2}$) is solved in the two-equation turbulence models. Improved descriptions involving the g-equation formulation of the mean square fluctuations of passive scalar quantities are currently included in preliminary form. The potential of these models, and the even more detailed turbulence descriptions available in higher-order closure models, are just beginning to be realized in exhaust plume applications.

DIFFERENTIAL CROSS SECTION

In view of the potential availability of plume solutions including a turbulence description, PRFIC includes a formulation for scattering from turbulent fluctuations of the index of refraction.* We have used the single scattering (Born) approximation, but with an added correction to account for attenuation by the mean flow of the incident and scattered wave.

*It is perhaps useful to point out the distinction between scattering and diffraction. Scattering is the more general term, and usually refers to the distribution of radiation at distances from the volume of nonuniform refractive index that are large compared to the wavelength and to the size of the nonuniform volumes. The effect of turbulence on RF waves, in which the size of the most effective nonuniformities is comparable to the wavelength and is small compared to the usual distances to the transmitter and receiver, is usually termed scattering. In contrast, the effect of the mean flow, for which the dimensions are usually large compared to the wavelength and can be comparable to the distances to the transmitter or receiver, is usually called diffraction. Another distinction is that scattering is a volume phenomenon, while diffraction is a surface phenomenon.

In the single scattering limit, the differential cross section per unit volume of scattering material is[8,9]

$$\frac{d^2\sigma}{dVd\Omega} = 2\pi k^4 \sin^2\chi\Phi(\vec{k} - k \cdot \vec{m}) \tag{23}$$

Φ is the power spectral density of the index of refraction fluctuations, evaluated at the wavenumber which is the difference between the wavenumber of the incident and scattered wave. $|\vec{k} - k\cdot\vec{m}| = 2k \sin \Theta/2$, where Θ is the scattering angle.

We have used the well-known Kolmogorov form of the energy spectrum for which

$$\Phi\,(\vec{k} - \vec{k} \cdot \vec{m}) = \frac{0.033\, C_n^2}{\left[1 + 4k^2\Lambda^2 \sin^2 \frac{\Theta}{2}\right]^{11/6}} \tag{24}$$

and the structure constant C_n^2 is

$$C_n^2 = 1.6\, \frac{\overline{n'^2}}{\Lambda^{2/3}} \quad . \tag{25}$$

We use a length scale Λ given by

$$\Lambda = \frac{1}{8}\,\frac{q^3}{\varepsilon}\,\frac{1}{2\sqrt{2}}\,\frac{k^{3/2}}{\varepsilon} \tag{26}$$

---

[8]Booker, H.G., and Gordon, W.E., "A Theory of Radio Scattering in the Troposphere," Proceedings of the I.R.E, April 1950, pp. 401-412.

[9]Tatarski, V.I., Wave Propagation in a Turbulent Medium, McGraw-Hill, New York, 1961, p. 68.

where k is the turbulence kinetic energy and ε the dissipation (both quantities are calculated in the SPF).

If we assume that n' is due only to the fluctuations in n_e', (see Appendix D), then

$$\overline{n'^2} = \overline{n_e'^2} \frac{\omega_p^4/n_e^2}{4(\omega^2 + \nu_{en}^2)^2} \tag{27}$$

$$\overline{n'^2} = \frac{4\pi^2}{k^4} \frac{\overline{n_e'^2}\, r_t^2}{\left[1 + \left(\frac{\nu_{en}}{\omega}\right)^2\right]^2} \tag{28}$$

with r_t being the Thompson radius of the electron

$$r_t = \frac{e^2}{4\pi\varepsilon_o mc^2} = 2.81 \times 10^{-15}\ \mathrm{m} \tag{29}$$

With these assumptions, the complete cross section per unit volume is

$$\frac{d^2\sigma}{dv d\Omega} = 8\pi^3\ (0.0528)\ \frac{\overline{n_e'^2}}{\overline{n_e^2}} \frac{\overline{n_e^2}\ r_t^2\ \Lambda^3}{\left[1 + \left(\frac{\nu_{en}}{\omega}\right)^2\right]^2} \frac{\sin^2\chi}{\left[1 + 4(k\Lambda)^2 \sin^2 \frac{\theta}{2}\right]^{11/6}} \tag{30}$$

The ratio of received scattered power to transmitted power is obtained from an integration over the entire plume volume

$$\frac{P_R}{P_T} = \frac{\lambda^2}{(4\pi)^3} \int_V G_T\ (\phi_T)\ \frac{G_R(\phi_R)}{r_T^2\ r_R^2} \left(\frac{d^2\sigma}{dV d\Omega}\right) dV \tag{31}$$

G_T and G_R are transmitter and receiver gains in the directions ϕ_T and ϕ_R between the antenna direction and the wave direction.

This is the standard formulation for the power received from a volume of distributed scatterers. We have modified this formulation to include the attenuation of the wave along the path prior to and subsequent to scattering from each point in the flow. The integrand in Eq. (31) is therefore reduced by the factor

$$\exp - \left[\left(\int_0^s \alpha \, ds \right)_i + \left(\int_0^s \alpha \, ds \right)_s \right] \tag{32}$$

where the integrals are the attenuation along the optical paths of the incident and scattered waves, respectively. These paths can be evaluated along straight lines-of-sight or also along refracted paths.

ATTENUATION DUE TO SCATTERING

For completeness, we note that scattering contributes to attenuation by removing radiation from the direction of propagation. It also reduces attenuation by adding radiation back into the direction of propagation. The cross section per unit volume for removal (extinction) is

$$\alpha_s = \int_{4\pi} \left(\frac{d^2\sigma}{dV d\Omega} \right) d\Omega \tag{33}$$

$$= 8\pi \, (.0528) \, \frac{\overline{n_e'^2}}{\overline{n}_e^2} \, \frac{\overline{n}_e^2 \, r_t^2 \, \Lambda^3}{\left[1 + \left(\frac{\nu_{en}}{\omega} \right)^2 \right]^2} \int_0^{2\pi} \int_0^{\pi} \frac{\sin^2\chi \, \sin\Theta d\Theta d\phi}{\left[1 + 4(k\Lambda)^2 \sin^2 \frac{\Theta}{2} \right]^{11/6}} \tag{34}$$

using

$$\sin^2\chi = 1 - \sin^2\Theta \, \sin^2\phi \tag{35}$$

the integral of $d^2\sigma/dVd\Omega$ over all directions is

$$Q(p) = \frac{6\pi}{p^3}\left\{\frac{1}{5}(2p^2 + 2p + 1)[1 - (1 + 2p)^{-5/6}] - 2(p + 1)[(1 + 2p)^{1/6} - 1]\right.$$

$$\left. + \frac{1}{7}[(1 + 2p)^{7/6} - 1]\right\} \quad \text{with } p = 2k^2\Lambda^2 \tag{36}$$

Limiting cases are

$$\lim_{p \to o} Q(p) = 8\pi \tag{37}$$

$$\lim_{p \to \infty} Q(p) = \frac{12}{5}\frac{\pi}{p} \tag{38}$$

The attenuation due to scattering by the turbulent fluctuations is then given by

$$\alpha_s = 8\pi^3 (.0528) \frac{\overline{n_e'^2}}{\overline{n}_e^2} \frac{\overline{n}_e^2 r_t^2 \Lambda^3 Q(2k^2\Lambda^2)}{\left[1 + \left(\frac{\nu_{en}}{\omega}\right)^2\right]^2} \tag{39}$$

This contribution to the attenuation along the line-of-sight is included in PRFIC. However, it has proved to be small compared to the attenuation due to absorption in all cases examined so far.

RADAR CROSS SECTION

In the special case of co-located antennas, the scattered power given by Eq. (31) reduces to the turbulent scattering component of the radar cross section of the plume

$$\frac{P_R}{P_T} = \frac{\lambda^2}{(4\pi)^3} \frac{G_T G_R}{R^4} \int_V \frac{d^2\sigma}{dV d\Omega} dV = \frac{\lambda^2}{(4\pi)^3} \frac{G_T G_R}{R^4} \bar{\sigma} \tag{40}$$

(when the range R is large compared to any plume dimension).

DOPPLER SHIFT

SHIFT OF DIRECTLY TRANSMITTED WAVE

Two Doppler shifts of the transmitted frequency are considered in PRFIC. One is the frequency shift of the directly transmitted wave due to relative motion between the transmitter and receiver. This shift is

$$\Delta\nu = \nu - \nu_o = \frac{\nu_o}{c}(\vec{V}_T - \vec{V}_R) \cdot \hat{s} \quad * \tag{41}$$

where $\hat{s}$ is a unit vector from the transmitter to the receiver. This shift occurs for any condition of relative motion between the transmitter and receiver and is independent of the presence of an exhaust plume.

TURBULENCE BROADENED SPECTRUM

The second Doppler shift occurs in the scattering of the radiation by the turbulence in the plume. This shift depends on the relative velocities of the transmitter and receiver, the mean velocity of the exhaust plume, and also on the fluctuations of the plume velocity. Since these fluctuations are random, they are described in a statistical sense; and, consequently, the frequency shift due to scattering is also given statistically. In this first version of PRFIC, the velocity fluctuations were assumed to have a Gaussian distribution in magnitude; and, consequently, the probability density of the frequency shift due to scattering is also Gaussian. The probability density is

$$P(\Delta\nu) = \frac{1}{\sqrt{2\pi\overline{q^2}}} \frac{c}{2\nu_o \sin\frac{\Theta}{2}} \exp\left\{\frac{1}{2}\frac{\left[\frac{c\Delta\nu}{\nu_o} - (\vec{V}_T \cdot \hat{s} - \vec{V}_R \cdot \hat{t}) - (\overline{w\hat{k}} + \vec{V}_m)(\hat{t} - \hat{s})\right]^2}{4\overline{q^2}\sin^2\frac{\Theta}{2}}\right\} \tag{42}$$

*Terms of order $|(\vec{V}_T - \vec{V}_R) \cdot \hat{s}/c|^2$ and higher are neglected.

(See Appendix E for the derivation.) $\overline{q^2}$ is the mean square turbulent velocity fluctuation ($\overline{q^2}=2k$, where k is the turbulence kinetic energy). $\vec{V}_T$, $\vec{V}_R$, $\vec{V}_m$, are the velocities of the transmitter, receiver, and missile, respectively (Figure 6). $\bar{w}$ is the local mean axial velocity of the plume, with respect to a coordinate system fixed in the missile, and is given directly by the output of the SPF.

The scattered power is frequency dependent, and the amplitude at each frequency $\nu=\nu_0+\Delta\nu$ is given by Eq. (31) weighted with the above frequency probability density. Note that the frequency probability density must be included within the volume integral because it depends on the local position within the plume. The result of this evaluation is the frequency spectrum of the scattered power (i.e., the AM noise spectrum). The total AM noise and total scattering cross sections are obtained from

$$\int_{-\infty}^{\infty} \frac{P_R}{P_T} (\Delta\nu)\, d(\Delta\nu). \tag{43}$$

APPLICATIONS OF PRFIC

This section contains summaries of some sample calculations with PRFIC to illustrate its capabilities. As with any code that makes predictions of physical quantities, the ultimate test is to compare the predictions with measurements. However, with RF interference, there is the equally important issue of the correct flowfield. Comparison between measured and predicted RF interference quantities therefore requires the additional effort of making accurate flowfield predictions. That was not part of the contractual effort summarized here and remains to be done. The emphasis in this initial effort was to verify that PRFIC computes correctly those quantities which it is supposed to provide, given a plume flowfield description.

TRANSVERSE ATTENUATION

We include one comparison of predictions and experiment with the objective of showing that PRFIC does provide correct attenuation predictions. An extensive set of transverse attenuation measurements was reported in Reference 1. We have made predictions for cases 21-23 of this set: a small static, solid propellant motor (84 percent solids, of which 18 percent is aluminum).

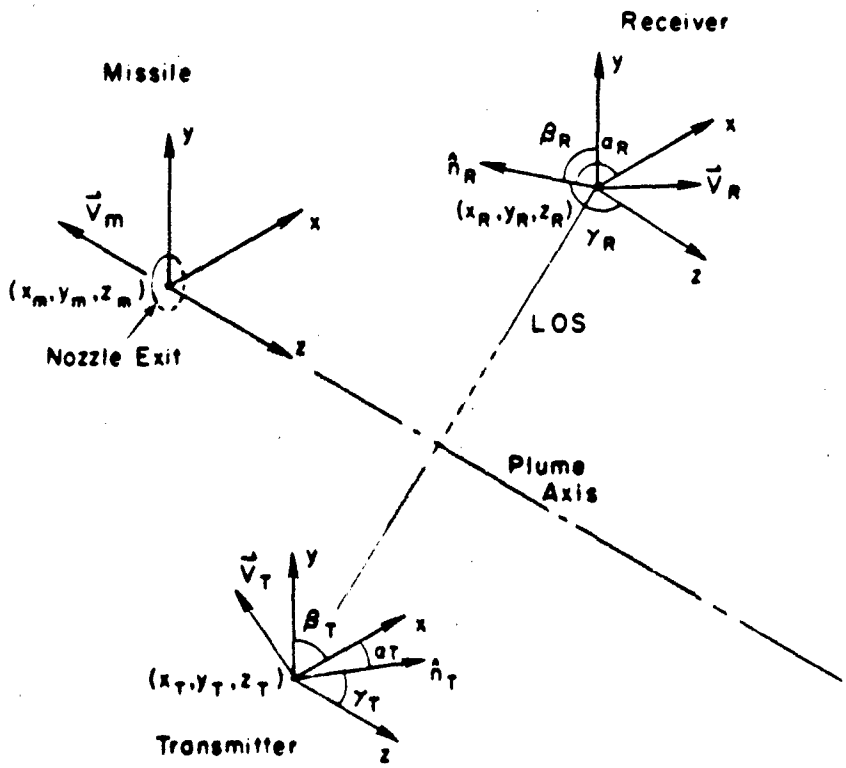

FIGURE 6. Coordinate System for PRFIC.

The full capability of the SPF was utilized. We input a user defined chemical system with species and reactions that included all the major afterburning and charged species and all the afterburning and charged species reactions. The impurity levels were 80 ppm potassium and 125 ppm sodium. Both equilibrium and finite rate chemistry during the expansion from the chamber were tried as initial conditions for the plume. In addition, a constant pressure mixing (fully pressure equilibrated to ambient pressure) case was compared to the more precise overlaid calculation (mixing layer superposed on the underexpanded plume boundary). In this particular case, there were no significant differences between the overlaid and constant pressure mixing solutions because the degree of underexpansion was not severe (ratio of exit to ambient pressure of about two).

There was a large difference between the predictions using the equilibrium and chemical kinetic initial conditions. The kinetics solution provided a higher electron number density, and consequently the attenuation through the initial region of the plume (along those paths penetrating the inviscid core of the plume) was too large. The difference between these two sets of initial conditions diminished downstream as the chemistry in the plume mixing region began to dominate over the initial concentrations. However, even with the lower electron concentrations of the equilibrium initial conditions, the predicted attenuation was too large. For the purpose of testing PRFIC, we took the approach of reducing the electron concentration uniformly throughout the plume until the predictions and measurements matched at the first measurement location, (about $z/r_j = 18$) near the end of the inviscid core. By reducing the electron number density uniformly by a multiplier of 1/8, it was possible to match the initial transverse attenuation at the three measurement frequencies of 9, 16, and 32 GHz. These results are given in Figures 7, 8, and 9, for these three frequencies. It is important to note that the downstream distribution of attenuation is also closely predicted. By calibrating the flowfield at the first measurement station, we have made good predictions of the attenuation downstream as well. We infer from this comparison that, when given the proper flowfield description, the attenuation predictions with PRFIC compare favorably with the three sets of measurements at different frequencies.

It is important to note that the plume prediction giving the best agreement with the attenuation measurements was made with the two-equation turbulence model, without the compressibility correction. The flowfield with the compressibility correction gave too much attenuation downstream. The exit Mach number was 3.2, and the inviscid core lengths were $29r_j$ and $14r_j$ with and without the correction, respectively. The same conclusion was reached independently in a study

Reproduced From
Best Available Copy

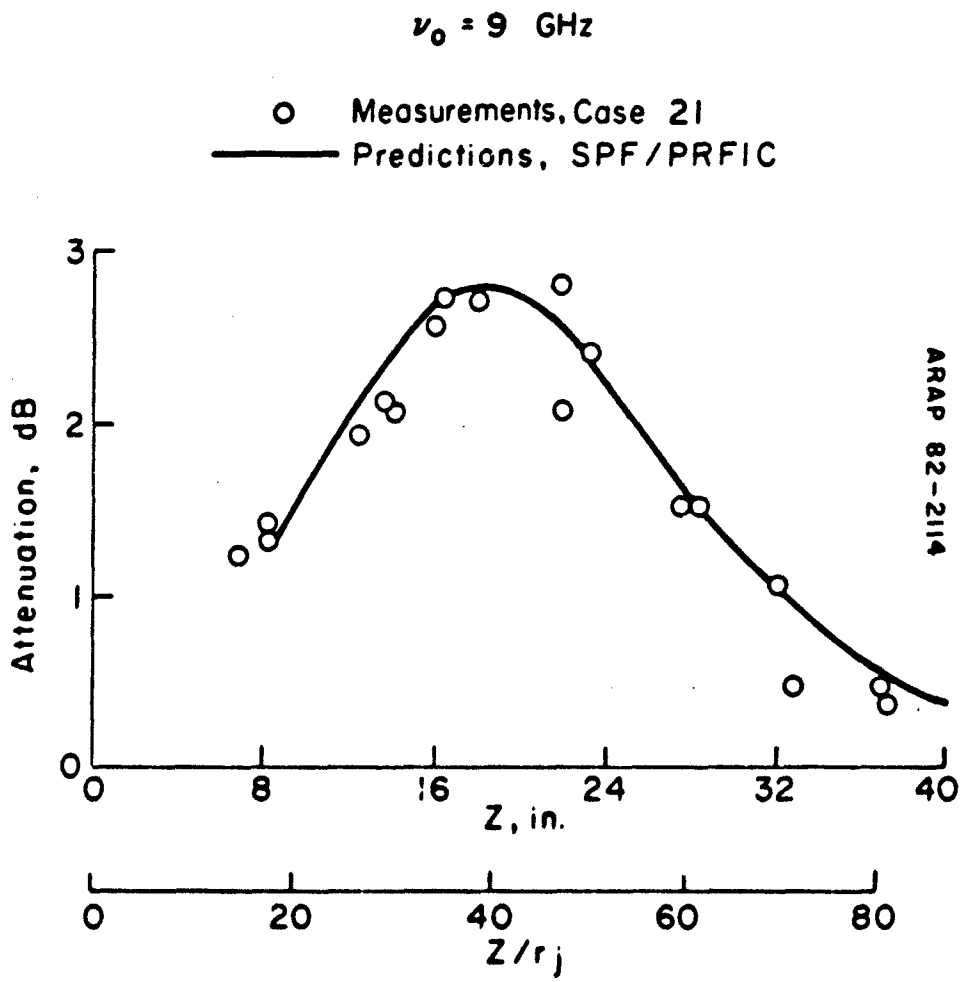

FIGURE 7. Transverse Attenuation at 9 GHz. NWC TP 5319, Part 1, Case 21.

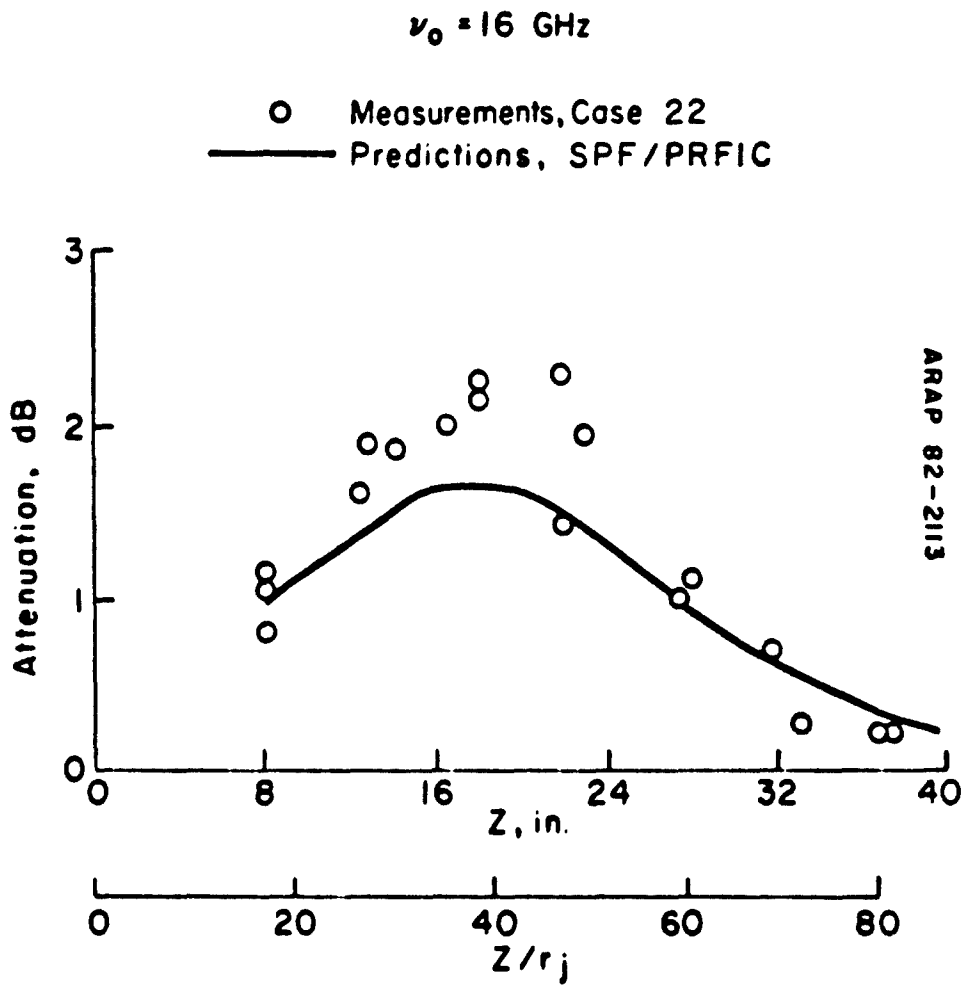

FIGURE 8. Transverse Attenuation at 16 GHz. NWC TP 5319, Part 1, Case 22.

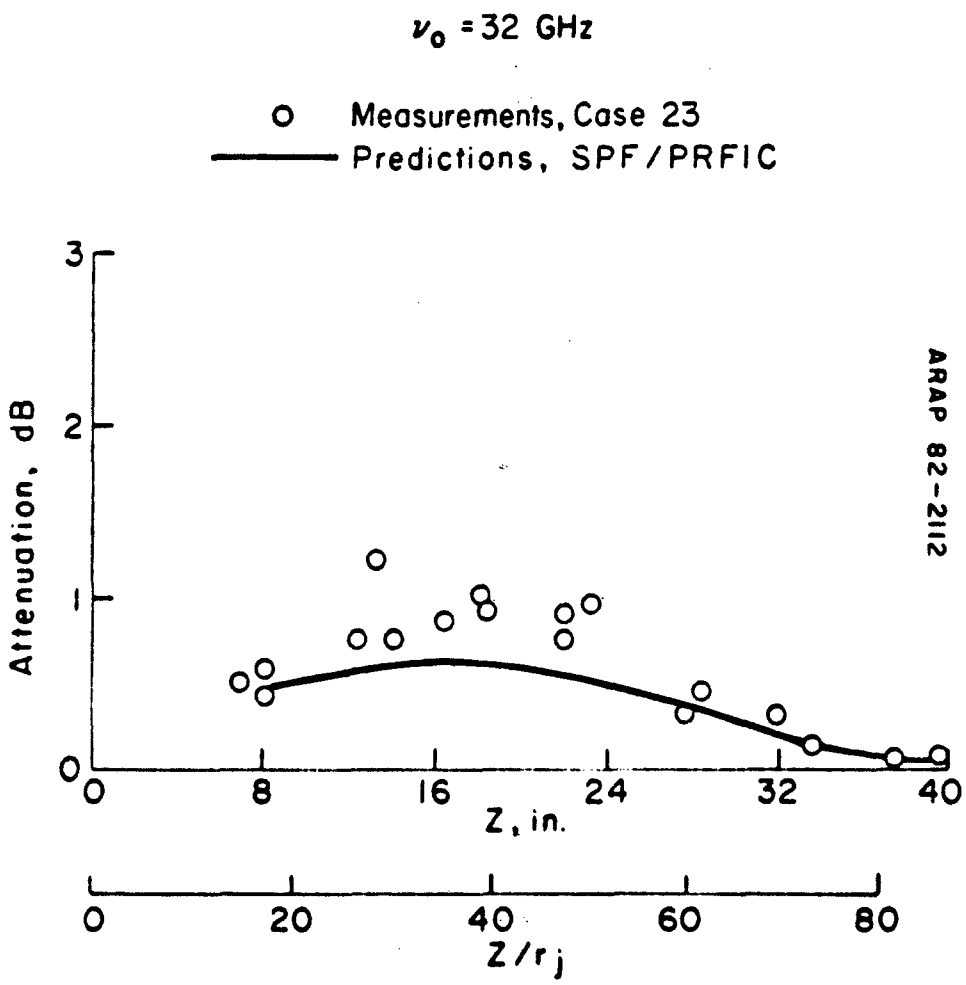

FIGURE 9. Transverse Attenuation at 32 GHz. NWC TP 5319, Part 1, Case 23.

of the gas dynamic structure of plumes.[10] This sensitivity suggests that both the magnitude and distribution of plume RF interference properties are strongly affected by our ability to predict turbulent flows.

An additional set of transverse attenuation and phase predictions is given for the exhaust plume shown in Figures 3, 4, and 5. A profile of transverse attenuation from the axis to the edge of the plume is given in Figure 10. At 5 meters downstream ($z/r_j = 37$), the peak electron number density and attenuation are located in an annular volume about the axis. The attenuation shows this, as the peak occurs at a radius of about 0.125 meters [$(y/r_j) \sim 1$]. This prediction suggests that the peak attenuation does not necessarily occur for a line-of-sight through the plume axis, at least for those regions where afterburning is most intense.

Attenuation predictions using the ray trace option are also shown in Figure 10. For this particular example, the refracted paths yield attenuation which is not substantially different from the straight line-of-sight. When there is a difference, the attenuation is uniformly larger for the refracted path.

The phase change for the same conditions as the attenuation in Figure 10 is shown in Figure 11. The phase difference, $\Delta\phi$,

$$\Delta\phi = \int_0^s \beta ds - 2\pi s/\lambda = \int_0^s 2\pi \frac{n}{\lambda} ds - 2\pi s/\lambda \tag{44}$$

between that along the actual path and that for the free space line-of-sight is shown. The peak phase shift occurs at the location of peak attenuation. We note that the coherent RF power ratio due to this phase difference is

$$\sim e^{21\Delta\phi} \tag{45}$$

The phase difference predicted for the refracted path is larger by a small amount in the highly attenuating region for this case.

[10] Pergament, H.S., "Assessment and Recommendation of Two-Equation Turbulence Models for Rocket and Aircraft Plume Flowfield Predictions," Naval Weapons Center, China Lake, Calif., July 1982. (NWC TP 6364, publication UNCLASSIFIED).

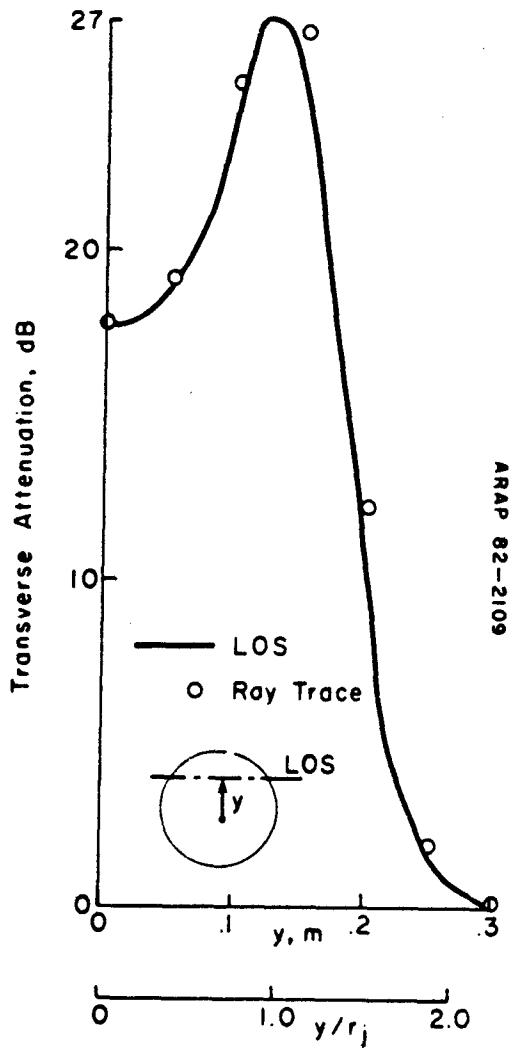

FIGURE 10. Transverse Attenuation Distribution Across the Plume. ν_0 = 1 GHz, z/r_j = 37.

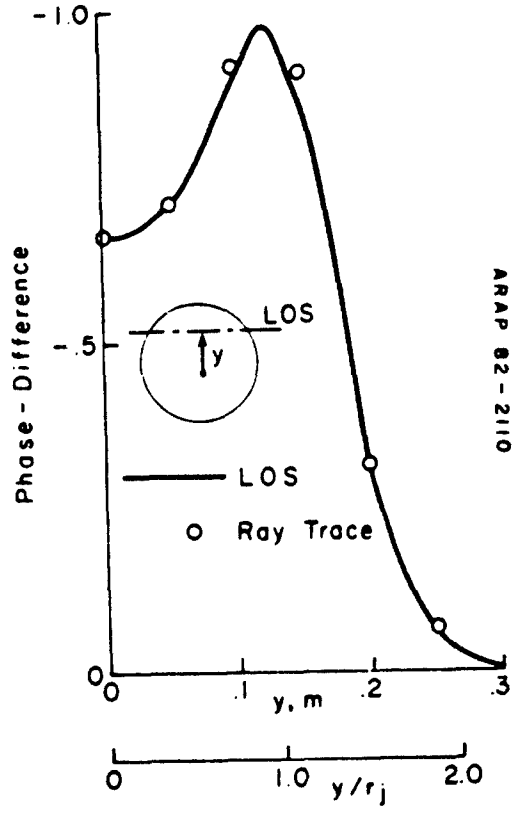

FIGURE 11. Transverse Phase Difference Across the Plume. ν_0 = 1 GHz, z/r_j = 37.

DIAGONAL ATTENUATION

An example of diagonal attenuation from near tail-on observation angles for the plumes shown in Figures 3-5 is given in Figure 12. These predictions show the rapid onset of severe attenuation as the line-of-sight passes through the edge of the plume and into the region where it passes through nearly the entire plume length. Calculations like this have shown that the attenuation for observation on the same side as the antenna ($\beta > 0$) is very sensitive to the radial location of the antenna. Additionally, this situation is one in which diffraction by the plume is important. The increased attenuation with decreasing angle is actually less than that shown in Figure 12, when the diffracted wave is included. For this particular geometry, the attenuation due to absorption calculated by PRFIC is a worst case, and the effects of diffraction should be included to provide an accurate description of the total plume interference.

An example of the three-dimensional capability of the PRFIC code is given in Figure 13 in which the attenuation of the transmission from a rolling missile is given. These calculations are for a large Minuteman class plume at 5 km altitude. The observation is from an aspect angle of 150 degrees (30 degrees from tail-on). A zero roll angle occurs when the transmitting and receiving antennas are on opposite sides of the plume. The attenuation diminishes as the antenna rolls out of the shadow of the plume. The calculation requires the capability of the code to deal with a fully three-dimensional line-of-sight through the axisymmetric plume. This observational condition is also one in which diffraction effects are important.

SCATTERING

There are several applications of the calculation of scattering from the turbulent fluctuations in the plume electrical properties. Scattering in the direction of propagation, like diffraction by the mean flow, increases the power received and reduces the apparent attenuation. In the limiting case where there is no direct propagation path from transmitter to receiver, scattering and diffraction are the only means of signal transmission. In the case of pure backscatter, scattering by turbulence is a component of the plume radar cross section in addition to that scattered by the mean flow. Finally, the fluctuating nature of scattering by the turbulence, and the fact that it has a large Doppler shifted frequency spectrum because of the turbulent velocity distribution, create a source of noise that is present in any portion of the received signal that has interacted with the exhaust plume.

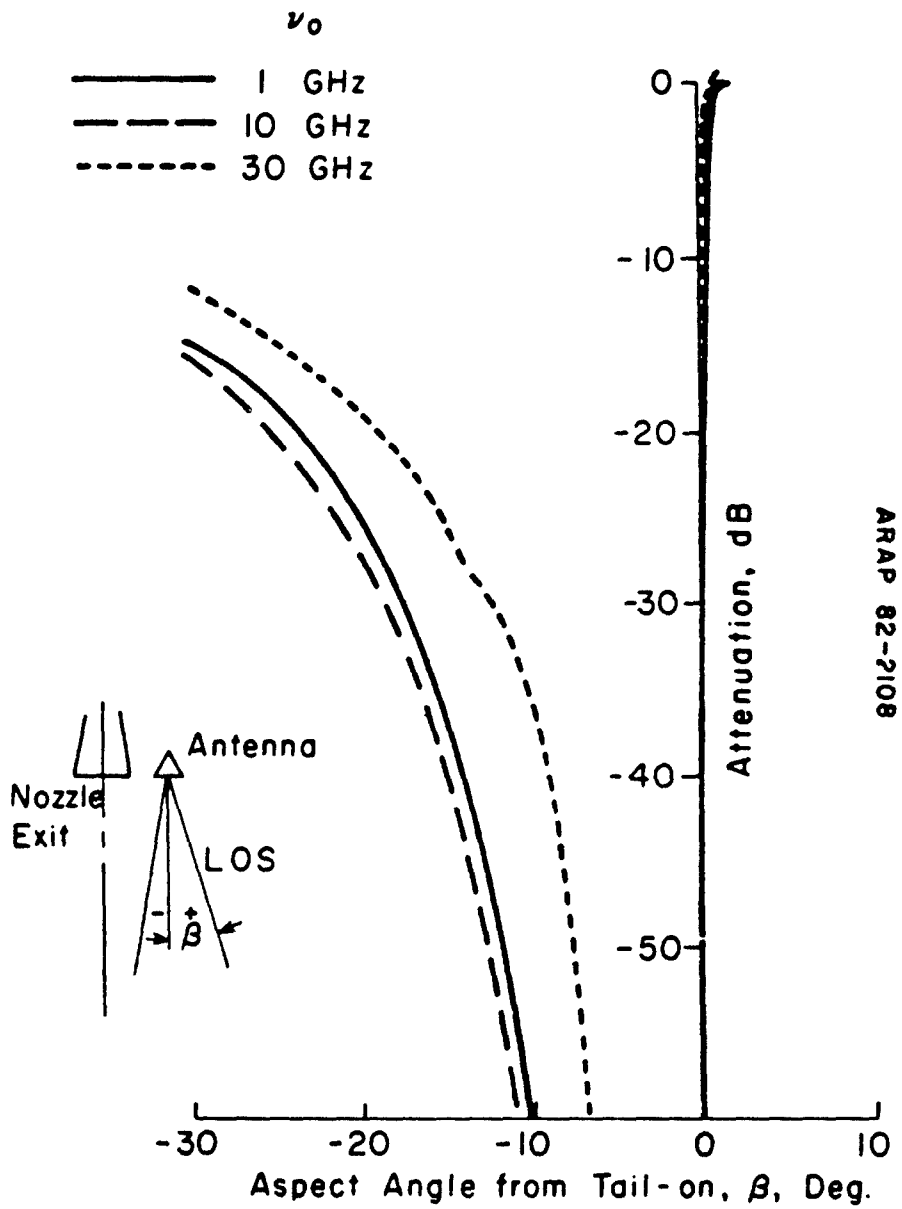

FIGURE 12. Diagonal Attenuation at Near Tail-on Aspect.

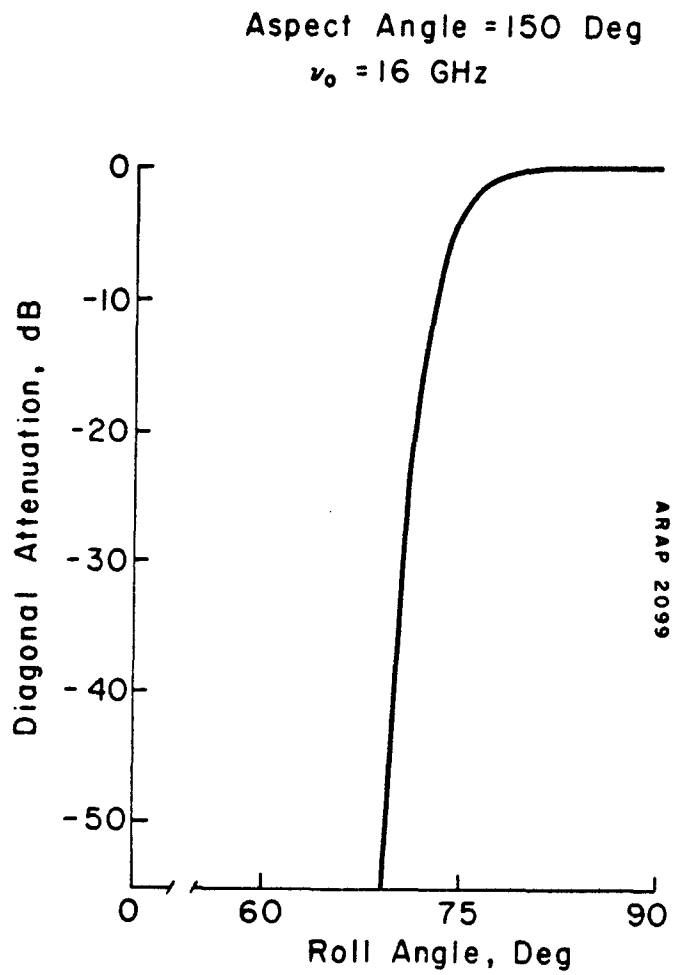

FIGURE 13. Diagonal Attenuation at Near Tail-on Aspect for a Rolling Missile, Minuteman Class Plume at 5 km Altitude.

As an initial example of the calculation of scattering, we include a tabulation of the scattered power for the transverse attenuation conditions shown in Figures 7, 8, and 9 (see Table 2). This is the power added back into the direction of propagation that reduces the effective attenuation. The contribution is that added incoherently, without regard to phase, and does not include attenuation of the incident and scattered wave (the added effect of attenuation is small for this plume.) In all cases, the power received by scattering is very much less than that absorbed from the directly transmitted wave.

TABLE 2. Transverse Attenuation and Scattering

Predictions for cases 21, 22, 23, of NWC TP 5319, Part 1 (Reference 1)
(scattering calculations do not include attenuation)

	9 GHz		16 GHz		32 GHz	
z/rj	Attn,dB	Scatt,dB	Attn,dB	Scatt,dB	Attn,dB	Scatt,dB
17.7	1.34	-91.79	1.104	-94.34	0.553	-100.16
35.4	2.69	-87.06	1.62	-88.85	0.599	- 94.85
53.1	2.19	-86.21	1.31	-89.28	0.470	- 97.27
70.7	1.03	-89.07	0.608	-92.80	0.169	-100.36
88.4	0.373	-95.74	0.203	-99.98	0.015	-107.37

These scattering results were computed with uniform gain for both the transmitter and receiver. If a highly directional antenna is used (for example, with a gain of 20 dB) for both the transmitter and receiver, the scattering contribution is still small compared to that of the direct transmission for this particular plume.

The contribution to the received signal due only to scattering was computed for a fixed receiver location and direction (a radial location of $y/r_j = 1.86$, pointed downstream, parallel to the plume axis). The plume properties are those shown in Figures 3-5. The scattered power received as the transmitter was moved around the vehicle is shown in Figure 14. Cases both with and without attenuation of the scattered waves are shown. The polar plot is for the situation in which the receiver, transmitter, and plume axis are all in the same plane. This result shows that, for this particular plume, the effect of attenuation of the scattered power contributes about a 10 dB loss to that scattered without attenuation. In both cases, there is very little aspect angle dependence in the forward hemisphere of scattering

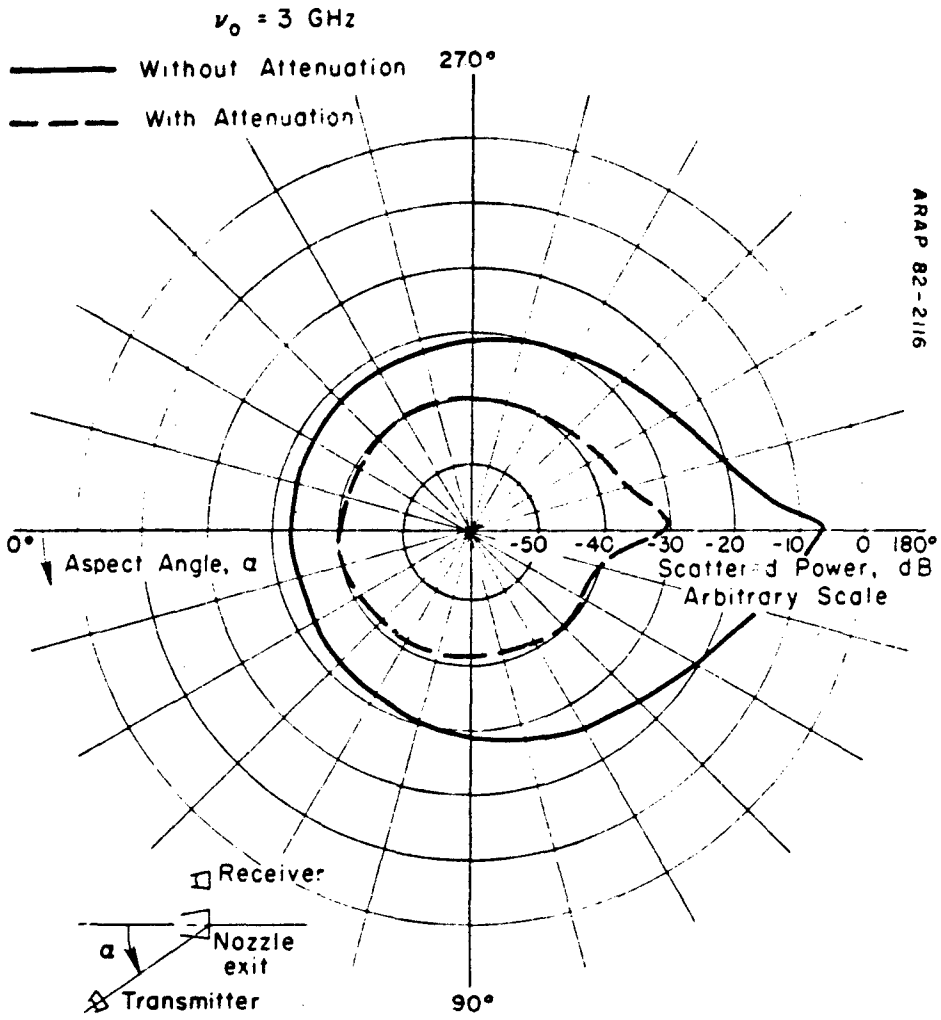

FIGURE 14. Aspect Angle Dependence of Scattering to a Fixed Antenna Location at the Nozzle Exit Plane (plume properties of Figures 3-5).

($0 < \alpha < 90$ degrees and $270 < \alpha < 360$ degrees). There is an aspect angle dependence in the rearward hemisphere, and there is an asymmetry about the plume axis because the transmitter and receiver are on the same side of the plume for 180 degrees $< \alpha <$ 360 degrees and on opposite sides for $0 < \alpha < 180$ degrees. It is important to note that, when the aspect angle is in the forward hemisphere, there is no direct transmission, and the received power is only that scattered by the mean flow and the turbulence.

Sample calculations of the aspect dependent backscatter (radar cross section) by the turbulent plume flow are shown in Figure 15. The same plume flowfield was used, and results for scattering with and without attenuation are shown. In the forward hemisphere, no allowance was made for occultation by the missile body. These results are symmetric with respect to the plume axis. There is very little aspect angle dependence of the scattering without attenuation (at sufficiently large distances, the total plume cross section depends only on the number of electrons and their fluctuations). In contrast, the scattering with attenuation decreases sharply at the near tail-on aspect angle because of absorption within the larger path lengths through the plume.

DOPPLER SHIFT

The Doppler shift of the scattered power due both to the mean relative missile, plume, and receiver velocities and to the turbulent fluctuations contributes a frequency spectrum of power. An example of this spectrum is given in Figure 16 for a Minuteman class missile with a velocity of 503 m/s. These calculations are for the backscattered power, and the spectra are shown with and without the effect of attenuation of the scattered power. There is an important effect of the attenuation on the frequency spectrum; and, qualitatively at least, the spectra with attenuation have the general appearance of the measurement of AM noise (Reference 2).

Additional examples of the scattering frequency spectra are shown in Figures 17 and 18, which are for aspect angles of 45 and 135 degrees, respectively. These two observations correspond to the missile approaching the observer and receding from the observer. The two results show the change in spectra for these two relative velocities. The static case is superposed for comparison.

Finally, we show several frequency distributions of the scattered power for different aspect angles in Figure 19. These results are for the Minuteman class plume, and are typical AM noise spectra. Although no quantitative comparisons have yet been made, it is encouraging that these predicted spectra have the general appearance of the several measurements summarized in Reference 2.

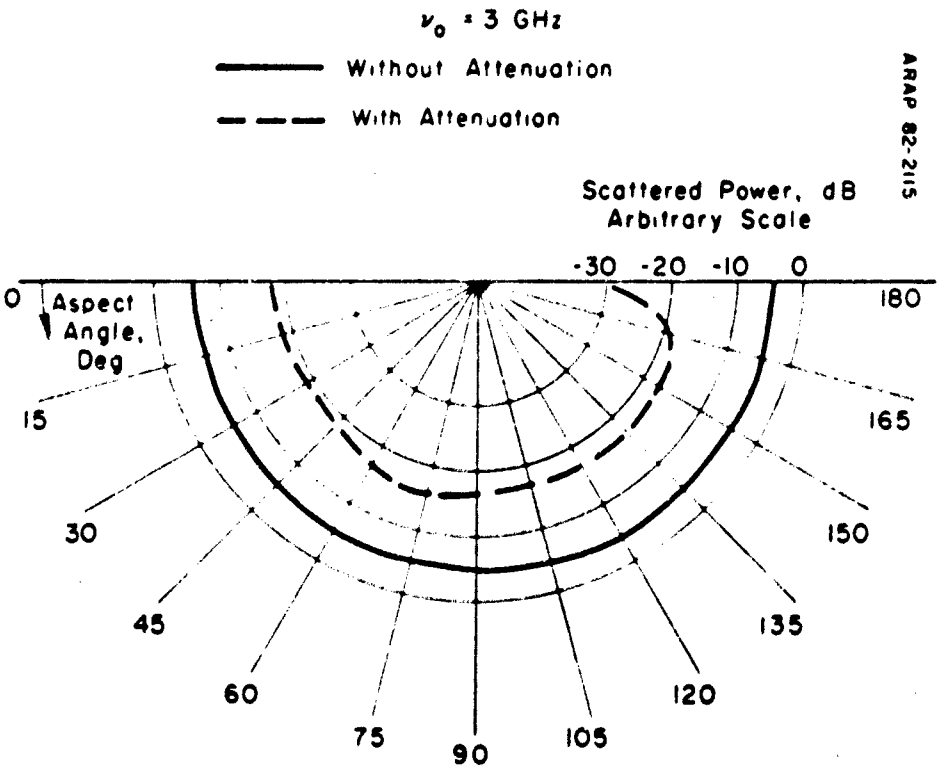

FIGURE 15. Plume Radar Cross Section (plume properties of Figures 3-5).

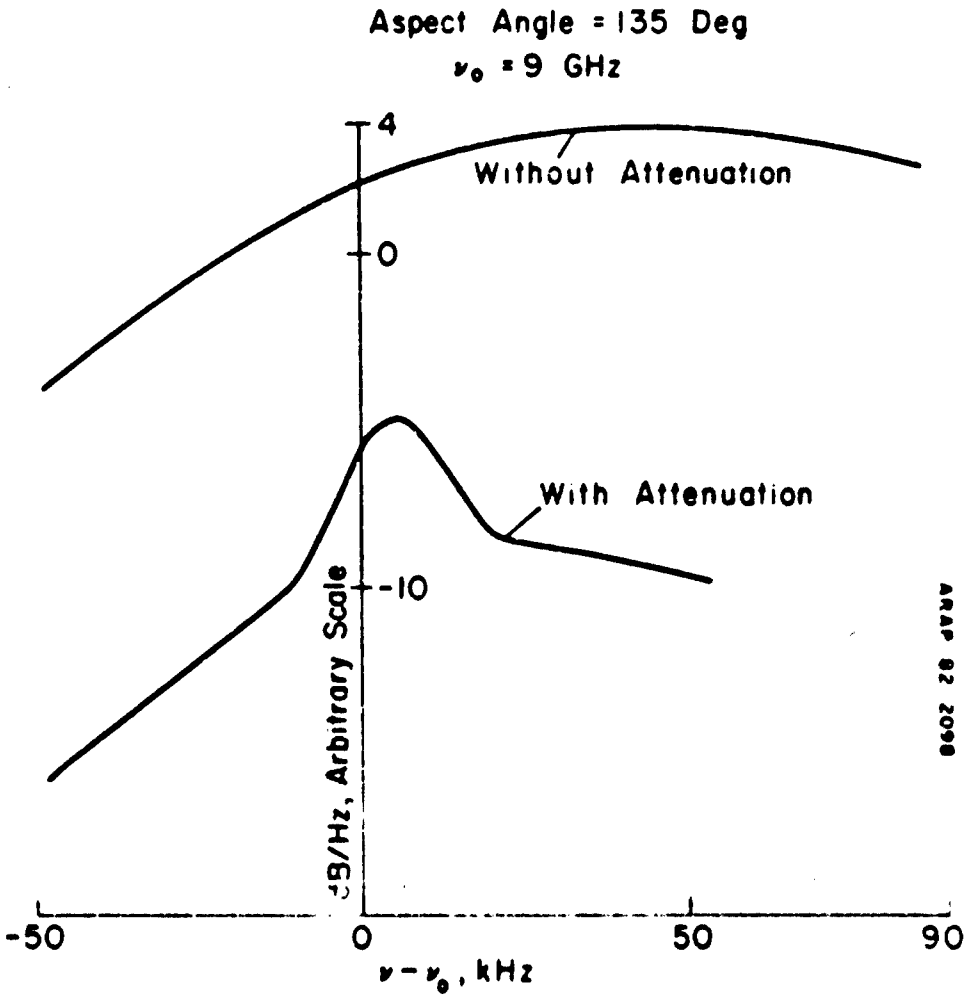

FIGURE 16. Doppler Shifted Frequency Spectra for Backscatter from a Minuteman Class Plume at 1.5 km Altitude, Velocity of 503 m/s, 135 degrees Aspect Angle.

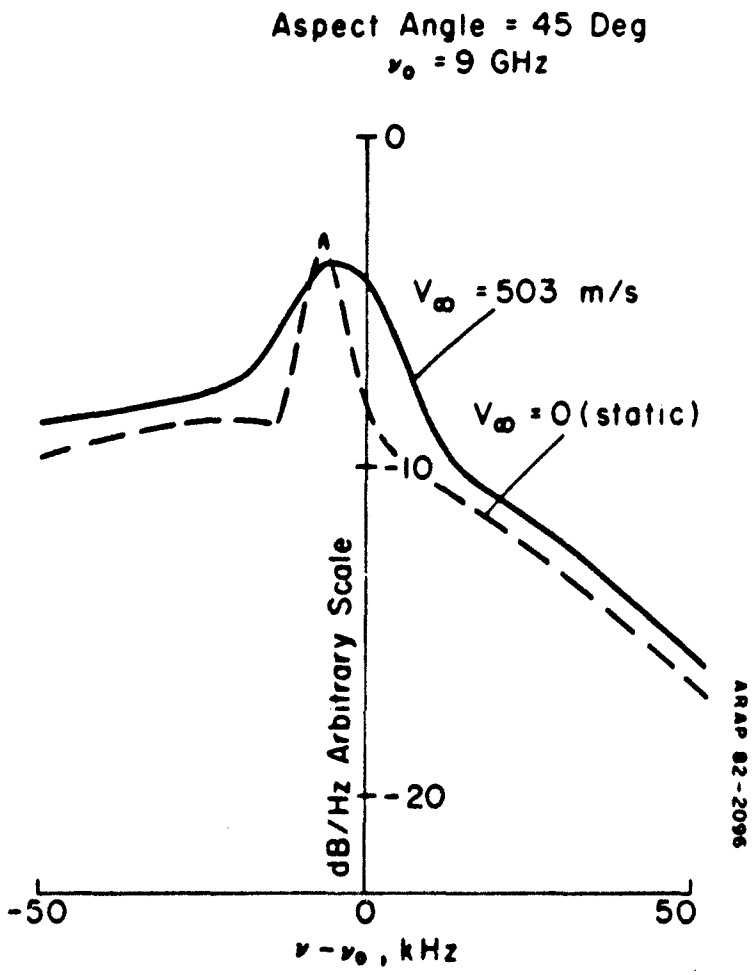

FIGURE 17. Doppler Shifted Frequency for Backscatter from a Minuteman Class Plume at 1.5 km Altitude, Velocity of 503 m/s, Aspect Angle of 45 degrees.

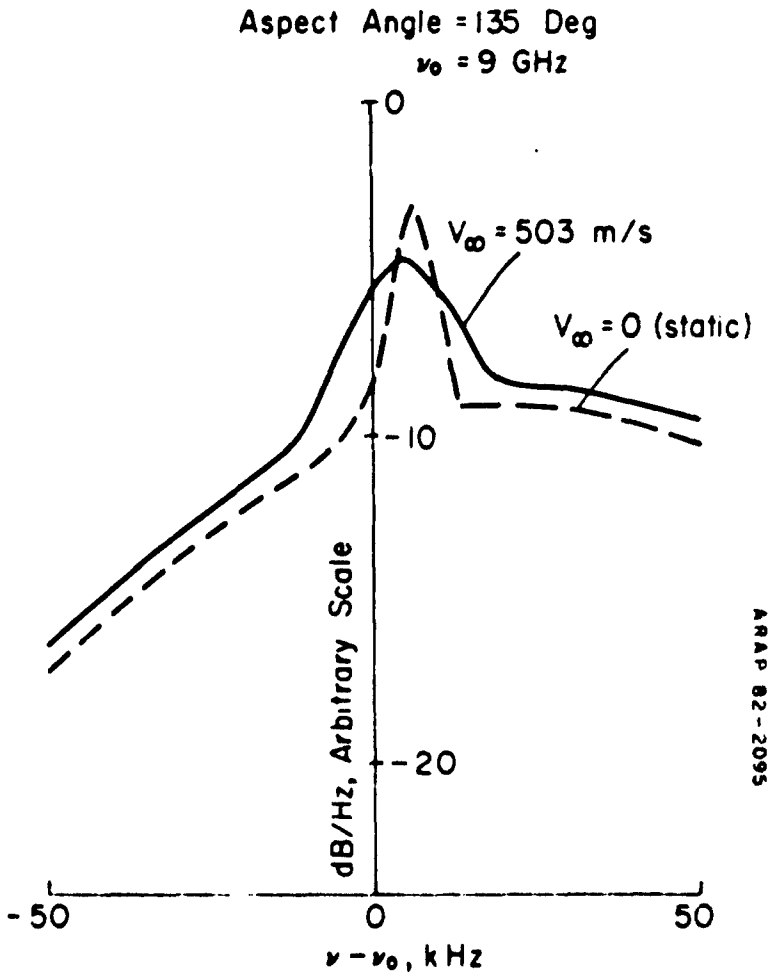

FIGURE 18. Doppler Shifted Frequency Spectra for Backscatter from a Minuteman Class Plume at 1.5 km Altitude, Velocity of 503 m/s, Aspect Angle of 135 degrees.

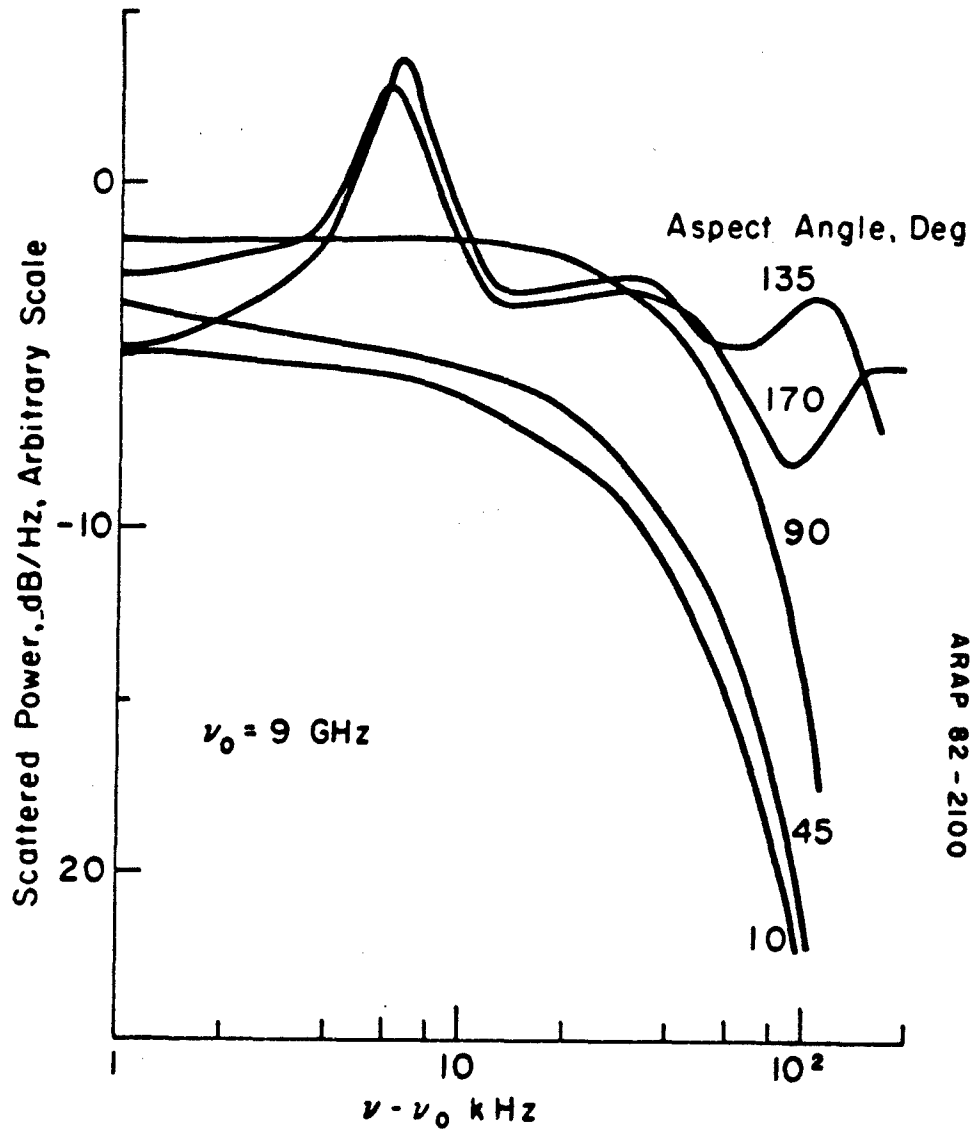

FIGURE 19. Frequency Spectra for Backscattering from a Minuteman Class Plume at 1.5 km Altitude, Velocity of 503 m/s.

These are representative samples of the Doppler spectra of the scattered signal. Their shape is affected to some extent by the choice of a Gaussian probability density for the magnitude of the turbulent velocity fluctuations. Other forms have not been examined, and so the sensitivity of the spectrum to this choice is unknown. However, it is an easy task to change the probability density in the code, and an assessment of various choices against experimental data can easily be made. We anticipate that PRFIC will be a valuable tool for this kind of analysis and predictions.

SUMMARY OF CAPABILITIES AND LIMITATIONS

The primary capabilities and limitations of PRFIC are summarized below.

1. Flowfield Input - SPF format: radial distribution of properties at successive axial stations

2. Geometry - Arbitrary location, orientation, and velocity of the missile, receiver, and transmitter (see Figure 6)
   (This generality was included to account for transmission between a moving missile and a fixed or moving observer, static test situations, and radar cross section predictions with a single code.)

3. Direct Transmission
   a. Attenuation and phase predictions, Doppler shift
   b. Line-of-sight, or ray trace option
      (The ray trace calculation is not reliable in its current form if there are very strong gradients in index of refraction.)

4. Scattering
   a. Single scattering from turbulence-induced index of refraction fluctuations, with attenuation of the incident and scattered wave
   b. Doppler frequency spectra of the scattered power
      (The current code uses a Gaussian distribution of the fluctuating velocity probability density.)
   c. Electron number density fluctuations which are obtained from the SPF
      (The modeling of n_e' is confined to the SPF, the specification of C_n^2, given n_e', is in PRFIC.)
      (The current version of PRFIC keeps track of the amplitude of the frequency spectra, the phase of the scattered wave is computed, but not currently utilized.)
      (The scattering path can be computed with either a line-of-sight or ray trace option.)

SUGGESTED IMPROVEMENTS

There are two classes of improvements to PRFIC that can be easily made. One set of improvements involves the addition of new physical phenomena to the code. In this category, the authors suggest the following:

1. Focusing effects of the refraction

2. Surface scattering effects (diffraction) at the overdense surface

Simple diffraction models have been quite successful in predicting attenuation by plumes with moderate to high electron density levels (References 1 and 3). However such models do not contain the scientific principles or details needed to assure accurate predictions in all cases. As originally conceived, PRFIC was expected to give the same effects as a plume diffraction calculation if absorption, scattering, and phase shift calculations are combined and a sufficiently fine computational grid is used. If PRFIC, as currently implemented, has a major weakness, it is probably the lack of a mechanism to account for surface scattering at the boundary that defines the overdense surface of plumes with high electron densities. The results of scattering in that region should be quite similar to those of a diffraction calculation.

The authors suggest that PRFIC is appropriate to serve as a basis for a solution which incorporates diffraction by the mean flowfield and/or scattering by turbulence at the boundary of the overdense region, whichever is determined to be the more appropriate approach. The addition of a diffraction capability has the added advantage that it would provide the code with the ability to calculate missile body effects on the radiation field in cases where body mounted antennas are involved. These extensions to PRFIC, along with the current capabilities, would provide an entire plume interference computational capability in one unified code.

Another category of suggested improvements involves strictly the computational aspects of the current code. Some improvement in the numerical solution for the refracted ray path is needed to make it more reliable. If there are very severe gradients in n, the current integration scheme does not always converge. In general, the solution converges for trajectories that remain in the same plane. For example, convergence is obtained for ray paths that remain either nearly

perpendicular to the nozzle axis (transverse attenuation), or nearly parallel to the axis. Solutions have been obtained for these cases even for the most severe index of refraction gradients. The solution seems to be most sensitive along those trajectories which do not remain planar. Our initial attempts to define the criteria for convergent solutions more precisely have not been successful. Since the departure of the ray trajectory from the straight line-of-sight depends both upon the index of refraction gradient normal to the trajectory and on the path length, the probability of non-convergence increases with the integral of the gradient along the ray path. However, at this point, we do not have a specific criterion to define those conditions where convergence is assured.

The two-point boundary value problem is one of the more difficult numerical integrations to perform, especially when the solution is very sensitive to the initial conditions as is the case in the present application. The algorithm used in the current version of PRFIC can be improved with the addition of a more refined logic to improve convergence for the more difficult ray trajectories.

Finally, an improvement in the integration procedure for both the straight line-of-sight and refraction solution is suggested. The current procedure is to choose the integration step size a priori and to use uniform increments throughout the entire path length within the plume velocity boundaries. However, often the significant electron number density is confined to a smaller, electrical plume. The small integration steps outside the effective electrical plume are wasted. An improvement would be to let the step size vary throughout the plume, and depend on the gradient of the plume electrical properties along the line-of-sight. This is an easily implemented improvement that would yield accurate solutions with less computational time.

SUMMARY AND CONCLUSIONS

We have presented a summary of the physics of the interaction of electromagnetic waves with radar frequencies with a weakly ionized rocket exhaust plume. A computer code, the Naval Weapons Center Plume Radar Frequency Interference Code (PRFIC), has been developed to calculate several aspects of this interaction. The code relies on the description of the exhaust plume given by the JANNAF Standard Plume Flowfield Model (SPF). Its current capabilities in addition to the SPF plume structure are:

1. full three-dimensional geometry of the transmitter, missile, and receiver locations
2. attenuation predictions for the directly transmitted power

along line-of-sight or refracted ray trajectories

3. scattering from turbulent fluctuations of electron number density
4. Doppler shift of the directly transmitted and scattered signal

There are two additional aspects of the refracted ray that are not currently included in PRFIC. One is the multipath effect in which rays leaving the transmitter in different directions can arrive at the receiver. The multiple effect can be obtained from PRFIC if enough raypaths are calculated. However, it is not an automated part of the calculation sequence. The second effect is that of focusing the incident energy (see Appendix C). Both of these effects are directly related to the refractive properties of the plume and are absent in a line-of-sight approximation. They are not included in the present, first version of the code. We have no a priori indication of their importance in actual exhaust plume attenuation predictions. Subsequent versions of PRFIC should account for these additional effects and calculations should be made to determine the circumstances for which they are important.

This code has the potential for dealing with many of the variables that affect plume RF interference. With the SPF, we can assess the effects of propellant composition, vehicle size (thrust), and flight conditions. With PRFIC, we can predict the effect of the geometry of transmission (antenna locations), frequency, and turbulence properties. Combined, these capabilities allow a very complete description of several aspects of plume RF interference.

We have given some examples of the predictions by both the SPF and PRFIC. These are included to illustrate their capabilities and limitations. Improvements have been identified. However, the full capability remains to be verified by intensive comparisons with detailed measurements, which we strongly recommend.

REFERENCES

1. Victor, A.C., "Plume-Signal Interference, Part 1. Radar Attenuation," Naval Weapons Center, China Lake, Calif., NWC TP 5319, June 1975.

2. ------. "Plume-Signal Interference, Part 2. Plume-Induced Noise," Naval Weapons Center, China Lake, Calif., NWC TP 5319, May 1972.

3. JANNAF Handbook, Rocket Exhaust Plume Technology, Chapter 4. Plume Electromagnetic Interactions, CPIA Pub. 263, April 1977.

4. Dash, S.M. and Pergament, H.S., "The JANNAF Standard Plume Flowfield Model (SPF)," Aeronautical Research Associates of Princeton, Inc., N.J., A.R.A.P. Report No. 448, April 1981.

5. Khalil, E.E., Spalding, D.B., and Whitelaw, J.H., "The Calculation of Local Flow Properties in Two-Dimensional Furnaces," Int. J. Heat Mass Transfer, Vol. 18, 1975, pp. 775-791.

6. Mitchner, M. and Kruger, C. H., Partially Ionized Gases, John Wiley and Sons, N.Y., 1973, pp. 156-61.

7. Marchand, E. W. , Gradient Index Optics, Academic Press, N.Y., 1978, p. 108.

8. Booker, H.G., and Gordon, W.E., "A Theory of Radio Scattering in the Troposphere," Proceedings of the I.R.E, April 1950, pp. 401-412.

9. Tatarski, V.I., Wave Propagation in a Turbulent Medium, McGraw-Hill, New York, 1961, p. 68.

10. Pergament, H.S., "Assessment and Recommendation of Two-Equation Turbulence Models for Rocket and Aircraft Plume Flowfield Predictions," Naval Weapons Center, China Lake, Calif., NWC TP 6364, July 1982.

11. Molmud, P., "Raybend, a Ray Tracing Program for Microwave Propagation Through Rocket Plumes," JANNAF 12th Plume Trajectory Meeting, U.S. Air Force Academy, Colorado Springs, Nov. 18-20, 1980. also (CPIA Publication 332, December 1980, pp. 273-312.

12. Kerr, D.E., Propagation of Short Radio Waves, McGraw Hill, New York, 1951, pp. 41-44.

Appendix A
USER'S MANUAL

INTRODUCTION

This appendix is the user's manual for the Naval Weapons Center Plume Radar Frequency Interference Code (PRFIC). It documents the code structure and detailed input instructions. Recommended values for those variables that define convergence criteria and number of iterations are given. Sample input and results from test cases are included. The physics involved in the calculations are described in the main text of this report, and the detailed software description is given in Appendix B.

CODE STRUCTURE

Essentially each type of calculation performed in PRFIC is separated into individual subroutines. A flow chart that identifies the subroutines, and the sequence in which they are called, is given in Figure A-1. A complete list of subroutines is given in Table A-1. More complete descriptions of the most important subroutines are given in Appendix B. The input flowfield file with the appropriate variables defining the electrical properties of the plume is obtained from the JANNAF SPF code or an equivalent calculation.

Table A-1. List of Subroutines and Their Function in PRFIC

Subroutine	Function
PRFIAG:	Computes antenna gain
PRFICM:	Common
PRFIDT:	Sets up initial and final points for integration through plume
PRFIEP:	Computes electrical properties
PRFIFF:	Reads flowfield
PRFIIC:	Reads changes for multiple runs
PRFIIN:	Reads input
PRFIIT:	Performs integration through plume

Table A-1. (Continued)

Subroutine	Function
PRFILI:	Linear interpolation
PRFIMM:	Main calling subroutine
PRFIPC:	Computes attenuation and phase constants
PRFIPI:	Computes intersection of line-of-sight with plume
PRFIPL:	Printer plot
PRFIRZ:	Computes plume radius
PRFISC:	Performs volume integration for scattering
DUMP :	Writes input conditions
PDF :	Turbulent velocity probability density function (currently Gaussian)
SCAT :	Computes total scattering cross section
SCALP :	Computes scalar product of two vectors
SFVMV :	Exchanges one-dimensional arrays (system subroutine)

CODE INPUT

A description of each input variable and the instructions for running multiple cases are given in this section. The coordinate system used in the code was shown in Figure 6 of this report. The primary input is listed in Table A-2.

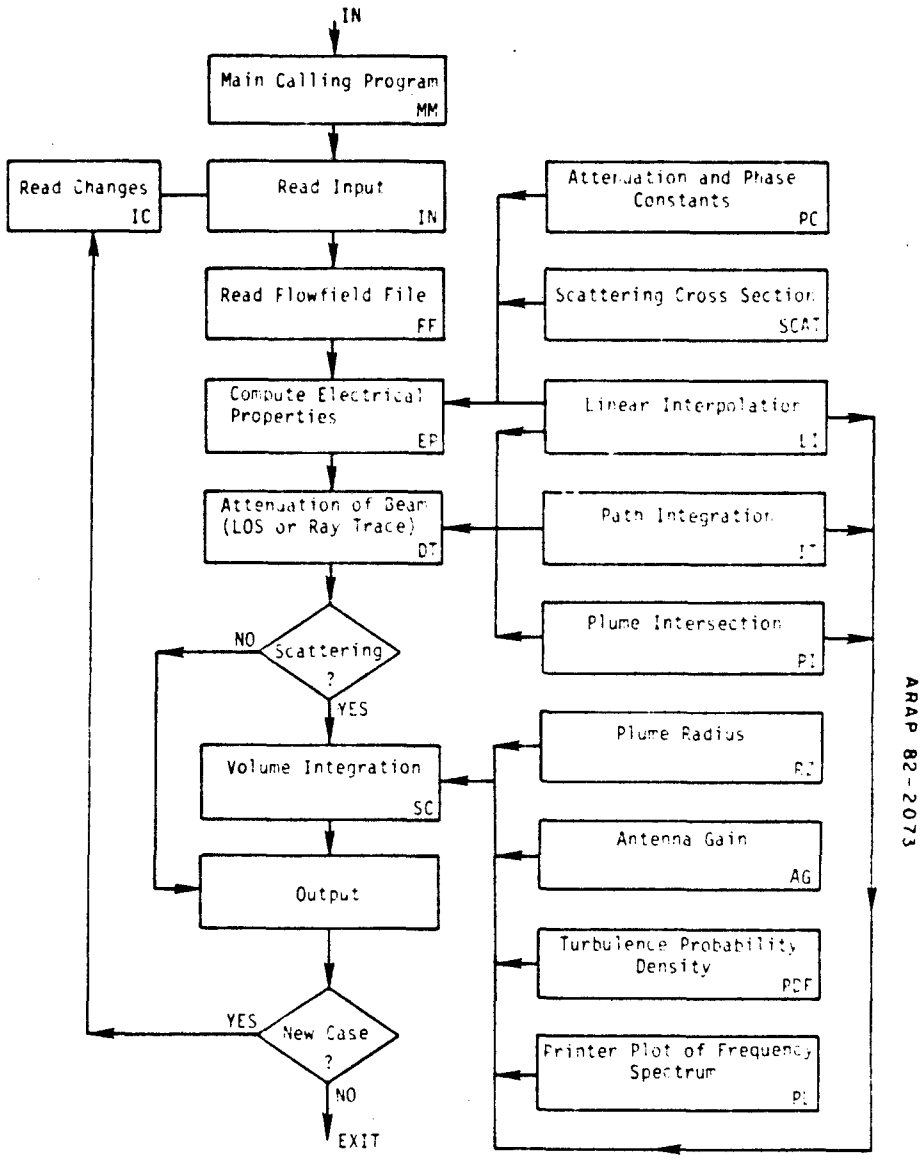

ARAP 82-2073

FIGURE A-1. Structure of the Naval Weapons Center Plume Radar Frequency Interference Code (PRFIC).

Table A-2. Primary Input

Card	Columns	Format	Variable No.	Variable
1	1-20	20A1	-	Flowfield file name, including extension (i.e., FILENAME.DAT)
2	1-72	18A4	-	Title
3	1-10*	E10.3	1	BFREQ, radar frequency, Hz
	11-20	F10.4	2	ZLL, upstream extent of flowfield to be considered. ZLL = 0, the first station on flowfield file is used. ZLL > 0, only Z ≥ ZLL considered.
	21-30	F10.4	3	ZUL, downstream extent of flowfield to be considered. ZUL ≤ 0, the last station on the flowfield file is used. ZUL > 0, only Z ≤ ZUL considered.
4				XT(1),XT(2),XT(3), components of position vector to the radar transmitter, m.
	1-10	F10.4	1	XT(1) - x-component
	11-20	F10.4	2	XT(2) - y-component
	21-30	F10.4	3	XT(3) - z-component

*In this and all subsequent cards, a list-directed input can be used in which the format is ignored and the variables are input in order and separated by commas.

Table A-2. (Continued)

Card	Columns	Format	Variable No.	Variable
5				DCT(1), DCT(2), DCT(3),* Direction of radar transmitter antenna with respect to the x,y,z coordinate system, degrees
	1-10	F10.4	1	DCT(1), angle between antenna direction and x-axis
	1-10	F10.4	2	DCT(2), angle between antenna direction and y-axis
	1-10	F10.4	3	DCT(3), angle between antenna direction and z-axis
6				DCTO(1), DCTO(2),** DCTO(3), Directions of a reference at the transmitter antenna, degrees
	1-10	F10.4	1	DCTO(1), angle between reference direction and x-axis

*See Figure 6 where these angles are called α, β, and γ, respectively. Subscripts, T, R, and M, refer to the transmitter, receiver, and missile. For all sets of these directions, it is necessary that $\cos^2\alpha + \cos^2\beta + \cos^2\gamma = 1$.

**These reference directions, for the transmitter, receiver, and missile, are included for future use (polarization effects, for example); none are used explicitly in the present calculations.

Table A-2. (Continued)

Card	Columns	Format	Variable No.	Variable
	11-10	F10.4	2	DCTO(2), angle between reference direction and y-axis
	21-20	F10.4	3	DCTO(3), angle between reference direction and z-axis
7				VT(1), VT(2), VT(3), components of velocity vector of the radar transmitter, m/s
	1-10	F10.4	1	VT(1) component in x-direction
	11-20	F10.4	2	VT(2) component in y-direction
	21-30	F10.4	3	VT(3) component in z-direction
8				XR(1), XR(2), XR(3) Component of position vector to the receiver, m
	1-10	F10.4	1	XR(1), x-component
	11-20	F10.4	2	XR(2), y-component
	21-30	F10.4	3	XR(3), z-component

Table A-2. (Continued)

Card	Columns	Format	Variable No.	Variable
9				DCR(1), DCR(2), DCR(3), Directions of the radar receiver antenna, degrees
	1-10	F10.4	1	DCR(1), angle between receiver direction and x-axis
	11-20	F10.4	2	DCR(2), angle between receiver direction and y-axis
	21-30	F10.4	3	DCR(3), angle between receiver direction and z-axis
10				DCRO(1), DCRO(2), DCRO(3)
	1-10	F10.4	1	DCTO(1), angle between reference direction and x-axis
	11-20	F10.4	2	DCTO(2), angle between reference direction and y-axis
	21-30	F10.4	3	DCTO(3), angle between reference direction and z-axis
11				VR(1), VR(2), VR(3) Components of velocity vector of radar receiver, m/s
	1-10	F10.4	1	VR(1), x-component
	11-20	F10.4	2	VR(2), y-component
	21-10	F10.4	3	VR(3), z-component

Table A-2. (Continued)

Card	Columns	Format	Variable No.	Variable
12				XM(1), XM(2), XM(3) Components of position vector of missile exit plane, m
	1-10	F10.4	1	XM(1), x-component
	11-20	F10.4	2	XM(2), y-component
	21-10	F10.4	3	XM(3), z-component
				Note: Normally, the missile exit plane is at the origin of the coordinate system so that XM(1) = XM(2) = XM(3) = 0.
13				DCM(1), DCM(2), DCM(3) Angles of normal to the missile exit plane, degrees
	1-10	F10.4	1	DCM(1), angle between normal and x-axis
	11-20	F10.4	2	DCM(2), angle between normal and y-axis
	21-30	F10.4	3	DCM(3), angle between normal and z-axis
				Note: Normally, the missile axis is pointed along the z-axis, so that DCM(1) = DCM(2) = 90 degrees, DCM(3) = 0.
14				DCMO(1), DCMO(2), DCMO(3) Angles of a reference direction at the missile exit plume, degrees

Table A-2. (Continued)

Card	Columns	Format	Variable No.	Variable
	1-10	F10.4	1	DCMO(1), angle between reference and x-axis
	11-20	F10.4	2	DCMO(2), angle between reference and y-axis
	21-30	F10.4	3	DCMO(3), angle between reference and z-axis
15				VM(1), VM(2), VM(3), components of missile velocity vector, m/s
	1-10	F10.4	1	VM(1), component in x-direction
	11-10	F10.4	2	VM(2), component in y-direction
	21-30	F10.4	2	VM(3), component in z-direction
16	1-10	F10.4	1	NCUTS - number of steps used in integration for attenuation along the ray path through the plume (NCUTS ~ 10-40)
	11-20	F10.4	2	RC - overrelaxation factor in ray trace iteration ($0.5 < RC < 1.0$)
	21-30	I10.4	3	NIT - number of iterations allowed in ray trace calculation ($10 \leq NIT \leq 20$)

Table A-2. (Continued)

Card	Columns	Format	Variable No.	Variable
17				EPSA(1), EPSA(2), error criteria for convergence of ray trace iterations, m
	1-10	F10.4	1	EPSA(1) - convergence in the interior of the plume
	11-20	F10.4	2	EPSA(2) - convergence at the receiving antenna EPSA(2) ≤ radius of antenna
18				
	1	L1	1	RAYTR - ray trace option flag. RAYTR = T, ray trace calculation RAYTR = F, line of sight calculation
	2	L1	2	FSCAT - scattering calculation flag. FSCAT = T, radar cross section calculation FSCAT = F, bypass radar cross section calculation Note: if RAYTR = T and FSCAT = T, the radar cross section calculation is also done with the ray trace option.

Table A-2. (Continued)

Card	Columns	Format	Variable No.	Variable
The following arrays specifying antenna gains are not required if FSCAT = F.				
19				
	1-5	I5	1	NANG(1) = Number of angles defining transmitter gain distribution. NANG(1) > 0, read NANG(1) points NANG(1) = 0, uniform gain, 0-90 degreees GAIN(1,J) = 0. NANG(1) < 0, transmitter gain set equal to receiver gain. NANG(1) ≤ 50
	6-10	I5	2	NANG(2) = number of angles defining receiver gain distribution NANG(2) > 0 read NANG(2) points. NANG(2) = 0 uniform gain. 0-90 degrees GAIN(2,J) = 0. NANG(2) < 0 receiver gain set equal to transmitter gain NANG(2) ≤ 50
20	1-80	10F8.0		ANGLE(1,J), J = 1, NANG(1), Angles for transmitter gain, degrees in ascending order
20+	1-80	10F8.0		GAIN(1,J), J = 1, NANG(1), Gain for transmitter, dB

Table A-2. (Continued)

Card	Columns	Format	Variable No.	Variable
20+	1-80	10F8.0		ANGLE(2,J) J = 1, NANG(2), Angles for receiver gain, degrees in ascending order
20+	1-80	10F8.0		GAIN(2,J), J = 1, NANG(2), Gain for receiver, dB

MULTIPLE CASES

The code can accommodate multiple cases for the same flowfield file and antenna gain patterns. That is, multiple cases for which changes occur in cards 3-18 (excluding BFREQ, which occurs on card 3) can be run. Only those variables which change need be specified. The format is given below and also in the FORTRAN Source Code (in PRFIIN).

After the entire set of input for the first card (including antenna gains):

Card	Columns	Format	Variable
1	1	free format	NC = total number of changes for next run
2	1	free format IC, IV, CV,...	IC = card number of change 3 ≤ IC ≤ 18 IV = number of variables on card IC to be changed (excluding IV=1, if IC=3) CV = new value of variable
2			repeat the sequence IC, IV, CV on card 2 or following cards up to NC times.
3			
.			
.			
.			

This sequence is repeated for each subsequent run. However, once the changes are made, they remain in effect until changed again. Also note that if an antenna gain is used, it must be read in the initial data set. The subroutine that reads subsequent cases does not go back to read the gain pattern.

OUTPUT

Page 1. Date, title, and all input quantities. Geometric and velocity inputs are grouped for the transmitter, receiver, and missile.

Page 2. Local and cumulative properties for beam propagation through the plume. If the ray trace option is used, only the final, converged path is printed. The columns are:

X,Y,Z : Position of points along the ray path, in meters beginning at the transmitter and ending at the receiver.

ALPHA, DB : Cumulative attenuation of beam power, in dB.

BETA*L : Cumulative phase along path: $\int_0^s \beta \, ds$.

N : Index of refraction.

ALPHA, 1/M: Local attenuation constant, m^{-1}.

BETA, 1/M : Local phase constant, m^{-1}.

K*LAMBDA : Local product of wavenumber and turbulence macroscale.

SIGMA, 1/M: Local scattering parameter, m^{-1} (that portion independent of angle).

$$\frac{(0.0528)8\pi^3 \, \overline{n_e'^2}/n_e^2 \; n_e^2 \; r_e^2 \; \Lambda^3}{[1 + (\nu_{en}/\omega)^2]^2}$$

U, M/S : Local axial velocity, m/s.

(Q/U)**2 : Local turbulence intensity, normalized by local axial velocity.

These quantities are printed for the beginning and end of the ray path and for the NCUTS-1 points within the plume.

Note: If there is no intersection of the ray path with the plume, or if the angle between the ray and normal to either the transmitter or receiver antenna is greater than 90 degrees, a flag will be printed and no integration will be performed.

A summary of the cumulative attenuation, in dB, and phase for the entire path is given (even if there is no intersection with the plume). Also, a phase difference (actual phase - $2\pi s/\lambda$), where s is the geometric length between the transmitter and receiver, is given. The Doppler shifted frequency of the transmitted ray is printed, in kHz.

Page 3. Listing of transmitter and receiver gain patterns (same as input) if the scattering option is chosen.

Page 4. Frequency spectrum of scattered power. The columns are the number of points; the difference between the shifted frequency and transmitter frequency, in kHz $[(\nu - \nu_0)/1000]$; a normalized frequency shift, $(\nu - \nu_0)c/\nu_0$, and the scattered power, in dB/Hz, referenced to the total transmitter power.

Frequency integrated scattered power, dB. The integral with respect to frequency of the spectral power.

Page 5. A printer plot of the frequency spectrum, dB/Hz, vs. $\nu - \nu_0$, in kHz.

DIAGNOSTICS

There are several built-in diagnostic messages which are printed. They are identified below, along with the subroutine in which they are located.

Subroutine	Message/Meaning/Program Action
PRFIFF:	FLOWFIELD EXCEEDS RADIAL DIMENSION There are more than 50 radial points in the flowfield file; program stops.
PRFIDT:	CO-LOCATED ANTENNAS There is no attenuation path between the transmitter and receiver; computation continues if FSCAT = T.

NO DIRECT PATH TO RECEIVER, S*NT < 0
The ray path is at an angle of more than 90 degrees with respect to the normal to the transmitter antenna; computation continues if FSCAT = T.

NO DIRECT PATH TO RECEIVER, S*NR < 0
The ray path is at an angle of more than 90 degrees with respect to the normal to the receiver antenna; computation continues if FSCAT = T.

IT = MAX, NO CONVERGENCE
The ray trace calculation failed to converge to an error < EPSA*(1) in NIT iterations; program stops.

PRFIPC: PLUME IS LOCALLY OVERDENSE
$(\omega_p/\omega)/(1 + (\nu_{en}/\omega)^2)$ at some point; computation continues.

COMMON PROBLEMS

It is anticipated that most problems will arise in the ray trace option. If a portion of the plume is overdense, there are no rays that can propagate through that region, and a ray trace calculation will not converge. The method of successively computing the curved path from the transmitter towards the receiver until it intersects within a prescribed distance EPSA(2) proved to require many iterations for some paths. The solution requires experience and may depend on relaxing the error criterion. The most sensitive paths were found to be those requiring corrections in two directions (i.e., those paths that were not wholly contained in the plane of symmetry of the plume).

LOGICAL UNIT ASSIGNMENTS

The following logical unit (LUN) assignments are used:

LUN	Assignment
5	Input
6	Output
7	Flowfield file

SAMPLE CASES

Several sample cases are included on the following pages to provide examples of the output for the several options available. In each case, the input file is given, followed by the output. The sample cases are defined in Table A-3.

Table A-3. Sample Cases

Case	Description
1	Line-of-sight calculation, with scattering
2	Ray trace calculation, with scattering
3	Radar cross section calculation
4	Multiple cases, without scattering

```
TESTFF.DAT
TEST CASE NUMBER 1 FOR PRFIC, TRANSVERSE ATTENUATION, LOS OPTION
3.E+10,0.,100.
1.5,5.,20.
90.,180.,90.
90.,0.,90.
0.,0.,0.
1.5,-5.,20.
90.,0.,90.
90.,0.,90.
0.,0.,0.
0.,0.,0.
90.,90.,0.
90.,0.,90.
0.,0.,0.
40.,1.,10
.1,.1
FT
0,0
```

NAVAL WEAPONS CENTER, CHINA LAKE

EXHAUST PLUME RADAR FREQUENCY INTERFERENCE CODE(PRFIC)

WRITTEN BY AERONAUTICAL RESEARCH ASSOCIATES OF PRINCETON

7-SEP-82

TEST CASE NUMBER 1 FOR PRFIC, TRANSVERSE ATTENUATION, LOS OPTION

TRANSMITTER FREQUENCY = 3.000E+01 GHZ
FLOWFIELD FILE = TESTFF.DAT

GEOMETRIC DATA

	TRANSMITTER			RECEIVER			MISSLE		
POSITION, M	X	Y	Z	X	Y	Z	X	Y	Z
	1.500E+00	5.000E+00	2.000E+01	1.500E+00	-5.000E+00	2.000E+01	0.000E+00	0.000E+00	0.000E+00
DIRECTION OF NORMAL, DEG	ALPHA	BETA	GAMMA	ALPHA	BETA	GAMMA	ALPHA	BETA	GAMMA
	9.000E+01	1.800E+02	9.000E+01	9.000E+01	0.000E+00	9.000E+01	9.000E+01	9.000E+01	0.000E+00
REFERENCE DIRECTION, DEG	ALPHA	BETA	GAMMA	ALPHA	BETA	GAMMA	ALPHA	BETA	GAMMA
	9.000E+01	0.000E+00	9.000E+01	9.000E+01	0.000E+00	9.000E+01	9.000E+01	0.000E+00	9.000E+01
VELOCITY COMPONENTS, M/SEC	U	V	W	U	V	W	U	V	W
	0.000E+00	0.000E+00	0.000E+00	0.000E+00	0.000E+00	0.000E+00	0.000E+00	0.000E+00	0.000E+00

RAYTRACE CALCULATION = F
SCATTERING CALCULATION = T

NO. OF STEPS IN INTEGRATION THROUGH PLUME = 4.000E+01
RELAXATION CONSTANT FOR RAYTRACE ITERATION = 1.000E+00
ERROR CRITERIA FOR RAYTRACE CONVERGENCE = 1.000E-01, 1.000E-01
NUMBER OF ITERATIONS IN RAY TRACE = 10
PLUME LENGTH BETWEEN 0.000E+00 AND 1.000E+02 M

PROPERTIES ALONG RAY TRAJECTORY

X,M	Y,M	Z,M	ALPHA,DB	BETA*L	N	ALPHA,1/M	BETA,1/M	K*LAMDA	SIGMA,1/M	U,M/S	(Q/U)**2
1.500E+00	5.000E+00	2.000E+01									
1.500E+00	2.718E+00	2.000E+01	0.000E+00	1.435E+03	1.000E+00	0.000E+00	6.287E+02	7.147E+01	5.784E-10	1.039E+01	4.351E-01
1.500E+00	2.582E+00	2.000E+01	3.837E-13	8.545E+01	1.000E+00	0.000E+00	6.287E+02	1.715E+02	1.750E-09	2.024E+01	1.047E+00
1.500E+00	2.446E+00	2.000E+01	6.686E-13	1.709E+02	1.000E+00	0.000E+00	6.287E+02	3.393E+02	7.900E-09	3.752E+01	2.113E+00
1.500E+00	2.310E+00	2.000E+01	2.551E-10	2.563E+02	1.000E+00	0.000E+00	6.287E+02	4.729E+02	2.556E-05	5.622E+01	2.848E+00
1.500E+00	2.174E+00	2.000E+01	1.196E-09	3.418E+02	1.000E+00	0.000E+00	6.287E+02	5.507E+02	9.353E-05	7.742E+01	3.044E+00
1.500E+00	2.039E+00	2.000E+01	5.709E-09	4.272E+02	1.000E+00	0.000E+00	6.287E+02	5.695E+02	5.579E-04	1.039E+02	2.656E+00
1.500E+00	1.903E+00	2.000E+01	1.869E-08	5.127E+02	1.000E+00	0.000E+00	6.287E+02	5.796E+02	1.383E-03	1.323E+02	2.228E+00
1.500E+00	1.767E+00	2.000E+01	1.180E-07	5.981E+02	1.000E+00	0.000E+00	6.287E+02	5.870E+02	1.397E-02	1.673E+02	1.916E+00
1.500E+00	1.631E+00	2.000E+01	1.814E-06	6.836E+02	1.000E+00	0.000E+00	6.287E+02	5.917E+02	2.527E-01	2.060E+02	1.655E+00
1.500E+00	1.495E+00	2.000E+01	8.866E-06	7.690E+02	1.000E+00	0.000E+00	6.287E+02	5.943E+02	8.645E-01	2.481E+02	1.439E+00
1.500E+00	1.359E+00	2.000E+01	1.242E-04	8.545E+02	1.000E+00	0.000E+00	6.287E+02	5.946E+02	1.746E+01	2.973E+02	1.269E+00
1.500E+00	1.223E+00	2.000E+01	1.549E-03	9.399E+02	1.000E+00	0.000E+00	6.287E+02	5.940E+02	2.086E+02	3.503E+02	1.122E+00
1.500E+00	1.087E+00	2.000E+01	7.061E-03	1.025E+03	1.000E+00	0.000E+00	6.287E+02	5.928E+02	6.627E+02	4.053E+02	9.965E-01
1.500E+00	9.513E-01	2.000E+01	3.591E-02	1.111E+03	1.000E+00	0.000E+00	6.287E+02	5.906E+02	3.866E+03	4.643E+02	8.944E-01
1.500E+00	8.154E-01	2.000E+01	1.566E-01	1.196E+03	9.999E-01	1.123E-02	6.287E+02	5.882E+02	1.390E+04	5.220E+02	8.076E-01
1.500E+00	6.795E-01	2.000E+01	5.349E-01	1.282E+03	9.998E-01	5.457E-02	6.286E+02	5.855E+02	3.853E+04	5.775E+02	7.368E-01
1.500E+00	5.436E-01	2.000E+01	1.549E+00	1.367E+03	9.997E-01	1.408E-01	6.285E+02	5.828E+02	9.907E+04	6.278E+02	6.806E-01
1.500E+00	4.077E-01	2.000E+01	3.958E+00	1.452E+03	9.994E-01	2.548E-01	6.284E+02	5.802E+02	2.309E+05	6.710E+02	6.383E-01
1.500E+00	2.718E-01	2.000E+01	8.114E+00	1.538E+03	9.992E-01	3.456E-01	6.283E+02	5.782E+02	3.418E+05	7.029E+02	6.077E-01
1.500E+00	1.359E-01	2.000E+01	1.384E+01	1.623E+03	9.991E-01	4.208E-01	6.282E+02	5.768E+02	4.480E+05	7.235E+02	5.898E-01
1.500E+00	5.662E-07	2.000E+01	2.058E+01	1.709E+03	9.990E-01	4.461E-01	6.281E+02	5.764E+02	4.837E+05	7.304E+02	5.838E-01
1.500E+00	-1.359E-01	2.000E+01	2.733E+01	1.794E+03	9.991E-01	4.208E-01	6.282E+02	5.768E+02	4.480E+05	7.235E+02	5.898E-01
1.500E+00	-2.718E-01	2.000E+01	3.305E+01	1.879E+03	9.992E-01	3.456E-01	6.283E+02	5.782E+02	3.418E+05	7.029E+02	6.077E-01
1.500E+00	-4.077E-01	2.000E+01	3.721E+01	1.965E+03	9.994E-01	2.548E-01	6.284E+02	5.802E+02	2.309E+05	6.710E+02	6.383E-01
1.500E+00	-5.436E-01	2.000E+01	3.962E+01	2.050E+03	9.997E-01	1.408E-01	6.285E+02	5.828E+02	9.907E+04	6.278E+02	6.806E-01
1.500E+00	-6.795E-01	2.000E+01	4.063E+01	2.136E+03	9.998E-01	5.457E-02	6.286E+02	5.855E+02	3.853E+04	5.775E+02	7.368E-01
1.500E+00	-8.154E-01	2.000E+01	4.101E+01	2.221E+03	9.999E-01	1.123E-02	6.287E+02	5.882E+02	1.390E+04	5.220E+02	8.076E-01
1.500E+00	-9.513E-01	2.000E+01	4.113E+01	2.306E+03	1.000E+00	0.000E+00	6.287E+02	5.906E+02	3.866E+03	4.643E+02	8.944E-01
1.500E+00	-1.087E+00	2.000E+01	4.116E+01	2.392E+03	1.000E+00	0.000E+00	6.287E+02	5.928E+02	6.627E+02	4.053E+02	9.965E-01
1.500E+00	-1.223E+00	2.000E+01	4.116E+01	2.477E+03	1.000E+00	0.000E+00	6.287E+02	5.940E+02	2.086E+02	3.503E+02	1.122E+00
1.500E+00	-1.359E+00	2.000E+01	4.117E+01	2.563E+03	1.000E+00	0.000E+00	6.287E+02	5.946E+02	1.746E+01	2.973E+02	1.269E+00
1.500E+00	-1.495E+00	2.000E+01	4.117E+01	2.648E+03	1.000E+00	0.000E+00	6.287E+02	5.943E+02	8.645E-01	2.481E+02	1.439E+00
1.500E+00	-1.631E+00	2.000E+01	4.117E+01	2.734E+03	1.000E+00	0.000E+00	6.287E+02	5.917E+02	2.527E-01	2.060E+02	1.655E+00
1.500E+00	-1.767E+00	2.000E+01	4.117E+01	2.819E+03	1.000E+00	0.000E+00	6.287E+02	5.870E+02	1.397E-02	1.673E+02	1.916E+00
1.500E+00	-1.903E+00	2.000E+01	4.117E+01	2.905E+03	1.000E+00	0.000E+00	6.287E+02	5.796E+02	1.383E-03	1.323E+02	2.228E+00
1.500E+00	-2.039E+00	2.000E+01	4.117E+01	2.990E+03	1.000E+00	0.000E+00	6.287E+02	5.695E+02	5.579E-04	1.039E+02	2.656E+00
1.500E+00	-2.174E+00	2.000E+01	4.117E+01	3.075E+03	1.000E+00	0.000E+00	6.287E+02	5.507E+02	9.353E-05	7.742E+01	3.044E+00
1.500E+00	-2.310E+00	2.000E+01	4.117E+01	3.161E+03	1.000E+00	0.000E+00	6.287E+02	4.729E+02	2.556E-05	5.622E+01	2.848E+00
1.500E+00	-2.446E+00	2.000E+01	4.117E+01	3.246E+03	1.000E+00	0.000E+00	6.287E+02	3.394E+02	7.900E-09	3.752E+01	2.113E+00
1.500E+00	-2.582E+00	2.000E+01	4.117E+01	3.332E+03	1.000E+00	0.000E+00	6.287E+02	1.715E+02	1.750E-09	2.024E+01	1.047E+00
1.500E+00	-2.718E+00	2.000E+01	4.117E+01	3.417E+03	1.000E+00	0.000E+00	6.287E+02	7.147E+01	5.784E-10	1.039E+01	4.351E-01
1.500E+00	-5.000E+00	2.000E+01	4.117E+01	6.287E+03							

INTERSECTION WITH PLUME= T
ATTENUATION= 41.1665 DB
PHASE= 6.28679E+03
PHASE DIFFERENCE= -5.89844E-01
DOPPLER SHIFTED FREQUENCY= 0.000E+00 KHZ

ANTENNA GAIN PATTERNS

TRANSMITTER

ANGLES,DEG: UNIFORM DISTRIBUTION, GAIN=0. FOR ALL ANGLES

GAIN, DB:

RECEIVER

ANGLES,DEG: UNIFORM DISTRIBUTION, GAIN=0. FOR ALL ANGLES

GAIN, DB:

VOLUME INTEGRATED SCATTERED ENERGY AT DOPPLER-SHIFTED FREQUENCY

N	DF, KHZ	DF*C/BFREQ	SCATTERED POWER, DB/HZ
1	-5.7698E+02	-5.7660E+03	-2.9006E+02
2	-5.5391E+02	-5.5354E+03	-2.8784E+02
3	-5.3083E+02	-5.3047E+03	-2.8568E+02
4	-5.0775E+02	-5.0741E+03	-2.8358E+02
5	-4.8467E+02	-4.8434E+03	-2.8152E+02
6	-4.6159E+02	-4.6128E+03	-2.7950E+02
7	-4.3851E+02	-4.3822E+03	-2.7749E+02
8	-4.1543E+02	-4.1515E+03	-2.7545E+02
9	-3.9235E+02	-3.9209E+03	-2.7328E+02
10	-3.6927E+02	-3.6902E+03	-2.7083E+02
11	-3.4619E+02	-3.4596E+03	-2.6785E+02
12	-3.2311E+02	-3.2290E+03	-2.6399E+02
13	-3.0003E+02	-2.9983E+03	-2.5899E+02
14	-2.7695E+02	-2.7677E+03	-2.5310E+02
15	-2.5387E+02	-2.5370E+03	-2.4699E+02
16	-2.3079E+02	-2.3064E+03	-2.4117E+02
17	-2.0771E+02	-2.0758E+03	-2.3593E+02
18	-1.8464E+02	-1.8451E+03	-2.3138E+02
19	-1.6156E+02	-1.6145E+03	-2.2758E+02
20	-1.3848E+02	-1.3838E+03	-2.2455E+02
21	-1.1540E+02	-1.1532E+03	-2.2231E+02
22	-9.2318E+01	-9.2256E+02	-2.2086E+02
23	-6.9238E+01	-6.9192E+02	-2.2018E+02
24	-4.6159E+01	-4.6128E+02	-2.2026E+02
25	-2.3080E+01	-2.3064E+02	-2.2015E+02
26	-1.6016E-04	-1.6005E-03	-2.1330E+02
27	2.3079E+01	2.3064E+02	-2.1151E+02
28	4.6159E+01	4.6128E+02	-2.1841E+02
29	6.9238E+01	6.9192E+02	-2.2740E+02
30	9.2317E+01	9.2256E+02	-2.2962E+02
31	1.1540E+02	1.1532E+03	-2.3128E+02
32	1.3848E+02	1.3838E+03	-2.3312E+02
33	1.6156E+02	1.6145E+03	-2.3515E+02
34	1.8463E+02	1.8451E+03	-2.3730E+02
35	2.0771E+02	2.0758E+03	-2.3951E+02
36	2.3079E+02	2.3064E+03	-2.4153E+02
37	2.5387E+02	2.5370E+03	-2.3104E+02
38	2.7695E+02	2.7677E+03	-2.4561E+02
39	3.0003E+02	2.9983E+03	-2.4725E+02
40	3.2311E+02	3.2290E+03	-2.4825E+02
41	3.4619E+02	3.4596E+03	-2.4887E+02
42	3.6927E+02	3.6902E+03	-2.4931E+02
43	3.9235E+02	3.9209E+03	-2.4968E+02
44	4.1543E+02	4.1515E+03	-2.5006E+02
45	4.3851E+02	4.3822E+03	-2.5049E+02
46	4.6159E+02	4.6128E+03	-2.5097E+02
47	4.8467E+02	4.8434E+03	-2.5151E+02
48	5.0775E+02	5.0741E+03	-2.5211E+02
49	5.3083E+02	5.3047E+03	-2.5277E+02
50	5.5391E+02	5.5354E+03	-2.5349E+02
51	5.7698E+02	5.7660E+03	-2.5428E+02

FREQUENCY INTEGRATED SCATTERED POWER= -163.660 DB

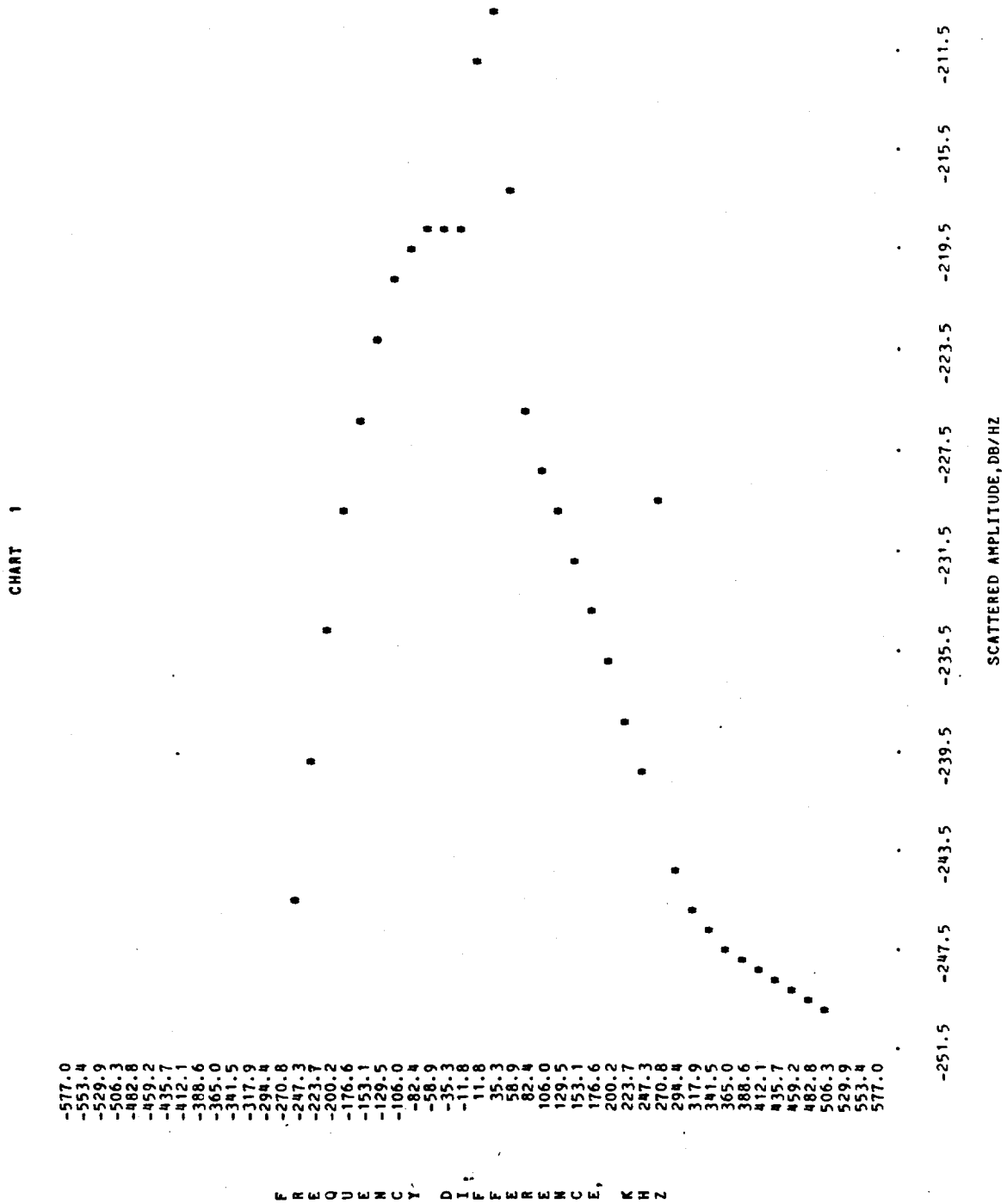
CHART 1
FREQUENCY DIFFERENCE, KHZ
-577.0
-553.4
-529.9
-506.3
-482.8
-459.2
-435.7
-412.1
-388.6
-365.0
-341.5
-317.9
-294.4
-270.8
-247.3
-223.7
-200.2
-176.6
-153.1
-129.5
-106.0
-82.4
-58.9
-35.3
-11.8
11.8
35.3
58.9
82.4
106.0
129.5
153.1
176.6
200.2
223.7
247.3
270.8
294.4
317.9
341.5
365.0
388.6
412.1
435.7
459.2
482.8
506.3
529.9
553.4
577.0
-251.5
-247.5
-243.5
-239.5
-235.5
-231.5
-227.5
-223.5
-219.5
-215.5
-211.5
SCATTERED AMPLITUDE,DB/HZ

```
TESTFF.DAT
TEST CASE NUMBER 2 FOR PRFIC, TRANSVERSE ATTENUATION, RAY TRACE OPTION
3.E+10,0.,100.
1.5,5.,20.
90.,180.,90.
90.,0.,90.
0.,0.,0.
1.5,-5.,20.
90.,0.,90.
90.,0.,90.
0.,0.,0.
0.,0.,0.
90.,90.,0.
90.,0.,90.
0.,0.,0.
40.,1.,10
.1,.1
TT
0,0
```

NAVAL WEAPONS CENTER, CHINA LAKE

EXHAUST PLUME RADAR FREQUENCY INTERFERENCE CODE(PRFIC)

WRITTEN BY AERONAUTICAL RESEARCH ASSOCIATES OF PRINCETON

7-SEP-82

TEST CASE NUMBER 2 FOR PRFIC, TRANSVERSE ATTENUATION, RAY TRACE OPTION

TRANSMITTER FREQUENCY = 3.000E+01 GHZ
FLOWFIELD FILE = TESTFF.DAT

GEOMETRIC DATA

	TRANSMITTER			RECEIVER			MISSLE		
POSITION, M	X	Y	Z	X	Y	Z	X	Y	Z
	1.500E+00	5.000E+00	2.000E+01	1.500E+00	-5.000E+00	2.000E+01	0.000E+00	0.000E+00	0.000E+00
DIRECTION OF NORMAL, DEG	ALPHA	BETA	GAMMA	ALPHA	BETA	GAMMA	ALPHA	BETA	GAMMA
	9.000E+01	1.800E+02	9.000E+01	9.000E+01	0.000E+00	9.000E+01	9.000E+01	9.000E+01	0.000E+00
REFERENCE DIRECTION, DEG	ALPHA	BETA	GAMMA	ALPHA	BETA	GAMMA	ALPHA	BETA	GAMMA
	9.000E+01	0.000E+00	9.000E+01	9.000E+01	0.000E+00	9.000E+01	9.000E+01	0.000E+00	9.000E+01
VELOCITY COMPONENTS, M/SEC	U	V	W	U	V	W	U	V	W
	0.000E+00	0.000E+00	0.000E+00	0.000E+00	0.000E+00	0.000E+00	0.000E+00	0.000E+00	0.000E+00

RAYTRACE CALCULATION = T
SCATTERING CALCULATION = T

NO. OF STEPS IN INTEGRATION THROUGH PLUME = 4.000E+01
RELAXATION CONSTANT FOR RAYTRACE ITERATION = 1.000E+00
ERROR CRITERIA FOR RAYTRACE CONVERGENCE = 1.000E-01, 1.000E-01
NUMBER OF ITERATIONS IN RAY TRACE = 10
PLUME LENGTH BETWEEN 0.000E+00 AND 1.000E+02 M

PROPERTIES ALONG RAY TRAJECTORY

X,M	Y,M	Z,M	ALPHA,DB	BETA*L	N	ALPHA,1/M	BETA,1/M	K*LAMDA	SIGMA,1/M	U,M/S	(Q/U)**2
1.500E+00	5.000E+00	2.000E+01									
1.487E+00	2.725E+00	2.000E+01	0.000E+00	1.430E+03	1.000E+00	0.000E+00	6.287E+02	7.147E+01	5.783E-10	1.039E+01	4.351E-01
1.486E+00	2.589E+00	2.000E+01	3.883E-13	8.594E+01	1.000E+00	0.000E+00	6.287E+02	1.735E+02	1.823E-09	2.045E+01	1.060E+00
1.485E+00	2.452E+00	2.000E+01	6.764E-13	1.719E+02	1.000E+00	0.000E+00	6.287E+02	3.435E+02	8.048E-09	3.794E+01	2.139E+00
1.484E+00	2.315E+00	2.000E+01	2.791E-10	2.578E+02	1.000E+00	0.000E+00	6.287E+02	4.759E+02	2.816E-05	5.703E+01	2.856E+00
1.484E+00	2.178E+00	2.000E+01	1.263E-09	3.438E+02	1.000E+00	0.000E+00	6.287E+02	5.547E+02	9.707E-05	7.853E+01	3.054E+00
1.483E+00	2.042E+00	2.000E+01	6.151E-09	4.297E+02	1.000E+00	0.000E+00	6.287E+02	5.702E+02	6.075E-04	1.058E+02	2.625E+00
1.482E+00	1.905E+00	2.000E+01	2.418E-08	5.157E+02	1.000E+00	0.000E+00	6.287E+02	5.803E+02	2.084E-03	1.352E+02	2.199E+00
1.481E+00	1.768E+00	2.000E+01	1.371E-07	6.016E+02	1.000E+00	0.000E+00	6.287E+02	5.877E+02	1.530E-02	1.709E+02	1.884E+00
1.481E+00	1.632E+00	2.000E+01	2.243E-06	6.875E+02	1.000E+00	0.000E+00	6.287E+02	5.921E+02	3.144E-01	2.113E+02	1.627E+00
1.480E+00	1.495E+00	2.000E+01	2.319E-05	7.735E+02	1.000E+00	0.000E+00	6.287E+02	5.944E+02	2.990E+00	2.554E+02	1.413E+00
1.479E+00	1.358E+00	2.000E+01	1.711E-04	8.594E+02	1.000E+00	0.000E+00	6.287E+02	5.947E+02	2.038E+01	3.058E+02	1.240E+00
1.478E+00	1.222E+00	2.000E+01	2.102E-03	9.454E+02	1.000E+00	0.000E+00	6.287E+02	5.938E+02	2.840E+02	3.619E+02	1.095E+00
1.477E+00	1.085E+00	2.000E+01	1.246E-02	1.031E+03	1.000E+00	0.000E+00	6.287E+02	5.923E+02	1.341E+03	4.201E+02	9.699E-01
1.477E+00	9.483E-01	2.000E+01	5.197E-02	1.117E+03	9.999E-01	0.000E+00	6.287E+02	5.900E+02	4.817E+03	4.809E+02	8.661E-01
1.476E+00	8.116E-01	2.000E+01	2.504E-01	1.203E+03	9.999E-01	2.772E-02	6.287E+02	5.872E+02	2.327E+04	5.431E+02	7.807E-01
1.475E+00	6.749E-01	2.000E+01	8.281E-01	1.289E+03	9.998E-01	8.651E-02	6.286E+02	5.843E+02	5.474E+04	6.010E+02	7.092E-01
1.474E+00	5.382E-01	2.000E+01	2.573E+00	1.375E+03	9.995E-01	2.128E-01	6.284E+02	5.811E+02	1.824E+05	6.551E+02	6.539E-01
1.474E+00	4.015E-01	2.000E+01	6.273E+00	1.461E+03	9.993E-01	3.331E-01	6.283E+02	5.784E+02	3.241E+05	6.995E+02	6.106E-01
1.473E+00	2.648E-01	2.000E+01	1.229E+01	1.547E+03	9.990E-01	4.589E-01	6.281E+02	5.762E+02	5.018E+05	7.338E+02	5.807E-01
1.473E+00	1.282E-01	2.000E+01	2.146E+01	1.633E+03	9.987E-01	5.771E-01	6.279E+02	5.746E+02	7.620E+05	7.554E+02	5.637E-01
1.473E+00	-8.538E-03	2.000E+01	3.310E+01	1.718E+03	9.986E-01	6.154E-01	6.279E+02	5.741E+02	8.498E+05	7.620E+02	5.586E-01
1.473E+00	-1.452E-01	2.000E+01	4.454E+01	1.804E+03	9.987E-01	5.646E-01	6.279E+02	5.748E+02	7.334E+05	7.533E+02	5.654E-01
1.474E+00	-2.819E-01	2.000E+01	5.334E+01	1.890E+03	9.990E-01	4.440E-01	6.281E+02	5.764E+02	4.808E+05	7.298E+02	5.843E-01
1.475E+00	-4.186E-01	2.000E+01	5.904E+01	1.976E+03	9.993E-01	3.148E-01	6.283E+02	5.788E+02	3.004E+05	6.937E+02	6.160E-01
1.476E+00	-5.553E-01	2.000E+01	6.240E+01	2.062E+03	9.996E-01	1.933E-01	6.285E+02	5.816E+02	1.598E+05	6.477E+02	6.612E-01
1.477E+00	-6.920E-01	2.000E+01	6.393E+01	2.148E+03	9.998E-01	7.257E-02	6.286E+02	5.848E+02	4.787E+04	5.925E+02	7.187E-01
1.478E+00	-8.287E-01	2.000E+01	6.442E+01	2.234E+03	9.999E-01	2.052E-02	6.287E+02	5.876E+02	1.918E+04	5.339E+02	7.924E-01
1.479E+00	-9.654E-01	2.000E+01	6.459E+01	2.320E+03	1.000E+00	0.000E+00	6.287E+02	5.904E+02	4.311E+03	4.721E+02	8.812E-01
1.480E+00	-1.102E+00	2.000E+01	6.462E+01	2.406E+03	1.000E+00	0.000E+00	6.287E+02	5.926E+02	7.836E+02	4.104E+02	9.865E-01
1.482E+00	-1.239E+00	2.000E+01	6.463E+01	2.492E+03	1.000E+00	0.000E+00	6.287E+02	5.940E+02	2.266E+02	3.531E+02	1.116E+00
1.483E+00	-1.375E+00	2.000E+01	6.463E+01	2.578E+03	1.000E+00	0.000E+00	6.287E+02	5.947E+02	1.775E+01	2.982E+02	1.266E+00
1.484E+00	-1.512E+00	2.000E+01	6.463E+01	2.663E+03	1.000E+00	0.000E+00	6.287E+02	5.943E+02	8.510E-01	2.476E+02	1.441E+00
1.485E+00	-1.649E+00	2.000E+01	6.463E+01	2.749E+03	1.000E+00	0.000E+00	6.287E+02	5.917E+02	2.356E-01	2.045E+02	1.663E+00
1.487E+00	-1.785E+00	2.000E+01	6.463E+01	2.835E+03	1.000E+00	0.000E+00	6.287E+02	5.866E+02	1.325E-02	1.653E+02	1.933E+00
1.488E+00	-1.922E+00	2.000E+01	6.463E+01	2.921E+03	1.000E+00	0.000E+00	6.287E+02	5.788E+02	1.275E-03	1.300E+02	2.255E+00
1.489E+00	-2.059E+00	2.000E+01	6.463E+01	3.007E+03	1.000E+00	0.000E+00	6.287E+02	5.685E+02	4.908E-04	1.013E+02	2.696E+00
1.490E+00	-2.196E+00	2.000E+01	6.463E+01	3.093E+03	1.000E+00	0.000E+00	6.287E+02	5.424E+02	8.629E-05	7.516E+01	3.023E+00
1.492E+00	-2.332E+00	2.000E+01	6.463E+01	3.179E+03	1.000E+00	0.000E+00	6.287E+02	4.633E+02	1.717E-05	5.360E+01	2.824E+00
1.493E+00	-2.469E+00	2.000E+01	6.463E+01	3.265E+03	1.000E+00	0.000E+00	6.287E+02	3.167E+02	7.069E-09	3.519E+01	1.969E+00
1.494E+00	-2.606E+00	2.000E+01	6.463E+01	3.351E+03	1.000E+00	0.000E+00	6.287E+02	1.519E+02	1.229E-09	1.826E+01	9.248E-01
1.496E+00	-2.742E+00	2.000E+01	6.463E+01	3.437E+03	1.000E+00	0.000E+00	6.287E+02	5.620E+01	4.548E-10	8.893E+00	3.421E-01
1.500E+00	-5.000E+00	2.000E+01	6.463E+01	6.287E+03							

INTERSECTION WITH PLUME= T
ATTENUATION= 64.6278 DB
PHASE= 6.28668E+03
PHASE DIFFERENCE= -6.93848E-01
DOPPLER SHIFTED FREQUENCY= 0.000E+00 KHZ

ANTENNA GAIN PATTERNS

TRANSMITTER

ANGLES,DEG:

UNIFORM DISTRIBUTION, GAIN=0. FOR ALL ANGLES

GAIN, DB:

RECEIVER

ANGLES,DEG:

UNIFORM DISTRIBUTION, GAIN=0. FOR ALL ANGLES

GAIN, DB:

VOLUME INTEGRATED SCATTERED ENERGY AT DOPPLER-SHIFTED FREQUENCY

N	DF, KHZ	DF*C/BFREQ	SCATTERED POWER, DB/HZ
1	-5.7698E+02	-5.7660E+03	-3.6843E+02
2	-5.5391E+02	-5.5354E+03	-3.5933E+02
3	-5.3083E+02	-5.3047E+03	-3.5073E+02
4	-5.0775E+02	-5.0741E+03	-3.4257E+02
5	-4.8467E+02	-4.8434E+03	-3.3485E+02
6	-4.6159E+02	-4.6128E+03	-3.2757E+02
7	-4.3851E+02	-4.3822E+03	-3.2073E+02
8	-4.1543E+02	-4.1515E+03	-3.1432E+02
9	-3.9235E+02	-3.9209E+03	-3.0836E+02
10	-3.6927E+02	-3.6902E+03	-3.0282E+02
11	-3.4619E+02	-3.4596E+03	-2.9773E+02
12	-3.2311E+02	-3.2290E+03	-2.9306E+02
13	-3.0003E+02	-2.9983E+03	-2.8884E+02
14	-2.7695E+02	-2.7677E+03	-2.8505E+02
15	-2.5387E+02	-2.5370E+03	-2.8169E+02
16	-2.3079E+02	-2.3064E+03	-2.7877E+02
17	-2.0771E+02	-2.0758E+03	-2.7628E+02
18	-1.8464E+02	-1.8451E+03	-2.7423E+02
19	-1.6156E+02	-1.6145E+03	-2.7262E+02
20	-1.3848E+02	-1.3838E+03	-2.7145E+02
21	-1.1540E+02	-1.1532E+03	-2.7073E+02
22	-9.2318E+01	-9.2256E+02	-2.7041E+02
23	-6.9238E+01	-6.9192E+02	-2.6960E+02
24	-4.6159E+01	-4.6128E+02	-2.6609E+02
25	-2.3080E+01	-2.3064E+02	-2.6328E+02
26	-1.6016E-04	-1.6005E-03	-2.4463E+02
27	2.3079E+01	2.3064E+02	-2.6966E+02
28	4.6159E+01	4.6128E+02	-2.7665E+02
29	6.9238E+01	6.9192E+02	-2.8108E+02
30	9.2317E+01	9.2256E+02	-2.8451E+02
31	1.1540E+02	1.1532E+03	-2.8828E+02
32	1.3848E+02	1.3838E+03	-2.9249E+02
33	1.6156E+02	1.6145E+03	-2.9713E+02
34	1.8463E+02	1.8451E+03	-3.0222E+02
35	2.0771E+02	2.0758E+03	-3.0774E+02
36	2.3079E+02	2.3064E+03	-3.1369E+02
37	2.5387E+02	2.5370E+03	-3.2007E+02
38	2.7695E+02	2.7677E+03	-3.2689E+02
39	3.0003E+02	2.9983E+03	-3.3415E+02
40	3.2311E+02	3.2290E+03	-3.4184E+02
41	3.4619E+02	3.4596E+03	-3.4996E+02
42	3.6927E+02	3.6902E+03	-3.5852E+02
43	3.9235E+02	3.9209E+03	-3.6754E+02
44	4.1543E+02	4.1515E+03	-3.7697E+02
45	4.3851E+02	4.3822E+03	-3.8000E+02
46	4.6159E+02	4.6128E+03	-3.8000E+02
47	4.8467E+02	4.8434E+03	-3.8000E+02
48	5.0775E+02	5.0741E+03	-3.8000E+02
49	5.3083E+02	5.3047E+03	-3.8000E+02
50	5.5391E+02	5.5354E+03	-3.8000E+02
51	5.7698E+02	5.7660E+03	-3.8000E+02

FREQUENCY INTEGRATED SCATTERED POWER= -203.328 DB

CHART 1

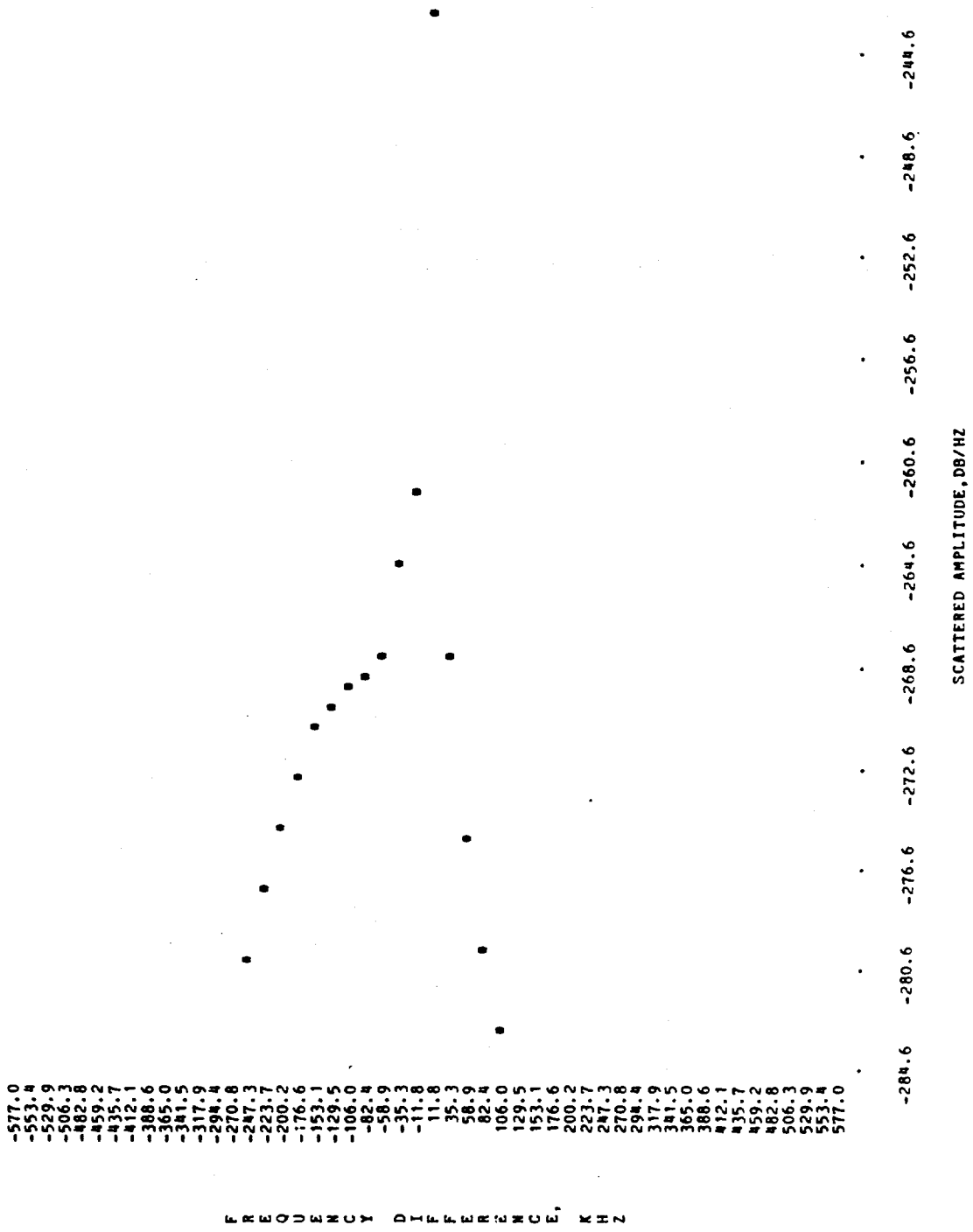
-577.0
-553.4
-529.9
-506.3
-482.8
-459.2
-435.7
-412.1
-388.6
-365.0
-341.5
-317.9
-294.4
-270.8
-247.3
-223.7
-200.2
-176.6
-153.1
-129.5
-106.0
-82.4
-58.9
-35.3
-11.8
11.8
35.3
58.9
82.4
106.0
129.5
153.1
176.6
200.2
223.7
247.3
270.8
294.4
317.9
341.5
365.0
388.6
412.1
435.7
459.2
482.8
506.3
529.9
553.4
577.0
FREQUENCY DIFFERENCE, KHZ
-284.6
-280.6
-276.6
-272.6
-268.6
-264.6
-260.6
-256.6
-252.6
-248.6
-244.6
SCATTERED AMPLITUDE, DB/HZ

```
TESTFF.DAT
TEST CASE NUMBER 3 FOR PRFIC, RADAR CROSS SECTION FROM BROADSIDE
3.E+10,0.,100.
0.,50.,50.
90.,180.,90.
90.,0.,90.
0.,0.,0.
0.,50.,50.
90.,180.,90.
90.,0.,90.
0.,0.,0.
0.,0.,0.
90.,90.,0.
90.,0.,90.
0.,0.,0.
40.,1.,10
.1,.1
FT
12,-1
0.,2.,4.,6.,8.,10.,12.,14.,16.,18.,
20.,22.
40.,35.,30.,25.,20.,15.,10.,5.,0.,-5.,
-10.,-15.
```

NAVAL WEAPONS CENTER, CHINA LAKE

EXHAUST PLUME RADAR FREQUENCY INTERFERENCE CODE(PRFIC)

WRITTEN BY AERONAUTICAL RESEARCH ASSOCIATES OF PRINCETON

8-SEP-82

TEST CASE NUMBER 3 FOR PRFIC, RADAR CROSS SECTION FROM BROADSIDE

TRANSMITTER FREQUENCY = 3.000E+01 GHZ
FLOWFIELD FILE = TESTFF.DAT

GEOMETRIC DATA

	TRANSMITTER			RECEIVER			MISSLE		
POSITION, M	X	Y	Z	X	Y	Z	X	Y	Z
	0.000E+00	5.000E+01	5.000E+01	0.000E+00	5.000E+01	5.000E+01	0.000E+00	0.000E+00	0.000E+00
DIRECTION OF NORMAL, DEG	ALPHA	BETA	GAMMA	ALPHA	BETA	GAMMA	ALPHA	BETA	GAMMA
	9.000E+01	1.800E+02	9.000E+01	9.000E+01	1.800E+02	9.000E+01	9.000E+01	9.000E+01	0.000E+00
REFERENCE DIRECTION, DEG	ALPHA	BETA	GAMMA	ALPHA	BETA	GAMMA	ALPHA	BETA	GAMMA
	9.000E+01	0.000E+00	9.000E+01	9.000E+01	0.000E+00	9.000E+01	9.000E+01	0.000E+00	9.000E+01
VELOCITY COMPONENTS, M/SEC	U	V	W	U	V	W	U	V	W
	0.000E+00	0.000E+00	0.000E+00	0.000E+00	0.000E+00	0.000E+00	0.000E+00	0.000E+00	0.000E+00

RAYTRACE CALCULATION = F
SCATTERING CALCULATION = T

NO. OF STEPS IN INTEGRATION THROUGH PLUME = 4.000E+01
RELAXATION CONSTANT FOR RAYTRACE ITERATION = 1.000E+00
ERROR CRITERIA FOR RAYTRACE CONVERGENCE = 1.000E-01, 1.000E-01
NUMBER OF ITERATIONS IN RAY TRACE = 10
PLUME LENGTH BETWEEN 0.000E+00 AND 1.000E+02 M

PROPERTIES ALONG RAY TRAJECTORY

X,M	Y,M	Z,M	ALPHA,DB	BETA*L	N	ALPHA,1/M	BETA,1/M	K*LAMDA	SIGMA,1/M	U,M/S	(Q/U)**2

COLOCATED ANTENNAS

INTERSECTION WITH PLUME= F
ATTENUATION= 0.0000 DB
PHASE= 0.00000E+00
PHASE DIFFERENCE= 0.00000E+00
DOPPLER SHIFTED FREQUENCY= 0.000E+00 KHZ

ANTENNA GAIN PATTERNS

TRANSMITTER

ANGLES, DEG:	0.00	2.00	4.00	6.00	8.00	10.00	12.00	14.00	16.00	18.00
	20.00	22.00								
GAIN, DB:	40.00	35.00	30.00	25.00	20.00	15.00	10.00	5.00	0.00	-5.00
	-10.00	-15.00								

RECEIVER

ANGLES, DEG:	0.00	2.00	4.00	6.00	8.00	10.00	12.00	14.00	16.00	18.00
	20.00	22.00								
GAIN, DB:	40.00	35.00	30.00	25.00	20.00	15.00	10.00	5.00	0.00	-5.00
	-10.00	-15.00								

VOLUME INTEGRATED SCATTERED ENERGY AT DOPPLER-SHIFTED FREQUENCY

N	DF, KHZ	DF*C/BFREQ	SCATTERED POWER, DB/HZ
1	-5.7698E+02	-5.7660E+03	-3.2992E+02
2	-5.5391E+02	-5.5354E+03	-3.2801E+02
3	-5.3083E+02	-5.3047E+03	-3.2613E+02
4	-5.0775E+02	-5.0741E+03	-3.2421E+02
5	-4.8467E+02	-4.8434E+03	-3.2214E+02
6	-4.6159E+02	-4.6128E+03	-3.1965E+02
7	-4.3851E+02	-4.3822E+03	-3.1644E+02
8	-4.1543E+02	-4.1515E+03	-3.1247E+02
9	-3.9235E+02	-3.9209E+03	-3.0801E+02
10	-3.6927E+02	-3.6902E+03	-3.0339E+02
11	-3.4619E+02	-3.4596E+03	-2.9885E+02
12	-3.2311E+02	-3.2290E+03	-2.9449E+02
13	-3.0003E+02	-2.9983E+03	-2.9038E+02
14	-2.7695E+02	-2.7677E+03	-2.8652E+02
15	-2.5387E+02	-2.5370E+03	-2.8294E+02
16	-2.3079E+02	-2.3064E+03	-2.7963E+02
17	-2.0771E+02	-2.0758E+03	-2.7659E+02
18	-1.8464E+02	-1.8451E+03	-2.7384E+02
19	-1.6156E+02	-1.6145E+03	-2.7136E+02
20	-1.3848E+02	-1.3838E+03	-2.6916E+02
21	-1.1540E+02	-1.1532E+03	-2.6724E+02
22	-9.2318E+01	-9.2256E+02	-2.6560E+02
23	-6.9238E+01	-6.9192E+02	-2.6423E+02
24	-4.6159E+01	-4.6128E+02	-2.6315E+02
25	-2.3080E+01	-2.3064E+02	-2.6233E+02
26	-1.6016E-04	-1.6005E-03	-1.8543E+02
27	2.3079E+01	2.3064E+02	-2.6156E+02
28	4.6159E+01	4.6128E+02	-2.6160E+02
29	6.9238E+01	6.9192E+02	-2.6191E+02
30	9.2317E+01	9.2256E+02	-2.6249E+02
31	1.1540E+02	1.1532E+03	-2.6336E+02
32	1.3848E+02	1.3838E+03	-2.6451E+02
33	1.6156E+02	1.6145E+03	-2.6593E+02
34	1.8463E+02	1.8451E+03	-2.6763E+02
35	2.0771E+02	2.0758E+03	-2.6961E+02
36	2.3079E+02	2.3064E+03	-2.7187E+02
37	2.5387E+02	2.5370E+03	-2.7440E+02
38	2.7695E+02	2.7677E+03	-2.7720E+02
39	3.0003E+02	2.9983E+03	-2.8026E+02
40	3.2311E+02	3.2290E+03	-2.8357E+02
41	3.4619E+02	3.4596E+03	-2.8706E+02
42	3.6927E+02	3.6902E+03	-2.9064E+02
43	3.9235E+02	3.9209E+03	-2.9409E+02
44	4.1543E+02	4.1515E+03	-2.9706E+02
45	4.3851E+02	4.3822E+03	-2.9927E+02
46	4.6159E+02	4.6128E+03	-3.0077E+02
47	4.8467E+02	4.8434E+03	-3.0183E+02
48	5.0775E+02	5.0741E+03	-3.0271E+02
49	5.3083E+02	5.3047E+03	-3.0356E+02
50	5.5391E+02	5.5354E+03	-3.0443E+02
51	5.7698E+02	5.7660E+03	-3.0535E+02

FREQUENCY INTEGRATED SCATTERED POWER= -154.200 DB

CHART 1

FREQUENCY DIFFERENCE, KHZ

-577.0
-553.4
-529.9
-506.3
-482.8
-459.2
-435.7
-412.1
-388.6
-365.0
-341.5
-317.9
-294.4
-270.8
-247.3
-223.7
-200.2
-176.6
-153.1
-129.5
-106.0
-82.4
-58.9
-35.3
-11.8
11.8
35.3
58.9
82.4
106.0
129.5
153.1
176.6
200.2
223.7
247.3
270.8
294.4
317.9
341.5
365.0
388.6
412.1
435.7
459.2
482.8
506.3
529.9
553.4
577.0

-225.4 -221.4 -217.4 -213.4 -209.4 -205.4 -201.4 -197.4 -193.4 -189.4 -185.4

SCATTERED AMPLITUDE, DB/HZ

```
TESTFF.DAT
TEST CASE NUMBER 4 FOR PRFIC, MULTIPLE CASES, TRANSVERSE ATTENUATION
3.E+10,0.,100.
.5,5.,20.
90.,180.,90.
90.,0.,90.
0.,0.,0.
.5,-5.,20.
90.,0.,90.
90.,0.,90.
0.,0.,0.
0.,0.,0.
90.,90.,0.
90.,0.,90.
0.,0.,0.
40.,1.,10
.1,.1
FF
2
4,1,1.
8,1,1.
2
4,1,1.5
8,1,1.5
```

NAVAL WEAPONS CENTER, CHINA LAKE

EXHAUST PLUME RADAR FREQUENCY INTERFERENCE CODE(PRFIC)

WRITTEN BY AERONAUTICAL RESEARCH ASSOCIATES OF PRINCETON

7-SEP-82

TEST CASE NUMBER 4 FOR PRFIC, MULTIPLE CASES, TRANSVERSE ATTENUATION

TRANSMITTER FREQUENCY = 3.000E+01 GHZ
FLOWFIELD FILE = TESTFF.DAT

GEOMETRIC DATA

	TRANSMITTER			RECEIVER			MISSLE		
POSITION, M	X	Y	Z	X	Y	Z	X	Y	Z
	5.000E-01	5.000E+00	2.000E+01	5.000E-01	-5.000E+00	2.000E+01	0.000E+00	0.000E+00	0.000E+00
DIRECTION OF	ALPHA	BETA	GAMMA	ALPHA	BETA	GAMMA	ALPHA	BETA	GAMMA
NORMAL, DEG	9.000E+01	1.800E+02	9.000E+01	9.000E+01	0.000E+00	9.000E+01	9.000E+01	9.000E+01	0.000E+00
REFERENCE	ALPHA	BETA	GAMMA	ALPHA	BETA	GAMMA	ALPHA	BETA	GAMMA
DIRECTION, DEG	9.000E+01	0.000E+00	9.000E+01	9.000E+01	0.000E+00	9.000E+01	9.000E+01	0.000E+00	9.000E+01
VELOCITY	U	V	W	U	V	W	U	V	W
COMPONENTS, M/SEC	0.000E+00	0.000E+00	0.000E+00	0.000E+00	0.000E+00	0.000E+00	0.000E+00	0.000E+00	0.000E+00

RAYTRACE CALCULATION = F
SCATTERING CALCULATION = F

NO. OF STEPS IN INTEGRATION THROUGH PLUME = 4.000E+01
RELAXATION CONSTANT FOR RAYTRACE ITERATION = 1.000E+00
ERROR CRITERIA FOR RAYTRACE CONVERGENCE = 1.000E-01, 1.000E-01
NUMBER OF ITERATIONS IN RAY TRACE = 10
PLUME LENGTH BETWEEN 0.000E+00 AND 1.000E+02 M

PROPERTIES ALONG RAY TRAJECTORY

X,M	Y,M	Z,M	ALPHA,DB	BETA*L	N	ALPHA,1/M	BETA,1/M	K*LAMDA	SIGMA,1/M	U,M/S	(Q/U)**2
5.000E-01	5.000E+00	2.000E+01									
5.000E-01	3.064E+00	2.000E+01	0.000E+00	1.217E+03	1.000E+00	0.000E+00	6.287E+02	7.147E+01	5.784E-10	1.039E+01	4.351E-01
5.000E-01	2.911E+00	2.000E+01	4.658E-13	9.632E+01	1.000E+00	0.000E+00	6.287E+02	2.187E+02	3.480E-09	2.510E+01	1.347E+00
5.000E-01	2.758E+00	2.000E+01	7.992E-13	1.926E+02	1.000E+00	0.000E+00	6.287E+02	4.357E+02	1.143E-08	4.743E+01	2.724E+00
5.000E-01	2.604E+00	2.000E+01	7.422E-10	2.890E+02	1.000E+00	0.000E+00	6.287E+02	5.436E+02	8.734E-05	7.549E+01	3.026E+00
5.000E-01	2.451E+00	2.000E+01	7.253E-09	3.853E+02	1.000E+00	0.000E+00	6.287E+02	5.722E+02	7.532E-04	1.114E+02	2.537E+00
5.000E-01	2.298E+00	2.000E+01	8.458E-08	4.816E+02	1.000E+00	0.000E+00	6.287E+02	5.846E+02	9.751E-03	1.559E+02	2.017E+00
5.000E-01	2.145E+00	2.000E+01	2.442E-06	5.779E+02	1.000E+00	0.000E+00	6.287E+02	5.921E+02	3.195E-01	2.117E+02	1.625E+00
5.000E-01	1.992E+00	2.000E+01	9.079E-05	6.742E+02	1.000E+00	0.000E+00	6.287E+02	5.945E+02	1.213E+01	2.819E+02	1.322E+00
5.000E-01	1.838E+00	2.000E+01	2.575E-03	7.706E+02	1.000E+00	0.000E+00	6.287E+02	5.936E+02	3.370E+02	3.700E+02	1.076E+00
5.000E-01	1.685E+00	2.000E+01	3.873E-02	8.669E+02	9.999E-01	0.000E+00	6.287E+02	5.901E+02	4.687E+03	4.787E+02	8.699E-01
5.000E-01	1.532E+00	2.000E+01	6.071E-01	9.632E+02	9.997E-01	1.038E-01	6.286E+02	5.837E+02	6.325E+04	6.114E+02	6.976E-01
5.000E-01	1.379E+00	2.000E+01	8.828E+00	1.059E+03	9.985E-01	6.594E-01	6.278E+02	5.735E+02	9.505E+05	7.696E+02	5.528E-01
5.000E-01	1.226E+00	2.000E+01	6.208E+01	1.155E+03	9.948E-01	2.246E+00	6.255E+02	5.583E+02	5.477E+06	9.507E+02	4.305E-01
5.000E-01	1.072E+00	2.000E+01	2.357E+02	1.251E+03	9.880E-01	5.082E+00	6.212E+02	5.372E+02	1.435E+07	1.152E+03	3.295E-01
5.000E-01	9.192E-01	2.000E+01	5.363E+02	1.346E+03	9.823E-01	7.493E+00	6.176E+02	5.124E+02	1.753E+07	1.367E+03	2.476E-01
5.000E-01	7.660E-01	2.000E+01	8.385E+02	1.440E+03	9.825E-01	7.468E+00	6.177E+02	4.860E+02	1.175E+07	1.588E+03	1.815E-01
5.000E-01	6.128E-01	2.000E+01	1.032E+03	1.535E+03	9.874E-01	5.415E+00	6.208E+02	4.574E+02	5.002E+06	1.803E+03	1.294E-01
5.000E-01	4.596E-01	2.000E+01	1.118E+03	1.631E+03	9.927E-01	3.195E+00	6.241E+02	4.258E+02	1.493E+06	1.999E+03	8.970E-02
5.000E-01	3.064E-01	2.000E+01	1.149E+03	1.726E+03	9.959E-01	1.793E+00	6.262E+02	3.928E+02	4.047E+05	2.157E+03	6.174E-02
5.000E-01	1.532E-01	2.000E+01	1.160E+03	1.822E+03	9.975E-01	1.136E+00	6.271E+02	3.655E+02	1.309E+05	2.260E+03	4.496E-02
5.000E-01	-1.788E-07	2.000E+01	1.165E+03	1.919E+03	9.979E-01	9.541E-01	6.274E+02	3.544E+02	8.246E+04	2.296E+03	3.933E-02
5.000E-01	-1.532E-01	2.000E+01	1.171E+03	2.015E+03	9.975E-01	1.136E+00	6.271E+02	3.655E+02	1.309E+05	2.260E+03	4.496E-02
5.000E-01	-3.064E-01	2.000E+01	1.182E+03	2.111E+03	9.959E-01	1.793E+00	6.262E+02	3.928E+02	4.047E+05	2.157E+03	6.174E-02
5.000E-01	-4.596E-01	2.000E+01	1.212E+03	2.206E+03	9.927E-01	3.195E+00	6.241E+02	4.258E+02	1.493E+06	1.999E+03	8.970E-02
5.000E-01	-6.128E-01	2.000E+01	1.299E+03	2.302E+03	9.874E-01	5.415E+00	6.208E+02	4.574E+02	5.002E+06	1.803E+03	1.294E-01
5.000E-01	-7.660E-01	2.000E+01	1.492E+03	2.397E+03	9.825E-01	7.468E+00	6.177E+02	4.860E+02	1.175E+07	1.588E+03	1.815E-01
5.000E-01	-9.192E-01	2.000E+01	1.794E+03	2.491E+03	9.823E-01	7.493E+00	6.176E+02	5.124E+02	1.753E+07	1.367E+03	2.476E-01
5.000E-01	-1.072E+00	2.000E+01	2.095E+03	2.586E+03	9.880E-01	5.082E+00	6.212E+02	5.372E+02	1.435E+07	1.152E+03	3.295E-01
5.000E-01	-1.226E+00	2.000E+01	2.268E+03	2.682E+03	9.948E-01	2.246E+00	6.255E+02	5.583E+02	5.477E+06	9.507E+02	4.305E-01
5.000E-01	-1.379E+00	2.000E+01	2.322E+03	2.778E+03	9.985E-01	6.594E-01	6.278E+02	5.735E+02	9.505E+05	7.696E+02	5.528E-01
5.000E-01	-1.532E+00	2.000E+01	2.330E+03	2.874E+03	9.997E-01	1.038E-01	6.286E+02	5.837E+02	6.325E+04	6.114E+02	6.976E-01
5.000E-01	-1.685E+00	2.000E+01	2.330E+03	2.970E+03	9.999E-01	0.000E+00	6.287E+02	5.901E+02	4.687E+03	4.787E+02	8.699E-01
5.000E-01	-1.838E+00	2.000E+01	2.330E+03	3.066E+03	1.000E+00	0.000E+00	6.287E+02	5.936E+02	3.370E+02	3.700E+02	1.076E+00
5.000E-01	-1.992E+00	2.000E+01	2.330E+03	3.163E+03	1.000E+00	0.000E+00	6.287E+02	5.945E+02	1.213E+01	2.819E+02	1.322E+00
5.000E-01	-2.145E+00	2.000E+01	2.330E+03	3.259E+03	1.000E+00	0.000E+00	6.287E+02	5.921E+02	3.195E-01	2.117E+02	1.625E+00
5.000E-01	-2.298E+00	2.000E+01	2.330E+03	3.355E+03	1.000E+00	0.000E+00	6.287E+02	5.846E+02	9.751E-03	1.559E+02	2.017E+00
5.000E-01	-2.451E+00	2.000E+01	2.330E+03	3.452E+03	1.000E+00	0.000E+00	6.287E+02	5.722E+02	7.532E-04	1.114E+02	2.537E+00
5.000E-01	-2.604E+00	2.000E+01	2.330E+03	3.548E+03	1.000E+00	0.000E+00	6.287E+02	5.436E+02	8.733E-05	7.549E+01	3.026E+00
5.000E-01	-2.758E+00	2.000E+01	2.330E+03	3.644E+03	1.000E+00	0.000E+00	6.287E+02	4.357E+02	1.143E-08	4.743E+01	2.724E+00
5.000E-01	-2.911E+00	2.000E+01	2.330E+03	3.741E+03	1.000E+00	0.000E+00	6.287E+02	2.187E+02	3.480E-09	2.510E+01	1.347E+00
5.000E-01	-3.064E+00	2.000E+01	2.330E+03	3.837E+03	1.000E+00	0.000E+00	6.287E+02	7.147E+01	5.784E-10	1.039E+01	4.351E-01
5.000E-01	-5.000E+00	2.000E+01	2.330E+03	6.272E+03							

INTERSECTION WITH PLUME= T
ATTENUATION= 2330.3416 DB
PHASE= 6.27162E+03
PHASE DIFFERENCE= -1.57588E+01
DOPPLER SHIFTED FREQUENCY= 0.000E+00 KHZ

1

NAVAL WEAPONS CENTER, CHINA LAKE

EXHAUST PLUME RADAR FREQUENCY INTERFERENCE CODE(PRFIC)

WRITTEN BY AERONAUTICAL RESEARCH ASSOCIATES OF PRINCETON

7-SEP-82

TEST CASE NUMBER 4 FOR PRFIC, MULTIPLE CASES, TRANSVERSE ATTENUATION

TRANSMITTER FREQUENCY = 3.000E+01 GHZ
FLOWFIELD FILE = TESTFF.DAT

GEOMETRIC DATA

	TRANSMITTER			RECEIVER			MISSLE		
POSITION, M	X	Y	Z	X	Y	Z	X	Y	Z
	1.000E+00	5.000E+00	2.000E+01	1.000E+00	-5.000E+00	2.000E+01	0.000E+00	0.000E+00	0.000E+00
DIRECTION OF NORMAL, DEG	ALPHA	BETA	GAMMA	ALPHA	BETA	GAMMA	ALPHA	BETA	GAMMA
	9.000E+01	1.800E+02	9.000E+01	9.000E+01	0.000E+00	9.000E+01	9.000E+01	9.000E+01	0.000E+00
REFERENCE DIRECTION, DEG	ALPHA	BETA	GAMMA	ALPHA	BETA	GAMMA	ALPHA	BETA	GAMMA
	9.000E+01	0.000E+00	9.000E+01	9.000E+01	0.000E+00	9.000E+01	9.000E+01	0.000E+00	9.000E+01
VELOCITY COMPONENTS, M/SEC	U	V	W	U	V	W	U	V	W
	0.000E+00	0.000E+00	0.000E+00	0.000E+00	0.000E+00	0.000E+00	0.000E+00	0.000E+00	0.000E+00

RAYTRACE CALCULATION = F
SCATTERING CALCULATION = F

NO. OF STEPS IN INTEGRATION THROUGH PLUME = 4.000E+01
RELAXATION CONSTANT FOR RAYTRACE ITERATION = 1.000E+00
ERROR CRITERIA FOR RAYTRACE CONVERGENCE = 1.000E-01, 1.000E-01
NUMBER OF ITERATIONS IN RAY TRACE = 10
PLUME LENGTH BETWEEN 0.000E+00 AND 1.000E+02 M

PROPERTIES ALONG RAY TRAJECTORY

X,M	Y,M	Z,M	ALPHA,DB	BETA*L	N	ALPHA,1/M	BETA,1/M	K*LAMDA	SIGMA,1/M	U,M/S	(Q/U)**2
1.000E+00	5.000E+00	2.000E+01									
1.000E+00	2.939E+00	2.000E+01	0.000E+00	1.296E+03	1.000E+00	0.000E+00	6.287E+02	7.147E+01	5.784E-10	1.039E+01	4.351E-01
1.000E+00	2.792E+00	2.000E+01	4.404E-13	9.239E+01	1.000E+00	0.000E+00	6.287E+02	2.010E+02	2.829E-09	2.327E+01	1.234E+00
1.000E+00	2.645E+00	2.000E+01	7.612E-13	1.848E+02	1.000E+00	0.000E+00	6.287E+02	3.993E+02	1.010E-08	4.369E+01	2.493E+00
1.000E+00	2.498E+00	2.000E+01	5.765E-10	2.772E+02	1.000E+00	0.000E+00	6.287E+02	5.167E+02	6.389E-05	6.818E+01	2.958E+00
1.000E+00	2.351E+00	2.000E+01	4.123E-09	3.696E+02	1.000E+00	0.000E+00	6.287E+02	5.672E+02	3.973E-04	9.763E+01	2.753E+00
1.000E+00	2.204E+00	2.000E+01	1.721E-08	4.620E+02	1.000E+00	0.000E+00	6.287E+02	5.798E+02	1.414E-03	1.330E+02	2.220E+00
1.000E+00	2.057E+00	2.000E+01	1.500E-07	5.544E+02	1.000E+00	0.000E+00	6.287E+02	5.891E+02	1.769E-02	1.774E+02	1.827E+00
1.000E+00	1.910E+00	2.000E+01	4.012E-06	6.467E+02	1.000E+00	0.000E+00	6.287E+02	5.934E+02	5.474E-01	2.311E+02	1.522E+00
1.000E+00	1.763E+00	2.000E+01	1.227E-04	7.391E+02	1.000E+00	0.000E+00	6.287E+02	5.946E+02	1.689E+01	2.957E+02	1.274E+00
1.000E+00	1.616E+00	2.000E+01	2.665E-03	8.315E+02	1.000E+00	0.000E+00	6.287E+02	5.936E+02	3.555E+02	3.729E+02	1.069E+00
1.000E+00	1.469E+00	2.000E+01	3.137E-02	9.239E+02	1.000E+00	0.000E+00	6.287E+02	5.907E+02	3.811E+03	4.633E+02	8.961E-01
1.000E+00	1.323E+00	2.000E+01	3.250E-01	1.016E+03	9.998E-01	4.647E-02	6.286E+02	5.860E+02	3.393E+04	5.671E+02	7.500E-01
1.000E+00	1.176E+00	2.000E+01	2.683E+00	1.109E+03	9.994E-01	2.855E-01	6.283E+02	5.795E+02	2.664E+05	6.826E+02	6.269E-01
1.000E+00	1.029E+00	2.000E+01	1.609E+01	1.201E+03	9.980E-01	8.800E-01	6.275E+02	5.707E+02	1.456E+06	8.076E+02	5.234E-01
1.000E+00	8.817E-01	2.000E+01	6.673E+01	1.293E+03	9.952E-01	2.081E+00	6.257E+02	5.596E+02	4.947E+06	9.377E+02	4.379E-01
1.000E+00	7.347E-01	2.000E+01	1.940E+02	1.385E+03	9.910E-01	3.819E+00	6.231E+02	5.466E+02	1.061E+07	1.067E+03	3.688E-01
1.000E+00	5.878E-01	2.000E+01	4.174E+02	1.476E+03	9.868E-01	5.585E+00	6.205E+02	5.332E+02	1.560E+07	1.187E+03	3.144E-01
1.000E+00	4.408E-01	2.000E+01	7.146E+02	1.567E+03	9.837E-01	6.885E+00	6.185E+02	5.211E+02	1.776E+07	1.292E+03	2.736E-01
1.000E+00	2.939E-01	2.000E+01	1.042E+03	1.658E+03	9.822E-01	7.543E+00	6.175E+02	5.116E+02	1.750E+07	1.374E+03	2.454E-01
1.000E+00	1.469E-01	2.000E+01	1.370E+03	1.749E+03	9.816E-01	7.812E+00	6.172E+02	5.055E+02	1.674E+07	1.425E+03	2.285E-01
1.000E+00	0.000E+00	2.000E+01	1.692E+03	1.839E+03	9.816E-01	7.819E+00	6.172E+02	5.034E+02	1.625E+07	1.443E+03	2.230E-01
1.000E+00	-1.469E-01	2.000E+01	2.014E+03	1.930E+03	9.816E-01	7.812E+00	6.172E+02	5.055E+02	1.674E+07	1.425E+03	2.285E-01
1.000E+00	-2.939E-01	2.000E+01	2.342E+03	2.021E+03	9.822E-01	7.543E+00	6.175E+02	5.116E+02	1.750E+07	1.374E+03	2.454E-01
1.000E+00	-4.408E-01	2.000E+01	2.669E+03	2.112E+03	9.837E-01	6.885E+00	6.185E+02	5.211E+02	1.776E+07	1.292E+03	2.736E-01
1.000E+00	-5.878E-01	2.000E+01	2.966E+03	2.203E+03	9.868E-01	5.585E+00	6.205E+02	5.332E+02	1.560E+07	1.187E+03	3.144E-01
1.000E+00	-7.347E-01	2.000E+01	3.190E+03	2.294E+03	9.910E-01	3.819E+00	6.231E+02	5.466E+02	1.061E+07	1.067E+03	3.688E-01
1.000E+00	-8.817E-01	2.000E+01	3.317E+03	2.386E+03	9.952E-01	2.081E+00	6.257E+02	5.596E+02	4.947E+06	9.377E+02	4.379E-01
1.000E+00	-1.029E+00	2.000E+01	3.368E+03	2.478E+03	9.980E-01	8.800E-01	6.275E+02	5.707E+02	1.456E+06	8.076E+02	5.234E-01
1.000E+00	-1.176E+00	2.000E+01	3.381E+03	2.570E+03	9.994E-01	2.855E-01	6.283E+02	5.795E+02	2.664E+05	6.826E+02	6.269E-01
1.000E+00	-1.323E+00	2.000E+01	3.383E+03	2.662E+03	9.998E-01	4.647E-02	6.286E+02	5.860E+02	3.393E+04	5.671E+02	7.500E-01
1.000E+00	-1.469E+00	2.000E+01	3.384E+03	2.755E+03	1.000E+00	0.000E+00	6.287E+02	5.907E+02	3.811E+03	4.633E+02	8.961E-01
1.000E+00	-1.616E+00	2.000E+01	3.384E+03	2.847E+03	1.000E+00	0.000E+00	6.287E+02	5.936E+02	3.555E+02	3.729E+02	1.069E+00
1.000E+00	-1.763E+00	2.000E+01	3.384E+03	2.940E+03	1.000E+00	0.000E+00	6.287E+02	5.946E+02	1.689E+01	2.957E+02	1.274E+00
1.000E+00	-1.910E+00	2.000E+01	3.384E+03	3.032E+03	1.000E+00	0.000E+00	6.287E+02	5.934E+02	5.474E-01	2.311E+02	1.522E+00
1.000E+00	-2.057E+00	2.000E+01	3.384E+03	3.124E+03	1.000E+00	0.000E+00	6.287E+02	5.891E+02	1.769E-02	1.774E+02	1.827E+00
1.000E+00	-2.204E+00	2.000E+01	3.384E+03	3.217E+03	1.000E+00	0.000E+00	6.287E+02	5.798E+02	1.414E-03	1.330E+02	2.220E+00
1.000E+00	-2.351E+00	2.000E+01	3.384E+03	3.309E+03	1.000E+00	0.000E+00	6.287E+02	5.672E+02	3.973E-04	9.763E+01	2.753E+00
1.000E+00	-2.498E+00	2.000E+01	3.384E+03	3.402E+03	1.000E+00	0.000E+00	6.287E+02	5.167E+02	6.389E-05	6.818E+01	2.958E+00
1.000E+00	-2.645E+00	2.000E+01	3.384E+03	3.494E+03	1.000E+00	0.000E+00	6.287E+02	3.993E+02	1.010E-08	4.369E+01	2.493E+00
1.000E+00	-2.792E+00	2.000E+01	3.384E+03	3.586E+03	1.000E+00	0.000E+00	6.287E+02	2.010E+02	2.829E-09	2.327E+01	1.234E+00
1.000E+00	-2.939E+00	2.000E+01	3.384E+03	3.679E+03	1.000E+00	0.000E+00	6.287E+02	7.147E+01	5.784E-10	1.039E+01	4.351E-01
1.000E+00	-5.000E+00	2.000E+01	3.384E+03	6.270E+03							

INTERSECTION WITH PLUME= T
ATTENUATION= 3383.6194 DB
PHASE= 6.27047E+03
PHASE DIFFERENCE= -1.69063E+01
DOPPLER SHIFTED FREQUENCY= 0.000E+00 KHZ

1

NAVAL WEAPONS CENTER, CHINA LAKE

EXHAUST PLUME RADAR FREQUENCY INTERFERENCE CODE(PRFIC)

WRITTEN BY AERONAUTICAL RESEARCH ASSOCIATES OF PRINCETON

7-SEP-82

TEST CASE NUMBER 4 FOR PRFIC, MULTIPLE CASES, TRANSVERSE ATTENUATION

TRANSMITTER FREQUENCY = 3.000E+01 GHZ
FLOWFIELD FILE = TESTFF.DAT

GEOMETRIC DATA

	TRANSMITTER			RECEIVER			MISSLE		
POSITION, M	X	Y	Z	X	Y	Z	X	Y	Z
	1.500E+00	5.000E+00	2.000E+01	1.500E+00	-5.000E+00	2.000E+01	0.000E+00	0.000E+00	0.000E+00
DIRECTION OF NORMAL, DEG	ALPHA	BETA	GAMMA	ALPHA	BETA	GAMMA	ALPHA	BETA	GAMMA
	9.000E+01	1.800E+02	9.000E+01	9.000E+01	0.000E+00	9.000E+01	9.000E+01	9.000E+01	0.000E+00
REFERENCE DIRECTION, DEG	ALPHA	BETA	GAMMA	ALPHA	BETA	GAMMA	ALPHA	BETA	GAMMA
	9.000E+01	0.000E+00	9.000E+01	9.000E+01	0.000E+00	9.000E+01	9.000E+01	0.000E+00	9.000E+01
VELOCITY COMPONENTS, M/SEC	U	V	W	U	V	W	U	V	W
	0.000E+00	0.000E+00	0.000E+00	0.000E+00	0.000E+00	0.000E+00	0.000E+00	0.000E+00	0.000E+00

RAYTRACE CALCULATION = F
SCATTERING CALCULATION = F

NO. OF STEPS IN INTEGRATION THROUGH PLUME = 4.000E+01
RELAXATION CONSTANT FOR RAYTRACE ITERATION = 1.000E+00
ERROR CRITERIA FOR RAYTRACE CONVERGENCE = 1.000E-01, 1.000E-01
NUMBER OF ITERATIONS IN RAY TRACE = 10
PLUME LENGTH BETWEEN 0.000E+00 AND 1.000E+02 M

PROPERTIES ALONG RAY TRAJECTORY

X,M	Y,M	Z,M	ALPHA,DB	BETA*L	N	ALPHA,1/M	BETA,1/M	K*LAMDA	SIGMA,1/M	U,M/S	(Q/U)**2
1.500E+00	5.000E+00	2.000E+01									
1.500E+00	2.718E+00	2.000E+01	0.000E+00	1.435E+03	1.000E+00	0.000E+00	6.287E+02	7.147E+01	5.784E-10	1.039E+01	4.351E-01
1.500E+00	2.582E+00	2.000E+01	3.837E-13	8.545E+01	1.000E+00	0.000E+00	6.287E+02	1.715E+02	1.750E-09	2.024E+01	1.047E+00
1.500E+00	2.446E+00	2.000E+01	6.686E-13	1.709E+02	1.000E+00	0.000E+00	6.287E+02	3.393E+02	7.900E-09	3.752E+01	2.113E+00
1.500E+00	2.310E+00	2.000E+01	2.551E-10	2.563E+02	1.000E+00	0.000E+00	6.287E+02	4.729E+02	2.556E-05	5.622E+01	2.848E+00
1.500E+00	2.174E+00	2.000E+01	1.196E-09	3.418E+02	1.000E+00	0.000E+00	6.287E+02	5.507E+02	9.353E-05	7.742E+01	3.044E+00
1.500E+00	2.039E+00	2.000E+01	5.709E-09	4.272E+02	1.000E+00	0.000E+00	6.287E+02	5.695E+02	5.579E-04	1.039E+02	2.656E+00
1.500E+00	1.903E+00	2.000E+01	1.869E-08	5.127E+02	1.000E+00	0.000E+00	6.287E+02	5.796E+02	1.383E-03	1.323E+02	2.228E+00
1.500E+00	1.767E+00	2.000E+01	1.180E-07	5.981E+02	1.000E+00	0.000E+00	6.287E+02	5.870E+02	1.397E-02	1.673E+02	1.916E+00
1.500E+00	1.631E+00	2.000E+01	1.814E-06	6.836E+02	1.000E+00	0.000E+00	6.287E+02	5.917E+02	2.527E-01	2.060E+02	1.655E+00
1.500E+00	1.495E+00	2.000E+01	8.866E-06	7.690E+02	1.000E+00	0.000E+00	6.287E+02	5.943E+02	8.645E-01	2.481E+02	1.439E+00
1.500E+00	1.359E+00	2.000E+01	1.242E-04	8.545E+02	1.000E+00	0.000E+00	6.287E+02	5.946E+02	1.746E+01	2.973E+02	1.269E+00
1.500E+00	1.223E+00	2.000E+01	1.549E-03	9.399E+02	1.000E+00	0.000E+00	6.287E+02	5.940E+02	2.086E+02	3.503E+02	1.122E+00
1.500E+00	1.087E+00	2.000E+01	7.061E-03	1.025E+03	1.000E+00	0.000E+00	6.287E+02	5.928E+02	6.627E+02	4.053E+02	9.965E-01
1.500E+00	9.513E-01	2.000E+01	3.591E-02	1.111E+03	1.000E+00	0.000E+00	6.287E+02	5.906E+02	3.866E+03	4.643E+02	8.944E-01
1.500E+00	8.154E-01	2.000E+01	1.566E-01	1.196E+03	9.999E-01	1.123E-02	6.287E+02	5.882E+02	1.390E+04	5.220E+02	8.076E-01
1.500E+00	6.795E-01	2.000E+01	5.349E-01	1.282E+03	9.998E-01	5.457E-02	6.286E+02	5.855E+02	3.853E+04	5.775E+02	7.368E-01
1.500E+00	5.436E-01	2.000E+01	1.549E+00	1.367E+03	9.997E-01	1.408E-01	6.285E+02	5.828E+02	9.907E+04	6.278E+02	6.806E-01
1.500E+00	4.077E-01	2.000E+01	3.958E+00	1.452E+03	9.994E-01	2.548E-01	6.284E+02	5.802E+02	2.309E+05	6.710E+02	6.383E-01
1.500E+00	2.718E-01	2.000E+01	8.114E+00	1.538E+03	9.992E-01	3.456E-01	6.283E+02	5.782E+02	3.418E+05	7.029E+02	6.077E-01
1.500E+00	1.359E-01	2.000E+01	1.384E+01	1.623E+03	9.991E-01	4.208E-01	6.282E+02	5.768E+02	4.480E+05	7.235E+02	5.898E-01
1.500E+00	5.662E-07	2.000E+01	2.058E+01	1.709E+03	9.990E-01	4.461E-01	6.281E+02	5.764E+02	4.837E+05	7.304E+02	5.838E-01
1.500E+00	-1.359E-01	2.000E+01	2.733E+01	1.794E+03	9.991E-01	4.208E-01	6.282E+02	5.768E+02	4.480E+05	7.235E+02	5.898E-01
1.500E+00	-2.718E-01	2.000E+01	3.305E+01	1.879E+03	9.992E-01	3.456E-01	6.283E+02	5.782E+02	3.418E+05	7.029E+02	6.077E-01
1.500E+00	-4.077E-01	2.000E+01	3.721E+01	1.965E+03	9.994E-01	2.548E-01	6.284E+02	5.802E+02	2.309E+05	6.710E+02	6.383E-01
1.500E+00	-5.436E-01	2.000E+01	3.962E+01	2.050E+03	9.997E-01	1.408E-01	6.285E+02	5.828E+02	9.907E+04	6.278E+02	6.806E-01
1.500E+00	-6.795E-01	2.000E+01	4.063E+01	2.136E+03	9.998E-01	5.457E-02	6.286E+02	5.855E+02	3.853E+04	5.775E+02	7.368E-01
1.500E+00	-8.154E-01	2.000E+01	4.101E+01	2.221E+03	9.999E-01	1.123E-02	6.287E+02	5.882E+02	1.390E+04	5.220E+02	8.076E-01
1.500E+00	-9.513E-01	2.000E+01	4.113E+01	2.306E+03	1.000E+00	0.000E+00	6.287E+02	5.906E+02	3.866E+03	4.643E+02	8.944E-01
1.500E+00	-1.087E+00	2.000E+01	4.116E+01	2.392E+03	1.000E+00	0.000E+00	6.287E+02	5.928E+02	6.627E+02	4.053E+02	9.965E-01
1.500E+00	-1.223E+00	2.000E+01	4.116E+01	2.477E+03	1.000E+00	0.000E+00	6.287E+02	5.940E+02	2.086E+02	3.503E+02	1.122E+00
1.500E+00	-1.359E+00	2.000E+01	4.117E+01	2.563E+03	1.000E+00	0.000E+00	6.287E+02	5.946E+02	1.746E+01	2.973E+02	1.269E+00
1.500E+00	-1.495E+00	2.000E+01	4.117E+01	2.648E+03	1.000E+00	0.000E+00	6.287E+02	5.943E+02	8.645E-01	2.481E+02	1.439E+00
1.500E+00	-1.631E+00	2.000E+01	4.117E+01	2.734E+03	1.000E+00	0.000E+00	6.287E+02	5.917E+02	2.527E-01	2.060E+02	1.655E+00
1.500E+00	-1.767E+00	2.000E+01	4.117E+01	2.819E+03	1.000E+00	0.000E+00	6.287E+02	5.870E+02	1.397E-02	1.673E+02	1.916E+00
1.500E+00	-1.903E+00	2.000E+01	4.117E+01	2.905E+03	1.000E+00	0.000E+00	6.287E+02	5.796E+02	1.383E-03	1.323E+02	2.228E+00
1.500E+00	-2.039E+00	2.000E+01	4.117E+01	2.990E+03	1.000E+00	0.000E+00	6.287E+02	5.695E+02	5.579E-04	1.039E+02	2.656E+00
1.500E+00	-2.174E+00	2.000E+01	4.117E+01	3.075E+03	1.000E+00	0.000E+00	6.287E+02	5.507E+02	9.353E-05	7.742E+01	3.044E+00
1.500E+00	-2.310E+00	2.000E+01	4.117E+01	3.161E+03	1.000E+00	0.000E+00	6.287E+02	4.729E+02	2.556E-05	5.622E+01	2.848E+00
1.500E+00	-2.446E+00	2.000E+01	4.117E+01	3.246E+03	1.000E+00	0.000E+00	6.287E+02	3.394E+02	7.900E-09	3.752E+01	2.113E+00
1.500E+00	-2.582E+00	2.000E+01	4.117E+01	3.332E+03	1.000E+00	0.000E+00	6.287E+02	1.715E+02	1.750E-09	2.024E+01	1.047E+00
1.500E+00	-2.718E+00	2.000E+01	4.117E+01	3.417E+03	1.000E+00	0.000E+00	6.287E+02	7.147E+01	5.784E-10	1.039E+01	4.351E-01
1.500E+00	-5.000E+00	2.000E+01	4.117E+01	6.287E+03							

INTERSECTION WITH PLUME= T
ATTENUATION= 41.1665 DB
PHASE= 6.28679E+03
PHASE DIFFERENCE= -5.89844E-01
DOPPLER SHIFTED FREQUENCY= 0.000E+00 KHZ

Appendix B
SOFTWARE DOCUMENTATION

This appendix contains the software documentation for the Naval Weapons Center Plume Radar Frequency Code (PRFIC). Brief descriptions are given of those subprograms that contain computations of physical quantities. Those subroutines that perform input and output operations, read files, or provide plots are not described in detail. A full list of the subroutines was given in Appendix A (Table A-1). The individual descriptions are given below, followed by a complete listing of the entire program.

SUBROUTINE PRFIAG(AANG,AGAIN,NA)

Subroutine PRFIAG provides the antenna gain pattern for the transmitter and receiver. AANG is the angle between the direction of propagation and normal to the antenna, in degrees. AGAIN is the gain at this angle, in dB, and NA is a code to define the gain distribution for the transmitter (NA = 1) and receiver (NA = 2). If the uniform distribution option is chosen, then

$$\text{AGAIN} = 0; \qquad 0 < \text{AANG} < 90. \tag{B-1}$$

If the gain distribution is nonuniform, a linear interpolation between angles is used. If G_i is the gain at the angle θ_i, then

$$\text{AGAIN} = G_i - (\theta_i - \text{AANG}) \times (G_i - G_{i+1})/(\theta_i - \theta_{i+1}) \tag{B-2}$$

where the input order is such that $\theta_{i+1} > \theta_i$. If AANG is beyond the range of the last angular entry, the subroutine returns the gain at the last entry.

SUBROUTINE PRFIDT(ATTEN,PHASE,DOPPS)

PRFIDT is the primary subroutine that governs the direct transfer of radiation from the transmitter to the receiver along the line-of-sight of a refracted ray trajectory. It returns the total attenuation (ATTEN) and phase (PHASE) for the path and the Doppler shift of this transmitted ray (DOPPS).

The primary function of PRFIDT is to set up the paths exterior and interior to the plume and then to call PRFIIT to do the integration for each segment. However, the first task is to determine if direct transfer can occur. No direct transfer is allowed for the three cases:

1. co-located transmitter and receiver (monostatic radar)

2. angle between the normal to the transmitter and the direction to the receiver > 90 degrees

3. angle between the normal to the receiver and the direction from the transmitter > 90 degrees

If any of the conditions occur, the subprogram returns and prints a message.

If the straight line-of-sight option is used, the direct transfer occurs in three steps: (1) transmitter to plume; (2) through the plume; (3) plume to receiver. PRFIPI is used to define the intersection with the plume (one intersection or two, if the line-of-sight enters the plume). If there is no intersection, the program returns the attenuation (= 0), phase and Doppler shift, and prints a flag, INTERSECTION WITH PLUME = F.

If the ray trace option is used, an iterative solution is required. The initial guess for the curved trajectory is taken to be the straight line-of-sight. At the endpoint of the integration, an error vector between the computed endpoint and actual endpoint (receiver location) is calculated. If this error exceeds a specified criterion (EPSA(1)), then a new guess for the initial direction at the transmitter is made. The current new guess for the direction cosines at the transmitter is

$$(\cos\alpha)^{n+1} = (\cos\alpha)^{n} + RC * ERV(I)/SL \qquad \text{(B-3)}$$

where n is the old guess, RC is an overrelaxation factor ($0.5 \leq RC \leq 1.0$), ERV(I) is the error vector from the computed endpoint to the desired endpoint, and SL is the length of the ray path. Similar expressions apply for the other two angles $\beta(I = 2)$ and $\gamma(I = 3)$. This is a simple iterative solution to the two-point boundary value problem that adjusts the initial ray direction to achieve convergence. The iteration is performed until convergence occurs or until the number of iterations exceeds NIT, an input variable. If no convergence occurs, a warning message is printed.

SUBROUTINE PRFIEP

The subroutine PRFIEP utilizes the input flowfield variables read directly from the SPF input file to create an array of quantities used in the RF interference calculations. It is called once at the beginning of each run when a new flowfield file is defined. The RF interference properties are then calculated at each point in the flowfield, once and for all. All subsequent interpolations required in the attenuation and scattering calculations throughout the plume volume are performed from these quantities directly, rather than for the flowfield variables initially on the input file. The objective of this calculation sequence is to minimize the number of operations. For example, calculating the RF properties first, and then interpolating, requires fewer calculations than interpolating for the flowfield properties and then computing the RF properties at each point along a ray trajectory.

The input flowfield file is stored in the array FF(I,J,K). PRFIEP calculates the RF interference properties and stores them back in FF(I,J,K). The individual quantities are defined below.

Input Flowfield Properties

K	FF(I,J,K)	Units
1	r, radius at axial location z(I), radial location J	m
2	T, temperature	K
3	p, pressure	n/m^2
4	n_e, mean electron number density	m^{-3}
5	$\overline{n_e'^2}/n_e^2$, normalized mean square electron number density fluctuation	---
6	ν_{en}, electron-neutral collision frequency	s^{-1}
7	Λ, turbulence macroscale	m
8	u, mean axial velocity	m/s
9	q^2/u^2, normalized mean square velocity fluctuation	---

Output RF Interference Properties

K	FF(I,J,K)	Units
1	r, radius at axial location z(I), radial location, J	m
2	n, real part of complex index of refraction	---
3	α, attenuation constant	m^{-1}
4	β, phase constant	m^{-1}
5	$k\Lambda$, product of wavenumber and turbulence macroscale	---
6	σ, common part of extinction cross section	m^{-1}
7	u, mean axial velocity	m/s
8	q^2/u^2, normalized mean square velocity fluctuations	---
9	$\partial n/\partial r$, radial derivative of index of refraction	m^{-1}
10	$\partial n/\partial z$, axial derivative of index of refraction	m^{-1}

These output quantities are obtained from the following equations.

K = 2,3,4, n,α,β, see subroutine PRFIPC

K = 5,

$$k\Lambda = 2\pi n\nu\Lambda/c$$

ν = radar frequency

K = 6,

$$\sigma = \frac{8\pi^3(0.0528)\left(\frac{\overline{n_e'^2}}{n_e^2}\right)n_e^2\ r_e^2\ \Lambda^3}{\left[1 + \left(\frac{\nu_{en}}{\omega}\right)^2\right]^2} \qquad \text{(B-4)}$$

This is a multiplier that is common to the scattering cross section used for both the attenuation and scattering calculation. For scattering, σ multiplies the angular dependent scattering function.*

$$\frac{\sin^2\chi}{\left[1 + 4(k\Lambda)^2\sin^2\frac{\theta}{2}\right]^{11/6}} \tag{B-5}$$

For extinction, σ multiplies the integral of this function over all directions. This integral is called Q and depends on $k\Lambda$. It is evaluated in function subprogram SCAT($k\Lambda$).

K = 7,8 u and q^2/u^2 carried over directly from flowfield.

K = 9,10 Radial and axial components of the index of refraction gradient.

The index of refraction gradients for use with the ray tracing option are calculated according to the following finite difference approximations. Subscripts i,j denote z,r locations, respectively.

$$\left(\frac{\partial n}{\partial r}\right)_{i,j} = \frac{1}{2}\left[\frac{n_{i,j+1} - n_{i,j}}{r_{i,j+1} - r_{i,j}} + \frac{n_{i,j} - n_{i,j-1}}{r_{i,j} - r_{i,j-1}}\right] \tag{B-6}$$

$$\left(\frac{\partial n}{\partial z}\right)_{i,j} = \frac{1}{2}\left[\frac{n_{i+1,j} - n_{i,j}}{z_{i+1} - z_i} + \frac{n_{i,j} - n_{i-1,j}}{z_i - z_{i-1}}\right] \tag{B-7}$$

```
SUBROUTINE PRFIIT(XO,SO,XF,ATTEN,PHASE,ERV,
                  ERVM,XFV,SFV,IN,RAY)
```

Subroutine PRFIIT computes the ray path between two points either outside or inside the plume. If the ray trace option is chosen, the ray trajectory within the plume is computed with the geometric optics approximation. If a line-of-sight option is chosen, the ray trajectory is a straight line. In both cases, the integrated attenuation and phase along the path are computed.

*For one choice of the turbulence spatial correlation.

XO(I), I=1,3 : Coordinates of initial point, m

SO(I), I=1,3 : Direction cosines of initial direction

XF(I), I=1,3 : Coordinates of final point of the straignt line-of-sight

ATTEN : Integrated attenuation along the path

PHASE : Integrated phase along the path

ERV(I), I=1,3: Error vector, ERV(I) = XF(I) - XFV(I)

ERVM : Magnitude of error, $ERVM = \left[\sum_{I=1}^{3} ERV(I) \right]^{1/2}$

XFV(I), I=1,3: Final point of integration

SFV(I), I=1,3: Direction of path at the endpoint

IN : IN = T, trajectory within the plume
= F, trajectory outside the plume

RAY : RAY = T, ray trace calculation
= F, line-of-sight calculation

Exterior to the plume, the attenuation and phase are given simply by ATTEN = 0, and

$$PHASE = 2\pi\nu_o s/c \tag{B-8}$$

where s is the path length between the initial and final point. The endpoint error, ERVM, is zero, the final points are equal, XF(I) = XFV(I), and the final direction and initial directions are the same SO(I) = SFV(I). This solution applies regardless of the ray trace option.

Interior to the plume, the line-of-sight is divided into increments according to

$$\Delta s = s/NCUTS \quad . \tag{B-9}$$

If the line-of-sight option is taken, the integration for the

attenuation and phase is summed along the straight line-of-sight by a trapezoidal rule

$$\text{ATTEN} = \sum_{i=1}^{\text{NCUTS}} \frac{\Delta s}{2}(\alpha_{i+1} + \alpha_i) \tag{B-10}$$

$$\text{PHASE} = \sum_{i=1}^{\text{NCUTS}} \frac{\Delta s}{2}(\beta_{i+1} + \beta_i) \tag{B-11}$$

In both cases, the attenuation and phase constants are obtained at each point i by interpolation between the values stored in the flowfield file.

If the ray trace option is chosen, then the integration within the exhaust plume proceeds along s, the arc length, but this no longer coincides with the straight line-of-sight. The equations defining the ray trajectory

$$\vec{r}(s) = \{x(s),\ y(s),\ z(s)\} \tag{B-12}$$

$$x(s + \Delta s) = x(s) + \left(\frac{dx}{ds}\right)_s \Delta s + \frac{1}{2n}\left(\frac{\partial n}{\partial x} - \frac{dx}{ds}(\vec{t} \cdot \nabla n)\right)_s (\Delta s)^2 \tag{B-13}$$

$$y(s + \Delta s) = y(s) + \left(\frac{dy}{ds}\right)_s \Delta s + \frac{1}{2n}\left(\frac{\partial n}{\partial y} - \frac{dy}{ds}(\vec{t} \cdot \nabla n)\right)_s (\Delta s)^2 \tag{B-14}$$

$$z(s + \Delta s) = z(s) + \left(\frac{dz}{ds}\right)_s \Delta s + \frac{1}{2n}\left(\frac{\partial n}{\partial z} - \frac{dz}{ds}(\vec{t} \cdot \nabla n)\right)_s (\Delta s)^2 \tag{B-15}$$

where

$$\vec{t} = \left\{\frac{dx}{ds}, \frac{dy}{ds}, \frac{dz}{ds}\right\}, \quad \text{and} \tag{B-16}$$

$$\nabla n = \cos\theta \frac{\partial n}{\partial r}, \sin\theta \frac{\partial n}{\partial r}, \frac{\partial n}{\partial z} \tag{B-17}$$

Solution of Eqs. (B-13)-(B-15) is achieved in a stepwise numerical integration throughout the plume. The initial point

$$\vec{r}(0) = x(0), y(0), z(0) \tag{B-18}$$

and direction

$$\vec{t}(0) = \frac{dx}{ds}(0), \frac{dy}{ds}(0), \frac{dz}{ds}(0) \tag{B-19}$$

are known. However, for a given initial point and direction, the endpoint and direction are unknown until the integration along the trajectory has been performed. For a known initial point and known endpoint, the solution for the ray trajectory is a two-point boundary value problem. An iterative solution must be performed until the initial direction is found which allows the trajectory to pass between these points.

This subroutine does not perform the iteration but simply integrates the ray equations between two points. The actual choice of a new direction is made in the individual subroutines PRFIDT and PRFISC (for the directly transmitted ray and scattered ray, respectively). Integration along the trajectory proceeds until the distance between the known endpoint XF(I) and point on the ray path is smaller than $\Delta s/2$. A check is included to insure that if the trajectory does not pass within $\Delta s/2$ of the known endpoint, the integration stops when the error is least. When this criterion is met, the subroutine returns the actual endpoint of the integration XFV(I), the actual direction of the ray at the endpoint, the error vector ERV(I), and magnitude of the displacement error ERVM. These quantities are used to choose a new initial direction. If the line-of-sight option is chosen, the errors are zero and the final direction is the same as the initial direction.

SUBROUTINE PRFILI(Z,R,VZR)

The subroutine PRFILI is a linear interpolation program that computes the RF interference properties at the axial location, z, and radial location, r which do not coincide with the grid points of the

input flowfield. Let i,j be indices identifying the axial and radial locations, respectively. Then, if f is any dependent variable such that $f_{i,j}$ is its value at the grid points i,j and $f_{z,r}$, the value at (z,r):

$$f_{i-1,r} = f_{i-1,j-1} + \frac{r - r_{i-1,j-1}}{r_{i-1,j} - r_{i-1,j-1}}\left(f_{i-1,j} - f_{i-1,j-1}\right) \tag{B-20}$$

$$f_{i,r} = f_{i,j-1} + \frac{r - r_{i,j-1}}{r_{i,j} - r_{i,j-1}}\left(f_{i,j} - f_{i,j-1}\right) \tag{B-21}$$

then

$$f_{z,r} = f_{i-1,r} + \frac{z - z_{i-1}}{z_i - z_{i-1}}\left(f_{i,r} - f_{i-1,r}\right) \tag{B-22}$$

The values of the nine quantities n, α, β, $k\Lambda$, σ, u, q^2/u^2, $\partial n/\partial r$, $\partial n/\partial z$ are returned in the array VZR for each point z,r, even though not all are used at each call. For example, $\partial n/\partial r$ and $\partial n/\partial z$ are not used when the line-of-sight option is chosen.

If the point is outside the plume boundary, ambient values are returned. The non-zero quantities are n=1, $\beta=2\pi\nu/c$, and $u=u_\infty$.

SUBROUTINE PRFIPC(ν, ν_p, ν_{en}, α, β, n)

The subroutine PRFIPC calculates the plasma index of refraction, attenuation, and phase constants, given the radar frequency, ν, plasma frequency, ν_p, and electron-neutral collision frequency, ν_{en}.

$$\nu_p = 8.97\ n_e^{1/2} \tag{B-23}$$

$$\omega_p = 2\pi\nu_p \tag{B-24}$$

$$\omega = 2\pi\nu \tag{B-25}$$

$$\left(\frac{kc}{\omega}\right)^2 = K_R + iK_I = 1 - \frac{(\omega_p/\omega)^2}{1 + \left(\frac{\nu_{en}}{\omega}\right)^2} + i\,\frac{(\omega_p/\omega)^2\,\frac{\nu_{en}}{\omega}}{1 + \left(\frac{\nu_{en}}{\omega}\right)^2} \tag{B-26}$$

$$|K| = (K_R^2 + K_I^2)^{1/2} \tag{B-27}$$

$$n = \left\{\frac{1}{2}\left(|K| + K_R\right)\right\}^{1/2} \tag{B-28}$$

$$\alpha = \frac{\omega}{c}\left\{\frac{1}{2}\left(|K| - K_R\right)\right\}^{1/2} \tag{B-29}$$

$$\beta = n\omega/c \tag{B-30}$$

SUBROUTINE PRFIPI(XO,XF,XI,XE,MTYPE,NTYPE)

It is convenient to separate the portions of the propagation path that are outside and inside the plume. Subroutine PRFIPI solves for the points at which a straight line-of-sight intersects the plume boundary. This subroutine is used to answer the following questions:

1. Does the line-of-sight intersect the plume?

2. If there is an intersection, how much of the line-of-sight is outside the plume? The attenuation and phase of the outside portion can be computed in one step because it is a homogeneous path (with $\alpha = 0$ and $\beta = 2\pi\nu/c$), while only the nonhomogeneous portion interior to the plume need be broken into smaller steps for integration.

   a. This calculation completely defines the propagation path when refraction is not considered.

   b. This calculation gives a first guess for the ray trajectory when refraction is considered.

The solution is determined by the following sequence of operations. Let $\vec{x}_1 = (x_1, y_1, z_1)$ be the initial point and $\vec{x}_2 = (x_2, y_2, z_2)$ be the final point along the path. Then any point along the path between $\vec{x}_2$ and $\vec{x}_1$ is $\vec{r} = (x, y, z)$,

$$\vec{r} = \vec{x}_1 + \xi\,\hat{s} \tag{B-31}$$

where ξ is a scalar distance ($\xi > 0$) and $\hat{s}$ is the unit vector in the direction of $\vec{r}_2$ from $\vec{r}_1$.

$$\hat{s} = (\vec{r}_2 - \vec{r}_1)/|\vec{r}_2 - \vec{r}_1| \quad . \tag{B-32}$$

The radius of the plume at any axial location is

$$r(z) = r_i + \frac{r_{i+1} - r_i}{z_{i+1} - z_i}(z - z_i) \ , \quad z_i \leq z \leq z_{i+1} \tag{B-33}$$

where r_i, z_i are the plume radius and axial location at the ith station given in the flowfield file [i.e., FF(I,NPTS(J),1), Z(I), $1 \leq I \leq$ NZ]. At the point of intersection

$$(\vec{r} \cdot \hat{i})^2 + (\vec{r} \cdot \hat{j})^2 = (x_1 + \xi\hat{s} \cdot \hat{i})^2 + (y_1 + \xi\hat{s} \cdot \hat{j})^2 = r^2(z) \tag{B-34}$$

and

$$\vec{r} \cdot \hat{k} = z_1 + \xi\hat{s} \cdot \hat{k} = z \tag{B-35}$$

where $\hat{i}$, $\hat{j}$, $\hat{k}$ are unit vectors in the x, y, and z directions. These two equations can be combined to give a single, quadratic equation for ξ:

$$a\xi^2 + 2b\xi + c = 0 \tag{B-36}$$

with

$$a = B^2 - (\hat{s} \cdot i)^2 - (\hat{s} \cdot \hat{j})^2; \quad A = r_i + \frac{r_{i+1} - r_i}{z_{i+1} - z_i}(z_1 - z_i) \tag{B-37}$$

$$b = AB - x_i(\hat{s} \cdot i) - (\hat{s} \cdot j); \quad B = \frac{r_{i+1} - r_i}{z_{i+1} - z_i}(\hat{s} \cdot \hat{k}) \tag{B-38}$$

$$c = A^2 - (x_1^2 + y_1^2) \tag{B-39}$$

and

$$\xi = \left(-b \pm \sqrt{b^2 - ac}\right)/a \tag{B-40}$$

The two roots to this equation are evaluated for each conical segment of the plume, $I = 1,\ldots,NZ$. The solution of interest must satisfy

$$z_i \leq z \leq z_{i+1} \quad . \tag{B-41}$$

That is, the line-of-sight must pass through the conical segment of the plume at which the radius is defined by Eq. (B-33).*

The exceptional cases occur when

$$b^2 - ac < 0 \tag{B-42}$$

for which there is no intersection, and when $a = 0$, for which there is only one solution (the line-of-sight can intersect the plume, but the angle of the plume expansion is such that it will never exit). In the event that the line-of-sight does not exit the plume, we define the line-of-sight interior to the plume to extend to the end of the input flowfield. (This situation can occur if the receiving antenna is downstream of the end of the flowfield and sufficiently close to the plume axis.)

*It is possible for the line-of-sight to intersect the upstream and downstream extensions of the conical volume defined by Eq. (B-33). That is, ξ is a root of Eq. (B-40), but $z < z_i$ or $z > z_{i+1}$. However, that is not a valid solution for the plume intersection.

In general, there are two real roots that result from the solution after all plume segments are examined. From the definition of $\xi > 0$, the root defining the incident intercept, ξ_i is the smaller of the two, $\xi_i < \xi_e$, where ξ_e defines the exit point. The positions of the intercepts are

$$\vec{r}_{i,e} = \vec{x}_1 + \xi_{i,e}\,\hat{s} \quad . \tag{B-43}$$

The same formulation applies if the initial point is outside the plume and the endpoint is inside, or vice versa. This situation occurs in the volume scattering calculation. If $\vec{x}_1$ is outside and $\vec{x}_2$ inside, then the single root of interest is ξ_i. If $\vec{x}_1$ is inside and $\vec{x}_2$ outside, then one of the two roots is negative, and we take the positive root to be ξ_e.

All these cases are computed in the subroutine PRFIPI, and are defined in the arguments, as follows:

XO = XO(I), I = 1,3	x,y,z coordinates of initial point
XF = XF(I), I = 1,3	MTYPE < 0; XF = direction cosines of direction to endpoint
	MTYPE > 0; XF = coordinates of endpoint
XI = XI(I), I = 1,3	coordinates of entry point
XE XE(I), I = 1,3	coordinates of exit point
MTYPE	= flag for type of input (coordinates or direction to final point)
NTYPE	= flag for type of path NTYPE = 1 Initial and endpoints outside the plume (solutions are XI and XE, or no intersection) NTYPE = 2 Initial point outside, final point inside, solution is XI. NTYPE = 3 Initial point inside, final point outside, solution is XE.

SUBROUTINE PRFIRZ(ZP,RP)

The integration in the radial direction of the volume scattering integral (see description of subroutine PRFISC) uses a radial coordinate normalized by the local plume radius r(z). Subroutine PRFIRZ interpolates between neighboring flowfield stations z_ℓ, $z_{\ell+1}$ to define the plume radius at the axial quadrature point z_i; $z_\ell < z_i < z_{\ell+1}$. A simple linear interpolation is used:

$$r(z_i) = r(z_\ell) + \frac{z_i - z_\ell}{z_{\ell+1} - z_\ell}\left[r(z_{\ell+1}) - r(z_\ell)\right] \qquad \text{(B-44)}$$

where $r(z_\ell)$ = FF[L,NPTS(L),1], the outermost radial location defined in the flowfield file at the axial location z(L).

SUBROUTINE PRFISC

Subroutine PRFISC computes the scattered signal due to fluctuations in the electron number density. It performs a numerical evaluation of the scattering from the entire plume volume. This requires a three-dimensional volume integration; the plume volume is axisymmetric, but the arbitrary locations of transmitter and receiver make the integrand dependent upon all three coordinates (r,θ,z).

The approach used in this report is to evaluate the volume integral by a succession of Gaussian quadratures. For a fixed number of points, these schemes yield the most accurate quadratures. The volume integral to be evaluated is

$$P(\nu) = \int_V C(r,\theta,z,\nu)\, dV \qquad \text{(B-45)}$$

where $P(\nu)$ is the frequency spectrum of the mean square scattered power and C is the scattering cross section at the point r,θ,z. The integrand also depends on the scattering angle between the directions of the incident and scattered waves and also the distances from the scattering location to both the transmitter and receiver. In the event of refraction, a separate curved ray trajectory must be computed between the point r,θ,z and both the transmitter and receiver. In addition, the attenuation and phase for each path, for both the curved ray trajectory or straight line-of-sight, is included. The detailed specification of $C(r,\theta,z,\nu)$ is

$$C(r,\theta,z,\nu) = \frac{\lambda^2}{8\pi^3} \frac{G_T G_A \sigma}{r_T^2 r_R^2} \frac{\sin\chi \; PDF(\nu - \nu_o)}{\left[1 + 4(k\Lambda)^2 \sin^2 \frac{\theta}{2}\right]^{11/6}} \tag{B-46}$$

where G_T, G_A, and r_T, r_R are the antenna gains and distances from the scattering point to the transmitter and receiver, respectively.

In PRFISC, the volume integral is evaluated according to

$$P = \int_{Z_i}^{Z_f} \int_0^{R(z)} \int_0^{2\pi} C(r,\theta,z) r d\theta \, dz \tag{B-47}$$

$$= \sum_i \sum_j \sum_k C(r_j,\theta_k,z_i) r_j \, w_k \, w_j \, w_i \tag{B-48}$$

$$= (z_f - z_i) \, \pi \sum_{i=1}^{M} R^2(z_i) \sum_j^N \eta_j \sum_{k=1}^{N} C(\eta_j,\zeta_k,\xi_i) w_k \, w_j \, w_i \tag{B-49}$$

where w_i, w_j, w_k are the weights and ζ_k, η_j, ξ_i are the roots of normalized variables in the θ, r, and z directions, respectively. The normalization, ranges, and number of points are given in the following table. In all three cases, the independent variables are scaled to the interval (-1,1) so the quadrature points are roots of Legendre polynomials.

Table B-1. Numerical Quadratures Used in Volume Scattering Calculation

Coordinate	Transformed	Range	No. of Points
θ	$\theta = \pi(1-\zeta)$	$-1 < \zeta < 1$	10
r	$r = \eta \, R(z)$	$0 < \eta < 1$ (1/2 of 20 point quadrature)	10
z	$z = \xi(z_f - z_i)$	$0 < \xi < 1$ (1/2 of 48 point quadrature)	24

The axial variable is scaled by an initial and final plume length z_i, z_f, respectively, that can be specified in the input. This allows the computation of scattering from a finite length of plume different from the length of flowfield in the input file.

The integral, Eq. (B-47), is also the temporal power spectral density of the scattered signal, i.e., $P = P(\nu)$, that accounts for the probability of both the spatial and temporal fluctuations in electron number density. The integrand contains a frequency dependent multiplier, the probability density function PDF(ν). $P(\nu)$ is evaluated at increments in frequency difference, $\Delta\nu = \nu - \nu_o$, from the transmitter frequency, ν_o.

If the ray trace option is chosen, the incident and scattered ray paths are curved. Iterative solutions are applied to both the segments in PRFISC. The procedure is like that outlined for the directly transmitted ray in PRFIDT.

FUNCTION PDF(DF,VMK,QQ,ANG,BFREQ)

Function subroutine PDF returns the probability density function for the Doppler shifted scattered wave. The Doppler shift includes the effect of the resultant mean velocity of the transmitter, missile, and exhaust plume relative to the receiver. There is a frequency spread about this mean shift due to the turbulent fluctuations. At present, it is assumed that the velocity fluctuations are isotropic with respect to direction at each point and have a Gaussian distribution with a mean square value of $\overline{q'^2}$ about the local time averaged velocity. With these assumptions, the probability density function of the Doppler shifted scattered wave at a point is

$$\mathrm{PDF}(\nu - \nu_o) = \frac{1}{\sqrt{2\pi\overline{q'^2}}} \exp\left[-\frac{\left(c\,\dfrac{\nu - \nu_o}{\nu_o} - v_s\right)^2}{2\,\overline{q'^2}\left[2\sin(\theta/2)\right]^2}\;\frac{c}{2\nu_o\sin(\theta/2)}\right] \qquad \text{(B-50)}$$

DF = frequency difference $(\nu - \nu_o)$, Hz

VMK = component of resultant velocity of transmitter, missile, and mean plume flow relative to the receiver, m/s.

QQ = mean square turbulence intensity, $\overline{q'^2}$, m^2/s^2.

ANG = magnitude of the resultant scattering wave vector, $2\sin(\theta/2)$.

BFREQ = transmitter frequency, ν_0.

PDF = probability density of mean square scattered power at the frequency, ν, $0 \leq PDF \leq 1$.

SUBPROGRAM SCAT($k\Lambda$)

The function subroutine SCAT($k\Lambda$) calculates the directionally averaged scattering component of the electron number density fluctuation. It depends on the single augment $k\Lambda$ and is given by

$$SCAT = \frac{6\pi}{p^3}\left\{\frac{1}{5}(2p^2 + 2p + 1)\left[1 - (1 + 2p)^{-5/6}\right]\right.$$

$$\left. -2(p + 1)\left[(1 + 2p)^{1/6} - 1\right] + \frac{1}{7}\left[(1 + 2p)^{7/6} - 1\right]\right\} \qquad \text{(B-51)}$$

where $p = 2(k\Lambda)^2$.

FUNCTION SCALP(A,B)

Function subroutine SCALP returns the scalar product of two vectors defined in rectangular Cartesian coordinates.

$$SCALP = \sum_{I=1}^{3} A(I) * B(I) \qquad \text{(B-52)}$$

A(I) and B(I), where I = 1,2,3, are the x, y, and z components of the two vectors, respectively.

Code Listing

```
      SUBROUTINE PRFIAG(AANG,AGAIN,NA)
C
C     COMPUTES ANTENNA GAIN AT ANGLE AANG
C
C     AANG=ANGLE, DEG
C     AGAIN=GAIN, DB
C     NA=1, TRANSMITTER
C       =2, RECEIVER
C
      INCLUDE'PRFICM.FOR/NOLIST'

      IF(NANG(NA).NE.0) GO TO 5
      AGAIN=0.
      RETURN

    5 CONTINUE
      NG=NANG(NA)-1
      DO 10 I=1,NG
      IF(AANG.GE.ANGLE(NA,I).AND.AANG.LT.ANGLE(NA,I+1)) GO TO 20
   10 CONTINUE
      AGAIN=GAIN(NA,NANG(NA))
      RETURN

   20 CONTINUE
      AGAIN=GAIN(NA,I)-(ANGLE(NA,I)-AANG)*(GAIN(NA,I)-GAIN(NA,I+1))/
     1 (ANGLE(NA,I)-ANGLE(NA,I+1))
      RETURN
      END
************************************************************************
C     PRFICM
C
C     COMMON FOR PROGRAM PRFIC
C     PLUME RADAR FREQUENCY INTERFERENCE CODE
C     WRITTEN FOR NWC, CHINA LAKE
C
      LOGICAL RAYTR,FSCAT,INSECT,PATH,EXTER
      REAL NCUTS
      BYTE FILEFF(20)

      PARAMETER (PI=3.141592653, C=2.998E+08)

C     DO NOT ALTER THE POSITIONS OF VARIABLES IN THE NEXT 8 LINES

      COMMON BFREQ,ZLL,ZUL
      COMMON XT(3),DCT(3),DCT0(3)
      COMMON VT(3),XR(3),DCR(3)
      COMMON DCR0(3),VR(3),XM(3)
```


Reproduced From
Best Available Copy

```
      COMMON DCM(3),DCMO(3),VM(3)
      COMMON NCUTS,RC,NIT
      COMMON EPSA(2),DUMX
      COMMON RAYTR,FSCAT

C     OK ...


      COMMON RTHOM,INSECT,PATH,EXTER
      COMMON TITLE(18),FILEFF
      COMMON FF(60,50,10),Z(60),NPTS(60)
      COMMON VZRAMB(9),ILAST,NZ
      COMMON NANG(2),ANGLE(2,50),GAIN(2,50)
C     END
*********************************************************************
      SUBROUTINE PRFIDT(ATTEN,PHASE,DOPPS)
C
C     CALCULATE RAY PATH FROM TRANSMITTER TO RECEIVER
C
      INCLUDE 'PRFICM.FOR/NOLIST'
      LOGICAL IN,RAY
      DIMENSION SU(3),DUM(3),ERV(3),XFV(3),SFV(3),XD(3),XI(3),
     1          XE(3),XF(3),VTR(3)

C
C     DETERMINE IF DIRECT TRANSFER CAN OCCUR
C

      PATH=.TRUE.
      DOPPS=0.
      SS=0.
      DO 10 I=1,3
      SS=SS+(XR(I)-XT(I))**2
   10 CONTINUE
      SL=SQRT(SS)
      ATTEN=0.
      PHASE=2.*PI*SL*BFREQ/C

      IF(SS.GT.0.) GO TO 30
      WRITE(6,20)
   20 FORMAT(1H ,'COLOCATED ANTENNAS')
      INSECT=.FALSE.
      RETURN

   30 CONTINUE
      DO 40 I=1,3
      SU(I)=(XR(I)-XT(I))/SL
```

```
      VTR(I)=VT(I)-VR(I)
   40 CONTINUE

      COSPT=SCALP(SU,DCT)
      IF(COSPT.GT.0.) GO TO 60
      WRITE(6,50)
   50 FORMAT(1H ,'NO DIRECT PATH TO RECEIVER, S*NT<0.')
      INSECT=.FALSE.
      RETURN
   60 CONTINUE
      COSPR=-SCALP(SU,DCR)
      IF(COSPR.GT.0.) GO TO 80
      WRITE(6,70)
   70 FORMAT(1H ,'NO DIRECT PATH TO RECEIVER, S*NR<0.')
      INSECT=.FALSE.
      RETURN
   80 CONTINUE

C     DOPPLER SHIFT OF DIRECT TRANSMISSION

      VTMS=SCALP(VTR,SU)
      DOPPS=BFREQ*VTMS/C


      IF(PATH) WRITE(6,300) (XT(I),I=1,3)

C
C     INTERSECTION WITH PLUME
C

C     LOS THROUGH PLUME
C
   90 CONTINUE

      IF(RAYTR) GO TO 100
      CALL PRFIPI(XT,XR,XI,XE,1,1)
      IF(INSECT) THEN
      PHASE=0.
      EXTER=.TRUE.
      IN=.FALSE.
      RAY=.FALSE.
      CALL PRFIIT(XT,SU,XI,ATTENT,PHASET,ERV,ERVM,XFV,SFV,IN,RAY)
      ATTEN=ATTEN+ATTENT
      PHASE=PHASE+PHASET

C
C     LOS CALCULATION
```


Reproduced From
Best Available Copy

```
C
      IN=.TRUE.
      CALL PRFIIT(XI,SU,XE,ATTENT,PHASET,ERV,ERVM,XFV,SFV,IN,RAY)
      ATTEN=ATTEN+ATTENT
      PHASE=PHASE+PHASET

      EXTER=.FALSE.
      IN=.FALSE.
      CALL PRFIIT(XFV,SU,XR,ATTENT,PHASET,ERV,ERVM,XFV,SFV,IN,RAY)
      ATTEN=ATTEN+ATTENT
      PHASE=PHASE+PHASET

      DB=ATTEN*8.6858
      IF(PATH) WRITE(6,300) (XR(I),I=1,3), DB,PHASE

      END IF
      RETURN
C
C     RAY TRACE CALCULATION
C

  100 CONTINUE
      IT=1
      PATH=.FALSE.
  105 CONTINUE


      ATTEN=0.
      PHASE=0.
C
C     OUTSIDE PLUME
C
      EXTER=.TRUE.
      IN=.FALSE.
      RAY=.FALSE.
      CALL PRFIPI(XT,SU,XI,XE,-1,1)
      CALL PRFIIT(XT,SU,XI,ATTENT,PHASET,ERV,ERVM,XFV,SFV,IN,RAY)
      ATTEN=ATTEN+ATTENT
      PHASE=PHASE+PHASET
C
C     INSIDE PLUME
C
      IN=.TRUE.
      RAY=.TRUE.
      CALL PRFIIT(XI,SU,XE,ATTENT,PHASET,ERV,ERVM,XFV,SFV,IN,RAY)
      ATTEN=ATTEN+ATTENT
```

```
      PHASE=PHASE+PHASET
C
C     OUTSIDE PLUME
C
      SA=0.
      DO 110 I=1,3
      SA=SA+(XFV(I)-XR(I))**2
      DUM(I)=SU(I)
  110 CONTINUE
      SA=SQRT(SA)
      DO 120 I=1,3
      XF(I)=XFV(I)+SA*SFV(I)
      XD(I)=XFV(I)
      SU(I)=SFV(I)
  120 CONTINUE
      EXTER=.FALSE.
      IN=.FALSE.
      RAY=.FALSE.
      CALL PRFIIT(XD,SU,XR,ATTENT,PHASET,ERV,ERVM,XFV,SFV,IN,RAY)
      ATTEN=ATTEN+ATTENT
      PHASE=PHASE+PHASET

      DB=ATTEN*8.6858
      IF(PATH) WRITE(6,300) (XR(I),I=1,3),DB,PHASE
      IF(PATH) RETURN

      IF(ERVM.LE.EPSA(I)) THEN
      PATH=.TRUE.
      END IF
C
C     NEW GUESS FOR INITIAL DIRECTION
C
      SS=0.
      DO 130 I=1,3
      SU(I)=DUM(I)+RC*ERV(I)/SL
      SS=SS+SU(I)**2
  130 CONTINUE
      SS=SQRT(SS)
      DO 135 I=1,3
      SU(I)=SU(I)/SS
  135 CONTINUE
      IF(PATH) GO TO 105
      IT=IT+1
      IF(IT.GT.NIT) GO TO 140
      GO TO 105
  140 CONTINUE
      WRITE(6,150)
```

```
  150 FORMAT(1H ,'IT=MAX, NO CONVERGENCE')
  300 FORMAT(1H ,5(1PE10.3,1X))
      RETURN
      END
*********************************************************************
      SUBROUTINE PRFIEP
C
C     CREATES FILE OF PLUME INTERFERENCE PROPERTIES FORM SPF
C     FLOWFIELD FILE FF(I,J,K)
C
C     REVISED FILE HAS THE QUANTITIES AS FOLLOWS
C     F(I,J,1)=RADIUS AT AXIAL LOCATION I, RADIAL LOCATION J
C           2 =INDEX OF REFRACTION
C           3 =ATTENUATION CONSTANT
C           4 =PHASE CONSTANT
C           5 =WAVENUMBER*TURBULENCE SCALE LENGTH
C           6 =SCATTERING CROSS-SECTION
C           7 =VELOCITY
C           8 =TURBULENCE INTENSITY
C           9 =RADIAL DERIVATIVE OF INDEX OF REFRACTION
C          10 =AXIAL DERIVATIVE OF INDEX OF REFRACTION
C

      INCLUDE 'PRFICM.FOR/NOLIST'
      DIMENSION GG(10),HM(9),HP(9)
      DATA RTHOM/2.8133E-15/

      DO 50 I=1,NZ
      DO 40 J=1,NPTS(I)
      GG(1)=FF(I,J,1)
      PFREQ=8.97*SQRT(FF(I,J,4))
      CALL PRFIPC(BFREQ,PFREQ,FF(I,J,6),GG(3),GG(4),GG(2))
      GG(5)=2.*PI*GG(2)*BFREQ*FF(I,J,7)/C
      DENOM=(1.+(FF(I,J,6)/(2.*PI*BFREQ))**2)**2
      GG(6)=8.*(PI**3)*.0528*FF(I,J,5)*((RTHOM*FF(I,J,4))**2)*
     1      (FF(I,J,7)**3)/DENOM
      GG(7)=FF(I,J,8)
      GG(8)=FF(I,J,9)

      DO 30 K=1,8
      FF(I,J,K)=GG(K)
   30 CONTINUE
   40 CONTINUE
   50 CONTINUE

C
C     COMPUTE RADIAL AND AXIAL DERIVATIVES OF INDEX OF REFRACTION IN
```

```
C     SEPARATE LOOP
C

      DO 70 I=1,NZ
      DO 60 J=1,NPTS(I)
      ANR=0.
      BNR=0.
      DRM=0.
      DRP=0.
      IF(J.GT.1) DRM=FF(I,J,1)-FF(I,J-1,1)
      IF(J.GT.1.AND.DRM.NE.0.) BNR=(FF(I,J,2)-FF(I,J-1,2))/DRM
      IF(J.LT.NPTS(I)) DRP=FF(I,J+1,1)-FF(I,J,1)
      IF(J.LT.NPTS(I).AND.DRP.NE.0.) ANR=(FF(I,J+1,2)-FF(I,J,2))/DRP
      IF(J.EQ.1) BNR=ANR
      IF(J.EQ.NPTS(I)) ANR=BNR
      FF(I,J,9)=.5*(ANR+BNR)

      IF(I.GT.1) CALL PRFILI(Z(I-1),FF(I,J,1),HM)
      IF(I.LT.NZ) CALL PRFILI(Z(I+1),FF(I,J,1),HP)
      IF(I.GT.1) BNZ=(FF(I,J,2)-HM(1))/(Z(I)-Z(I-1))
      IF(I.LT.NZ) ANZ=(HP(1)-FF(I,J,2))/(Z(I+1)-Z(I))
      IF(I.EQ.1) BNZ=ANZ
      IF(I.EQ.NZ) ANZ=BNZ
      FF(I,J,10)=.5*(ANZ+BNZ)

   60 CONTINUE
   70 CONTINUE
      RETURN
      END
*************************************************************************
        SUBROUTINE PRFIFF
C
C       READS SPF FLOWFIELD FILE INTO ARRAY FF(I,J,K)
C
C        .
C       FF(I,J,1) = RADIUS(M) AT AXIAL LOCATION I, RADIAL LOCATION J
C              2  = TEMPERATURE(K)
C              3  = PRESSURE(NT/M**2)
C              4  = ELECTRON NUMBER DENSITY
C              5  = MEAN SQUARE ELECTRON NUMBER DENSITY
C              6  = CFREQ
C              7  = TURBULENCE MACRO SCALE
C              8  = MEAN VELOCITY
C              9  = MEAN SQUARE TURBULENCE VELOCITY
C
C
        INCLUDE 'PRFICM.FOR/NOLIST'
```

```
      DATA NFF / 7 /,  I / 1 /,  NZMAX,NRMAX / 60,50 /


      OPEN(UNIT=NFF, STATUS='OLD', FILE=FILEFF, READONLY)

100   READ(NFF,1000,END=300) Z(I), NPTS(I)
D     WRITE(6,2001) I,Z(I),NPTS(I)
      IF(NPTS(I).GT.NRMAX) THEN
      WRITE(6,*) ' FLOWFIELD EXCEEDS RADIAL DIMENSION.'
      STOP
      END IF

      DO 200 J=1,NPTS(I)
      READ(NFF,2000) (FF(I,J,K),K=1,9)
D     WRITE(6,2002) J,(FF(I,J,K),K=1,9)
200 CONTINUE

      I = I + 1
      IF(I.LE.NZMAX) GO TO 100
  300 NZ = I - 1


 1000 FORMAT(E10.3,I10)
 2000 FORMAT(9E10.3)
 2001 FORMAT(I5,E10.3,I5)
 2002 FORMAT(I5,9E10.3)

      RETURN
      END
************************************************************************
      SUBROUTINE PRFIIN
C
C     READS IN INITIAL DATA FOR PRFIC
C

      INCLUDE 'PRFICM.FOR/NOLIST'

      DATA PRAD/1.745329252E-02/


C  CARD 1
      READ(5,6) I, FILEFF
      FILEFF(I+1)=0

C  CARD 2
      READ(5,7) TITLE
```

```
C  CARD 3
      READ(5,1) BFREQ,ZLL,ZUL

C  CARD 4
      READ(5,1) (XT(J),J=1,3)

C  CARD 5
      READ(5,1) (DCT(J),J=1,3)

C  CARD 6
      READ(5,1) (DCTO(J),J=1,3)

C  CARD 7
      READ(5,1) (VT(J),J=1,3)

C  CARD 8
      READ(5,1) (XR(J),J=1,3)

C  CARD 9
      READ(5,1) (DCR(J),J=1,3)

C  CARD 10
      READ(5,1) (DCRO(J),J=1,3)

C  CARD 11
      READ(5,1) (VR(J),J=1,3)

C  CARD 12
      READ(5,1) (XM(J),J=1,3)

C  CARD 13
      READ(5,1) (DCM(J),J=1,3)

C  CARD 14
      READ(5,1) (DCMO(J),J=1,3)

C  CARD 15
      READ(5,1) (VM(J),J=1,3)

C  CARD 16
      READ(5,2) NCUTS,RC,NIT

C  CARD 17
      READ(5,2) EPSA

C  CARD 18
```

```
      READ(5,5) RAYTR,FSCAT
C
C     READ ANTENNA GAIN DISTRIBUTIONS
C
C
      IF(FSCAT) THEN
      READ(5,60) NANG
   60 FORMAT(2I5)
      IF(NANG(1).LE.0) GO TO 80
      READ(5,70) (ANGLE(1,J),J=1,NANG(1))
      READ(5,70) (GAIN(1,J),J=1,NANG(1))
   80 CONTINUE
      IF(NANG(2).LE.0) GO TO 90
      READ(5,70) (ANGLE(2,J),J=1,NANG(2))
      READ(5,70) (GAIN(2,J),J=1,NANG(2))
      GO TO 130
   90 CONTINUE
   70 FORMAT(10F8.0)
      IF(NANG(1).EQ.0.AND.NANG(2).EQ.0) GO TO 130
      IF(NANG(2).GT.0) GO TO 110
      DO 100 I=1,NANG(1)
      ANGLE(2,I)=ANGLE(1,I)
      GAIN(2,I)=GAIN(1,I)
  100 CONTINUE
      NANG(2)=NANG(1)
      GO TO 130
  110 CONTINUE
      DO 120 I=1,NANG(2)
      ANGLE(1,I)=ANGLE(2,I)
      GAIN(1,I)=GAIN(2,I)
  120 CONTINUE
      NANG(1)=NANG(2)
      END IF
  130 CONTINUE

    1 FORMAT(3F10.0)
    2 FORMAT(2F10.0,I3)
    5 FORMAT(2L1)
    6 FORMAT(Q,20A1)
    7 FORMAT(18A4)
      DO 3 I=1,3
      DCT(I)=COS(DCT(I)*PRAD)
      DCTO(I)=COS(DCTO(I)*PRAD)
      DCR(I)=COS(DCR(I)*PRAD)
      DCRO(I)=COS(DCRO(I)*PRAD)
      DCM(I)=COS(DCM(I)*PRAD)
```

```
      DCMO(I)=COS(DCMO(I)*PRAD)
    3 CONTINUE

C     OUTPUT INITIAL CONDITIONS

      CALL DUMPIN

      RETURN
      END


      SUBROUTINE PRFIIC
C
C     READS INPUT CHANGES FOR MULTIPLE CASE RUNS -
C     ALLOWS ONE TO INPUT NEW VALUES FOR VARIABLES
C     ON CARDS 3-18.
C

C     INPUT CHANGES PROCEDURE :

C     1) A CARD CONTAINING THE TOTAL NUMBER OF VARIABLES
C        TO BE CHANGED FOR THE NEXT RUN.

C     2) CARD(S) CONTAINING THE SEQUENCE OF CHANGES DESIRED.
C        THE FORMAT OF THIS CARD(S) IS :

C     CARD NO. OF VARIABLE TO CHANGE,VARIABLE NO. ON THIS CARD,
C     NEW VALUE FOR THIS VARIABLE ...

C     REPEAT THIS SEQUENCE FOR AS MANY CHANGES SPECIFIED ON
C     CARD 1). CARD 2) MAY BE REPEATED AS MANY TIMES AS NECESSARY
C     TO COMPLETE THE NUMBER OF CHANGES SPECIFIED.

C     FOR EXAMPLE, TO CHANGE THE VARIABLE "ZUL" ON CARD 3 TO THE
C     QUANTITY 5000 AND TO CHANGE THE VARIABLE "RAYTR" ON CARD 18
C     TO THE VALUE FALSE, THE FOLLOWING CARDS SHOULD BE INPUT ...

C     2
C     3,3,5000, 18,1,F


      INCLUDE 'PRFICM.FOR/NOLIST'

      LOGICAL DINP(2)
      DIMENSION CV(3,3:18),IC(65),IV(65)

      EQUIVALENCE (BFREQ,CV(1,3))
```

```
      EQUIVALENCE (RAYTR,DINP(1))

      PRAD=1.745329252E-02


      READ(5,*,END=400) NC
100   READ(5,*,END=200) (IC(N),IV(N),CV(IV(N),IC(N)),N=1,NC)

200   DO 300 N=1,NC
      IF(IC(N).EQ.5 .OR. IC(N).EQ.6 .OR. IC(N).EQ.9
     #.OR. IC(N).EQ.10 .OR. IC(N).EQ.13 .OR. IC(N).EQ.14) THEN
      CV(IV(N),IC(N))=COS(CV(IV(N),IC(N))*PRAD)
      END IF
300   CONTINUE

C     OUTPUT INITIAL CONDITIONS

      WRITE(6,*) '1'
      CALL DUMPIN
      RETURN

400   STOP
      END


      SUBROUTINE DUMPIN
C
C     DUMPS INITIAL DATA TO PRINTER
C

      INCLUDE 'PRFICM.FOR/NOLIST'

      BYTE IDATE(9)
      DIMENSION ACT(3),ACR(3),ACM(3),ACTO(3),ACRO(3),ACMO(3)

      PRAD=1.745329252E-02

      CALL DATE(IDATE)

      DO 10 I=1,3
      ACT(I)=ACOS(DCT(I))/PRAD
      ACR(I)=ACOS(DCR(I))/PRAD
      ACM(I)=ACOS(DCM(I))/PRAD
      ACTO(I)=ACOS(DCTO(I))/PRAD
      ACRO(I)=ACOS(DCRO(I))/PRAD
      ACMO(I)=ACOS(DCMO(I))/PRAD
   10 CONTINUE
```

```
      WRITE(6,1000) IDATE, TITLE
      WRITE(6,2000) BFREQ/1.E9, FILEFF
      WRITE(6,3000) XT, XR, XM
      WRITE(6,4000) ACT, ACR, ACM
      WRITE(6,5000) ACTO, ACRO, ACMO
      WRITE(6,6000) VT, VR, VM
      WRITE(6,7000) RAYTR, FSCAT
      WRITE(6,8000) NCUTS, RC, EPSA, NIT

C     FORMATS:

1000  FORMAT(1H1,/// 50X,'NAVAL WEAPONS CENTER, CHINA LAKE'//
     #39X,'EXHAUST PLUME RADAR FREQUENCY INTERFERENCE CODE(PRFIC)'
     #//38X,'WRITTEN BY AERONAUTICAL RESEARCH ASSOCIATES OF PRINCETON'
     #//62X,9A1///45X,18A4///)
2000  FORMAT(45X,'TRANSMITTER FREQUENCY = ',1PE10.3,' GHZ'/
     #45X,'FLOWFIELD FILE = ',20A1///)
3000  FORMAT(59X,'GEOMETRIC DATA'//
     #33X,'TRANSMITTER',23X,'RECEIVER',26X,
     #'MISSLE'//' POSITION, M',4X,3(4X,9X,'X',9X,'Y',9X,'Z')/'6X,
     #3(4X,3(1PE10.3))/)
4000  FORMAT(' DIRECTION OF',3X,3(4X,5X,'ALPHA',6X,'BETA',5X,'GAMMA')/
     #' NORMAL, DEG',4X,3(4X,3(1PE10.3))/)
5000  FORMAT(' REFERENCE',6X,3(4X,5X,'ALPHA',6X,'BETA',5X,'GAMMA')/
     #' DIRECTION, DEG',1X,3(4X,3(1PE10.3))/)
6000  FORMAT(' VELOCITY',7X,3(4X,9X,'U',9X,'V',9X,'W')/
     #' COMPONENTS, M/SEC',2X,3(1PE10.3),2(4X,3(1PE10.3))//)
7000  FORMAT(45X,'RAYTRACE CALCULATION = ',L1/45X,'SCATTERING ',
     #'CALCULATION = ',L1/)
8000  FORMAT(45X,'NO. OF STEPS IN INTEGRATION THROUGH PLUME = ',
     1 1PE10.3/
     #45X,'RELAXATION CONSTANT FOR RAYTRACE ITERATION = ',1PE10.3/
     #45X,'ERROR CRITERIA FOR RAYTRACE CONVERGENCE = ',1PE10.3,', ',
     #1PE10.3/45X,'NUMBER OF ITERATIONS IN RAY TRACE = ',I5)

      RETURN
      END
*********************************************************************
      SUBROUTINE PRFIIT(XO,SO,XF,ATTEN,PHASE,ERV,ERVM,XFV,SFV,IN,RAY)
C
C     COMPUTES THE PATH FROM THE INITIAL POINT XO TO THE FINAL POINT
C     XF WITH INITIAL DIRECTION SO
C
C     ATTEN=INTEGRATED ATTENUATION DUE TO ABSORPTION AND SCATTERING
C     PHASE=INTEGRATED PHASE CHANGE
```


Reproduced From
Best Available Copy

```
C     ERV=ERROR VECTOR BETWEEN ACTUAL END POINT AND COMPUTED END POINT
C     ERVM=MAGNITUDE OF ERROR
C     XFV=COMPUTED END POINT
C     SFV=COMPUTED DIRECTION OF RAY AT END POINT
C     IN=T ; XO AND XF INSIDE THE PLUME
C        F ;            OUTSIDE THE PLUME
C     RAY=T ; DO RAY TRACE CALCULATION
C         F ; DO LOS CALCULATION

      INCLUDE'PRFICM.FOR/NOLIST'
      LOGICAL IN,RAY
      DIMENSION XO(3),SO(3),XF(3),ERV(3),XFV(3),SFV(3),X(3),SU(3),
     1          HOLD(9),HNEW(9),CURV(3)

C
C     FIRST SEGMENT DOES THE LOS CALCULATION FOR POINTS OUTSIDE THE
C     PLUME
C

      ATTEN=0.
      PHASE=0.
      SQ=0.
      ERVM=0.
      DO 10 I=1,3
      SQ=SQ+(XF(I)-XO(I))**2
   10 CONTINUE
      SL=SQRT(SQ)
      IF(IN) GO TO 20
      DO 15 I=1,3
      XFV(I)=XO(I)+SL*SO(I)
      ERV(I)=XF(I)-XFV(I)
      ERVM=ERVM+ERV(I)**2
      SFV(I)=SO(I)
   15 CONTINUE
      R=SQRT(XFV(1)**2+XFV(2)**2)
      CALL PRFILI(XFV(3),R,HNEW)
      ERVM=SQRT(ERVM)
      PHASE=2.*PI*BFREQ*SL/C
      IF(PATH.AND.EXTER) WRITE(6,200) (XFV(I),I=1,3),ATTEN,PHASE,
     1 (HNEW(I),I=1,7)
      RETURN

C
C     SECOND SEGMENT DOES LOS CALCULATION WITHIN THE PLUME
C

   20 CONTINUE
```

```
      DS=SL/NCUTS
      HDS=0.5*DS
      DO 30 I=1,3
      X(I)=X0(I)
      SU(I)=S0(I)
   30 CONTINUE
      R=SQRT(X(1)**2+X(2)**2)
      CALL PRFILI(X(3),R,HOLD)
      SS=0.
      IF(RAY) GO TO 70
   40 CONTINUE
      DO 50 I=1,3
      X(I)=X(I)+SU(I)*DS
   50 CONTINUE
      R=SQRT(X(1)**2+X(2)**2)
      CALL PRFILI(X(3),R,HNEW)
      ATTEN=ATTEN+.5*(HOLD(2)+HOLD(5)*SCAT(HOLD(4))+HNEW(2)+HNEW(5)*
     1       SCAT(HNEW(4)))*DS
      PHASE=PHASE+.5*(HOLD(3)+HNEW(3))*DS
      DO 60 J=1,9
      HOLD(J)=HNEW(J)
   60 CONTINUE
      SS=SS+DS
      DIF=ABS(SL-SS)
      DB=ATTEN*8.6858

C     WRITE STATEMENT FOR DETAILED DISTRIBUTION ALONG FINAL
C     INTEGRTION PATH

C     IF(PATH) WRITE(6,200) (X(I),I=1,3),DB,PHASE,(HNEW(I),I=1,7)
      IF(SS.LT.SL.AND.DIF.GT.HDS) GO TO 40
      ERVM=0.
      DO 65 I=1,3
      XFV(I)=X(I)
      ERV(I)=XF(I)-X(I)
      SFV(I)=S0(I)
   65 CONTINUE
      ERVM=SCALP(ERV,ERV)
      ERVM=SQRT(ERVM)
      RETURN

C
C     THIS SEGMENT DOES THE CALCULATION WITHIN THE PLUME WITH RAY
C     CURVATURE
C

   70 CONTINUE
```


Reproduced From
Best Available Copy

```
      ERVM=SL
   80 CONTINUE
      ERVMO=ERVM
      R=SQRT(X(1)**2+X(2)**2)
      COST=X(1)/R
      SINT=X(2)/R
      TDOTGN=SU(1)*HOLD(8)*COST+SU(2)*HOLD(8)*SINT+SU(3)*HOLD(9)
      CURV(1)=(HOLD(8)*COST-SU(1)*TDOTGN)/HOLD(1)
      CURV(2)=(HOLD(8)*SINT-SU(2)*TDOTGN)/HOLD(1)
      CURV(3)=(HOLD(9)     -SU(3)*TDOTGN)/HOLD(1)
      DO 90 I=1,3
      X(I)=X(I)+SU(I)*DS+.5*CURV(I)*DS*DS
      SU(I)=SU(I)+CURV(I)*DS
   90 CONTINUE
      R=SQRT(X(1)**2+X(2)**2)
      CALL PRFILI(X(3),R,HNEW)
      ATTEN=ATTEN+.5*(HOLD(2)+HOLD(5)*SCAT(HOLD(4))+HNEW(2)+HNEW(5)*
     1       SCAT(HNEW(4)))*DS
      PHASE=PHASE+.5*(HOLD(3)+HNEW(3))*DS
      SS=SS+DS
      DO 100 J=1,9
      HOLD(J)=HNEW(J)
  100 CONTINUE
      ERVM=0.
      DO 110 I=1,3
      ERV(I)=XF(I)-X(I)
      ERVM=ERVM+ERV(I)**2
  110 CONTINUE
      ERVM=SQRT(ERVM)
      DB=ATTEN*8.6858

C     WRITE STATEMENT FOR DETAILED DISTRIBUTION ALONG FINAL
C     INTEGRTION PATH

      IF(PATH) WRITE(6,200) (X(I),I=1,3),DB,PHASE,(HNEW(I),I=1,7)
      IF(ERVM.LT.ERVMO.AND.ERVM.GT.HDS) GO TO 80
      DO 120 I=1,3
      XFV(I)=X(I)
      SFV(I)=SU(I)
  120 CONTINUE
  200 FORMAT(1H ,12(1PE10.3,1X))
      RETURN
      END
*********************************************************************
        SUBROUTINE PRFILI(ZL,RL,VZR)
C
C       GIVEN AXIAL LOCATION, ZL, AND RADIAL LOCATION, RL,
```

```
C       PRFILI LINEARLY INTERPOLATES TO FIND THE FLOWFIELD
C       PROPERTIES AT ZL,RL AND RETURNS THEIR VALUES IN VZR.
C

        INCLUDE 'PRFICM.FOR/NOLIST'

        DIMENSION VZR(9), DATZ(2:10), DATZP(2:10)

        DATA VZRAMB / 1., 8*0. /,  ILAST / 2 /

        VZRAMB(3) = 2.*PI*BFREQ/C
        VZRAMB(6) = FF(NZ,NPTS(NZ),7)

C
C       SEARCH FOR BOUNDING AXIAL STATIONS
C
        IF((ZL.LT.Z(1)) .OR. (ZL.GT.Z(NZ))) GO TO 600
        DO 100 I=ILAST,NZ
100     IF(ZL.LE.Z(I)) GO TO 200
200     I = I - 1
C       ILAST = I

        DO 400 IZ=1,2
        DO 300 J=2,NPTS(I)
300     IF(ABS(RL).LT.FF(I,J,1)) GO TO 310
        CALL SFVMV(VZRAMB,DATZ,9)
        GO TO 330
310     RRAT = (ABS(RL)-FF(I,J-1,1))/(FF(I,J,1)-FF(I,J-1,1))
        DO 320 K=2,10
320     DATZ(K) = FF(I,J-1,K) + RRAT*(FF(I,J,K)-FF(I,J-1,K))
C
C       SAVE RADIALLY INTERPOLATED VALUES AT THE LOWER BOUNDING
C       AXIAL STATION AND REPEAT FOR UPPER BOUNDING STATION.
C
330     IF(IZ.EQ.1) CALL SFVMV(DATZ,DATZP,9)
400     I = I + 1

C
C       INTERPOLATE BETWEEN AXIAL STATIONS
C
        I = I - 1
        ZRAT = (ZL-Z(I-1))/(Z(I)-Z(I-1))
        DO 500 K=2,10
500     VZR(K-1) = DATZP(K) + ZRAT*(DATZ(K)-DATZP(K))
        RETURN

600     CALL SFVMV(VZRAMB,VZR,9)
        RETURN
        END
*****************************************************************************
```

```
      PROGRAM PRFIMM
C
C     MAIN CALLING PROGRAM FOR PRFIC
C
      INCLUDE 'PRFICM.FOR/NOLIST'

      CALL PRFIIN
      CALL PRFIFF
      CALL PRFIEP
    5 CONTINUE
      IF(ZLL.LE.0.) ZLL=Z(1)
      IF(ZUL.LE.0.) ZUL=Z(NZ)
      WRITE(6,20) ZLL,ZUL
      WRITE(6,30)
      CALL PRFIDT(ATTEN,PHASE,DOPP)

      DPHASE=0.
      DO 15 I=1,3
      DPHASE=DPHASE+(XR(I)-XT(I))**2
   15 CONTINUE
      DPHASE=2.*PI*BFREQ*SQRT(DPHASE)/C
      DPHASE=PHASE-DPHASE
      ATTEN=ATTEN*8.6858
      DOPP=DOPP/1000.

      WRITE(6,10) INSECT,ATTEN,PHASE,DPHASE,DOPP

      IF(FSCAT) THEN
      WRITE(6,100)
      IF(NANG(1).NE.0) WRITE(6,110) (ANGLE(1,J),J=1,NANG(1))
      IF(NANG(1).EQ.0) WRITE(6,150)
      WRITE(6,120)
      IF(NANG(1).NE.0) WRITE(6,110) (GAIN(1,J),J=1,NANG(1))
      WRITE(6,130)
      IF(NANG(2).NE.0) WRITE(6,110) (ANGLE(2,J),J=1,NANG(2))
      IF(NANG(2).EQ.0) WRITE(6,150)
      WRITE(6,140)
      IF(NANG(2).NE.0) WRITE(6,110) (GAIN(2,J),J=1,NANG(2))
      CALL PRFISC
      END IF

      CALL PRFIIC
      GO TO 5
   10 FORMAT(1H ,/// 40X,'INTERSECTION WITH PLUME= ',L1/52X,
```

```
     1 'ATTENUATION= ',F10.4,' DB'/
     2 58X,'PHASE=  ',1PE12.5/47X,'PHASE DIFFERENCE=  ',1PE12.5/
     3 38X,'DOPPLER SHIFTED FREQUENCY=  ',1PE10.3,' KHZ')
  20 FORMAT(1H ,44X,'PLUME LENGTH BETWEEN',1PE10.3,' AND ',1PE10.3,
     1 ' M'///)
  30 FORMAT(1H1,44X,'PROPERTIES ALONG RAY TRAJECTORY'//
     1 5X,'X,M',8X,'Y,M',8X,'Z,M',3X,'ALPHA,DB',5X,'BETA*L',10X,'N',
     2 2X,'ALPHA,1/M',3X,'BETA,1/M',4X,'K*LAMDA',2X,'SIGMA,1/M',
     3 6X,'U,M/S',3X,'(Q/U)**2'/)
 100 FORMAT(1H1,///44X,'ANTENNA GAIN PATTERNS'////44X,
     1 'TRANSMITTER'///1X,'ANGLES,DEG:')
 110 FORMAT(1H ,15X,10(F10.2)/(16X,10(F10.2)))
 120 FORMAT(1H ,//3X,'GAIN, DB:')
 130 FORMAT(1H ,////12X,'RECEIVER'///1X,'ANGLES,DEG:')
 140 FORMAT(1H ,//3X,'GAIN, DB:')
 150 FORMAT(1H ,20X,'UNIFORM DISTRIBUTION, GAIN=0. FOR ALL ANGLES')
     END
*********************************************************************
      SUBROUTINE PRFIPC(BFREQ,PFREQ,CFREQ,ALPHA,BETA,RI)

C     CALCULATE ATTENUATION AND PHASE CONSTANT

C     BFREQ=PROPAGATION FREQUENCY,HZ
C     PFREQ=PLASMA FREQUENCY,HZ
C     CFREQ=ELECTRON-NEUTRAL COLLISION FREQUENCY, 1/SEC
C     ALPHA=ATTENUATION CONSTANT,1/M
C     BETA =PHASE CONSTANT,1/M
C     RI=INDEX OF REFRACTION

      REAL KR,KI,KMAG
      DATA C,PI/2.998E+08,3.141592653/

      R1=PFREQ/BFREQ
      WPROP=2.*PI*BFREQ
      R2=CFREQ/WPROP
      R1S=R1*R1
      R2S=R2*R2

      KR=1.-R1S/(1.+R2S)
      IF(KR.LT.0.) WRITE(6,1)
      KI=R1S*R2/(1.+R2S)
      KMAG=SQRT(KR*KR+KI*KI)

      ALPHA=SQRT(.5*(KMAG-KR))*WPROP/C
      RI=SQRT(.5*(KMAG+KR))
      BETA=RI*WPROP/C
```

```
      RETURN

    1 FORMAT(1H ,'PLUME IS LOCALLY OVERDENSE')
      END
*********************************************************************
      SUBROUTINE PRFIPI(XO,XF,XI,XE,MTYPE,NTYPE)
C
C     COMPUTE THE POINT(S) AT WHICH THE LOS FROM XO TO XF INTERSECTS
C     THE PLUME BOUNDARIES
C

C     MTYPE.LT.0 : XF=INITIAL DIRECTION COSINES
C     MTYPE.GE.0 : XF=COORDINATES OF FINAL POINT
C     NTYPE=1, LOS PASSES COMPLETELY THROUGH THE PLUME (TWO SOLUTIONS,
C              XI,AND XE, OR NO INTERSECTION, INSECT=FALSE)
C     NTYPE=2, XO OUTSIDE THE PLUME, XF INSIDE PLUME (ONE SOLUTION, XI)
C     NTYPE=3, XO INSIDE THE PLUME, XF OUTSIDE PLUME (ONE SOLUTION, XE)
C
      INCLUDE 'PRFICM.FOR/NOLIST'
      LOGICAL ROOT1
      DIMENSION XO(3),XF(3),XI(3),XE(3),XD(3),SU(3),ROOT(2)

      INSECT=.FALSE.
      ROOT1=.FALSE.
      IF(MTYPE.GE.0) GO TO 5
      DO 1 I=1,3
      SU(I)=XF(I)
    1 CONTINUE
      GO TO 20
    5 CONTINUE
      SS=0.
      DO 10 I=1,3
      XD(I)=XF(I)-XO(I)
      SS=SS+XD(I)**2
   10 CONTINUE
      SL=SQRT(SS)
      DO 20 I=1,3
      SU(I)=XD(I)/SL
   20 CONTINUE
      NZM1=NZ-1
      DO 90 I=1,NZM1
      IP=I+1
      SLOPE=(FF(IP,NPTS(IP),1)-FF(I,NPTS(I),1))/(Z(IP)-Z(I))
      A=FF(I,NPTS(I),1)+SLOPE*(XO(3)-Z(I))
      B=SLOPE*SU(3)
      XP=XO(1)*SU(1)+XO(2)*SU(2)
      XPS=XO(1)**2+XO(2)**2
```

```
      CPS=SU(1)**2+SU(2)**2
      AR=B*B-CPS
      BR=A*B-XP
      CR=A*A-XPS
      DISC=BR*BR-AR*CR
      IF(DISC.LT.0.) GO TO 90
      IF(AR.EQ.0.) GO TO 60
      DISC=SQRT(DISC)
      R1=(-BR-DISC)/AR
      R2=(-BR+DISC)/AR
      IF(R1.LT.0..AND.R2.LT.0.) GO TO 90
      INSECT=.TRUE.
      ROOT(1)=AMIN1(R1,R2)
      IF(R1.LT.0.) ROOT(1)=R2
      IF(R2.LT.0.) ROOT(1)=R1
      Z1=X0(3)+ROOT(1)*SU(3)
      IF(Z1.LT.Z(1).OR.Z1.GT.Z(IP)) GO TO 40
      DO 30 J=1,3
      XI(J)=X0(J)+ROOT(1)*SU(J)
   30 CONTINUE
      ROOT1=.TRUE.
      IF(NTYPE.EQ.2) RETURN
   40 CONTINUE
      ROOT(2)=AMAX1(R1,R2)
      IF(ROOT(2).NE.ROOT(1)) GO TO 44
      ROOT(2)=ABS(Z(NZ)-X0(3))
      GO TO 45
   44 CONTINUE
      Z2=X0(3)+ROOT(2)*SU(3)
      IF(Z2.LT.Z(1).OR.Z2.GT.Z(IP)) GO TO 90
   45 CONTINUE
      DO 50 J=1,3
      XE(J)=X0(J)+ROOT(2)*SU(J)
   50 CONTINUE
      IF(NTYPE.EQ.3) RETURN
      IF(ROOT1) RETURN
      GO TO 90
   60 CONTINUE
      R1=-1.
      IF(BR.NE.0.) R1=-.5*CR/BR
      IF(R1.LT.0.) GO TO 90
      INSECT=.TRUE.
      IF(NTYPE.EQ.3) GO TO 70
      ROOT(1)=R1
      DO 65 J=1,3
      XI(J)=X0(J)+ROOT(1)*SU(J)
   65 CONTINUE
```

```
      ROOT1=.TRUE.
      IF(NTYPE.EQ.2) RETURN
      GO TO 90
   70 CONTINUE
      ROOT(2)=R1
      DO 75 J=1,3
      XE(J)=X0(J)+ROOT(2)*SU(J)
   75 CONTINUE
      IF(NTYPE.EQ.3) RETURN
      IF(ROOT1) RETURN
   90 CONTINUE

      IF(.NOT.INSECT) RETURN
      IF(NTYPE.EQ.3) GO TO 105
      IF(Z1.GE.Z(NZ).AND.SU(3).NE.0.) ROOT(1)=(Z(NZ)-X0(3))/SU(3)
      DO 100 I=1,3
      XI(I)=X0(I)+ROOT(1)*SU(I)
  100 CONTINUE
      IF(NTYPE.EQ.2) RETURN
  105 CONTINUE
      IF(Z2.GE.Z(NZ).AND.SU(3).NE.0.) ROOT(2)=(Z(NZ)-X0(3))/SU(3)
      DO 110 I=1,3
      XE(I)=X0(I)+ROOT(2)*SU(I)
  110 CONTINUE
      RETURN
      END
*********************************************************************
      SUBROUTINE PLOT(NO,A,N,M)
      INTEGER*2 YLAB(50)
      DIMENSION OUT(101),YPR(11),ANG(9),A(1)
      DATA MX,MY/6,5/
      DATA YLAB/13*'  ','F ','R ','E ','Q ','U ','E ','N ','C ','Y ',
     #'  ','D ','I ','F ','F ','E ','R ','E ','N ','C ','E','  ',
     #'K ','H ','Z ',13*'  '/
      DATA ANG(1)/'*'/, BLANK/' '/
    1 FORMAT ('1',60X,7H CHART ,I3,//)
    2 FORMAT (1X,A2,1X,F11.1,5X,101A1)
    3 FORMAT (1X,A2)
    5 FORMAT(10A1)
    7 FORMAT(    16X,101H.         .         .         .         .
     1         .         .         .         .         .         .)
    8 FORMAT (//,9X,11F10.1)
    9 FORMAT (//,53X,'  SCATTERED AMPLITUDE,DB/HZ ')

      NLL=50
C        PRINT TITLE
   20 WRITE(MX,1)NO
```

```
C         FIND SCALE FOR BASE VARIABLE
      XSCAL=(A(N)-A(1))/(FLOAT(NLL-1))
C         FIND SCALE FOR CROSS-VARIABLES
      M1=N+1
      M2=M*N
      YMAX=A(M1)
      DO 40 J=M1,M2
      IF(A(J)-YMAX) 40,40,30
   30 YMAX=A(J)
   40 CONTINUE
      YMIN=YMAX-40.
      YSCAL=(YMAX-YMIN)/100.0
C         FIND BASE VARIABLE PRINT POSITION
      XB=A(1)
      L=1
      MYX = M-1
      I=1
   45 F=I-1
      XPR=XB+F*XSCAL
      IF(A(L)-XPR) 50,50,70
C         FIND CROSS-VARIABLES
   50 DO 55 IX=1,101
   55 OUT(IX)=BLANK
      DO 60 J=1,MYX
      LL=L+J*N
      IF(A(LL).LT.YMIN) GOTO 60
      JP=((A(LL)-YMIN)/YSCAL)+1.0
      OUT(JP)=ANG(J)
   60 CONTINUE
C         PRINT LINE AND CLEAR, OR SKIP
      WRITE(MX,2)YLAB(I),XPR,(OUT(IZ),IZ=1,101)
      L=L+1
      GO TO 80
   70 WRITE(MX,3) YLAB(I)
   80 I=I+1
      IF(I-NLL)45,84,86
   84 XPR=A(N)
      GO TO 50
C         PRINT CROSS-VARIABLES NUMBERS
   86 WRITE(MX,7)
      YPR(1)=YMIN
      DO 90 KN=1,9
   90 YPR(KN+1)=YPR(KN)+YSCAL*10.0
      YPR(11)=YMAX
      WRITE(MX,8)(YPR(IP),IP=1,11)
      WRITE(MX,9)
      RETURN
      END
*****************************************************************************
```

```
      SUBROUTINE PRFIRZ(ZP,RP)
C
C     COMPUTES PLUME BOUNDARY RADIUS R AT AXIAL LOCATION Z
C
      INCLUDE 'PRFICM.FOR/NOLIST'

      IF(ZP.LT.ZLL.OR.ZP.GT.ZUL) GO TO 30
      I=1
   10 CONTINUE
      IF(ZP.LE.Z(I+1).AND.ZP.GE.Z(I)) GO TO 20
      I=I+1
      IF(I.GT.NZ) GO TO 30
      GO TO 10
   20 CONTINUE
      RP=FF(I,NPTS(I),1)+
     1 (ZP-Z(I))*(FF(I+1,NPTS(I+1),1)-FF(I,NPTS(I),1))/(Z(I+1)-Z(I))
      RETURN
   30 CONTINUE
      WRITE(6,40) ZP,RP,ZLL,ZUL
   40 FORMAT(1H ,'NO BOUNDARY SOLUTION',2X,4(1PE10.3))
      RETURN
      END
*********************************************************************
      SUBROUTINE PRFISC
C
C     COMPUTES VOLUME SCATTERING CONTRIBUTION TO ENERGY RECEIVED AT
C     THE ANTENNA
C

C     USES GAUSSIAN QUADRATURES FOR INTEGRATIONS OVER CIRCUMFERENCE,
C     RADIUS, AND AXIAL LENGTH
C
C

      INCLUDE 'PRFICM.FOR/NOLIST'
      LOGICAL IN,RAY
      DIMENSION RTHETA(10),WTHETA(10),RRAD(10),WRAD(10),RZ(24),WZ(24),
     1 X(3),ST(3),SR(3),H(9),DUM(3),XI(3),XE(3),ERV(3),XFV(3),SFV(3),
     2 SN(3),VP(3),SD(3)
      DIMENSION VOLTH(500),VOLR(500),VOLZ(500),FVOLZ(102)

      DATA TWOPI/6.283185307/
      DATA NNZ,NNR,NNTH,NF/24,10,10,50/

      DATA RTHETA/.97390653,.86506337,.67940956,.43339539,.14887434,
```

```
     1 -.14887434,-.43339539,-.67940956,-.86506337,-.97390653/
      DATA WTHETA/.06667134,.14945135,.21908636,.26926672,.29552422,
     1            .29552422,.26926672,.21908636,.14945135,.06667134/
      DATA RRAD/.07652652,.22778585,.37370609,.51086700,.63605368,
     1          .74633191,.83911697,.91223443,.96397193,.99312860/
      DATA WRAD/.15275339,.14917299,.14209611,.13168864,.11819453,
     1          .10193012,.08327674,.06267205,.04060143,.01761401/
      DATA RZ/.001229 ,.0064699,.0158755,.0294085,.0470123,.0686134,
     1        .0941209,.123428 ,.1564188,.1929338,.232841 ,.2759659,
     2        .3221277,.3711326,.4227752,.476864,.533097 ,.5913136,
     3        .6512442,.7126376,.7752363,.8387777,.9029953,.9676199/
      DATA WZ/.00315335,.00732755,.01147723,.0155793,.01961616,
     1        .02357076,.02742651,.03116723,.03477722,.03824135,
     2        .04154509,.04467456,.04761666,.05035904,.05289019,
     3        .05519950,.05727729,.05911484,.06070444,
     4        .06203942,.06311419,.0639242,.06446616,.06473770/

      PATH=.FALSE.
C
C     DOPPLER SHIFT PARAMETERS
C
      VTM=SCALP(VT,VT)
      VRM=SCALP(VR,VR)
      VPM=FF(1,1,7)+VM(3)
      VTM=SQRT(VTM)
      VRM=SQRT(VRM)

C     ESTIMATE OF MAXIMUM FREQUENCY SHIFT

      DDF=BFREQ*(VTM+VRM+2.*VPM)/C
      DFO=-DDF
      DNF=NF
      DELDF=2.*DDF/DNF
      NFP=NF+1
C     OUTER, Z-INTEGRAL
C
      ALAM=C/BFREQ
      CONST=(ALAM**2)/((2.*TWOPI)**3)
      ZNORM=ZUL-ZLL
      AEXP=11./6.
      VOLZZ=0.

      DO 600 L=1,NFP
      VOLZ(L)=0.
  600 CONTINUE
C
      DO 300 I=1,NNZ
```

```
      X(3)=ZLL+RZ(I)*ZNORM
      CALL PRFIRZ(X(3),RPZ)
C
C     MIDDLE, R-INTEGRAL
C
      VOLZR=0.

      DO 610 L=1,NFP
      VOLR(L)=0.
  610 CONTINUE
      DO 200 J=1,NNR
      R=RRAD(J)*RPZ
C
C     INNER, THETA-INTEGRAL
C
      VOLZA=0.

      DO 620 L=1,NFP
      VOLTH(L)=0.
  620 CONTINUE
      CALL PRFILI(X(3),R,H)
      IF(H(5).LE.0.) GO TO 100
      DO 100 K=1,NNTH
      THETA=PI*(1.-RTHETA(K))
      X(1)=R*COS(THETA)
      X(2)=R*SIN(THETA)
C
C     CHECK FOR ADMISSIBLE DIRECTIONS
C
      SST=0.
      SSR=0.
      DO 50 L=1,3
      ST(L)=X(L)-XT(L)
      SR(L)=XR(L)-X(L)
   50 CONTINUE
      SST=SCALP(ST,ST)
      SSR=SCALP(SR,SR)
      SST=SQRT(SST)
      SSR=SQRT(SSR)
      DO 60 L=1,3
      ST(L)=ST(L)/SST
      SR(L)=SR(L)/SSR
   60 CONTINUE
      COSPT=SCALP(DCT,ST)
      COSPR=-SCALP(DCR,SR)
      IF(COSPT.LE.0.) GO TO 100
      IF(COSPR.LE.0.) GO TO 100
```

```
C
C     ATTENUATION AND PHASE FOR THE INCIDENT AND SCATTERED RAY
C
C     INCIDENT RAY
C
      IT=1
   70 CONTINUE
      CALL PRFIPI(XT,ST,XI,DUM,-1,2)
      IN=.FALSE.
      RAY=.FALSE.
      CALL PRFIIT(XT,ST,XI,ATTEN1,PHASE1,ERV,ERVM,XFV,SFV,IN,RAY)
      IN=.TRUE.
      RAY=RAYTR
      CALL PRFIIT(XI,ST,X,ATTEN2,PHASE2,ERV,ERVM,XFV,SFV,IN,RAY)
      IF(RAYTR) THEN
      IF(ERVM.LE.EPSA(2)) GO TO 85
      SS=0.
      DO 75 L=1,3
      XI(L)=XI(L)+RC*ERV(L)
      ST(L)=XI(L)-XT(L)
      SS=SS+ST(L)**2
   75 CONTINUE
      SS=SQRT(SS)
      DO 80 L=1,3
      ST(L)=ST(L)/SS
   80 CONTINUE

C     ATTENUATION SET TO LARGE VALUE IF NO CONVERGENCE

      IT=IT+1
      IF(IT.GT.NIT) ATTEN2=40.
      IF(IT.GT.NIT) GO TO 85
      GO TO 70
      END IF
   85 CONTINUE
C
C     TRANSMITTER GAIN
C
      COSTA=SCALP(ST,DCT)
      IF(COSTA.LT.-1.) COSTA=-1.
      IF(COSTA.GT. 1.) COSTA= 1.
      TAANG=ACOS(COSTA)*180./PI
      EXPTG=0.
      IF(TAANG.GE.90.) GO TO 87
      CALL PRFIAG(TAANG,TAG,1)
      EXPTG=10.**(TAG/10.)
C
```

```
   87 CONTINUE

      ATTENT=ATTEN1+ATTEN2
      PHASET=PHASE1+PHASE2
C
C     SCATTERED RAY
C
      IT=1
      CALL PRFIPI(X,SR,DUM,XE,-1,3)
   90 CONTINUE
      IN=.TRUE.
      RAY=RAYTR
      CALL PRFIIT(X,SR,XE,ATTEN1,PHASE1,ERV,ERVM,XFV,SFV,IN,RAY)
      IN=.FALSE.
      RAY=.FALSE.
      DO 95 L=1,3
      SR(L)=SFV(L)
      XE(L)=XFV(L)
   95 CONTINUE
      CALL PRFIIT(XE,SR,XR,ATTEN2,PHASE2,ERV,ERVM,XFV,SFV,IN,RAY)
      IF(RAYTR) THEN
      IF(ERVM.LE.EPSA(1)) GO TO 105
      SS=0.
      DO 110 L=1,3
      XE(L)=XE(L)+RC*ERV(L)
      SR(L)=XE(L)-X(L)
      SS=SS+SR(L)**2
  110 CONTINUE
      SS=SQRT(SS)
      DO 115 L=1,3
      SR(L)=SR(L)/SS
  115 CONTINUE

C     ATTENUATION SET TO LARGE VALUE IF NO CONVERGENCE

      IT=IT+1
      IF(IT.GT.NIT) ATTEN2=40.
      IF(IT.GT.NIT) GO TO 105
      GO TO 90
      END IF
  105 CONTINUE
C
C     RECEIVER GAIN
C
      COSRA=-SCALP(SFV,DCR)
      IF(COSRA.LT.-1.) COSRA=-1.
      IF(COSRA.GT. 1.) COSRA= 1.
```

```
      RAANG=ACOS(COSRA)*180./PI
      EXPRG=0.
      IF(RAANG.GE.90.) GO TO 107
      CALL PRFIAG(RAANG,RAG,2)
      EXPRG=10.**(RAG/10.)
C
  107 CONTINUE
      ATTENR=ATTEN1+ATTEN2
      PHASER=PHASE1+PHASE2
      PHASE=PHASET+PHASER
      ATTEN=ATTENT+ATTENR
      COSSC=SCALP(ST,SR)
      IF(COSSC.GT.1.) COSSC=1.0
      IF(COSSC.LT.-1.) COSSC=-1.0
      SCANG=ACOS(COSSC)
      SCATA=SIN(.5*SCANG)
      DENOM=(1.+4.*(H(4)*SCATA)**2)**AEXP
      COSX=SCALP(DCTO,SR)
      XANG=ACOS(COSX)
      SINX=SIN(XANG)
      CROSS=H(5)*(SINX**2)/DENOM
      VOLTHT=CROSS*EXPTG*EXPRG*EXP(-2.*ATTEN)*WTHETA(K)/((SST*SSR)**2)
C
C     DOPPLER SHIFT CALCULATIONS
C
      DO 630 L=1,3
      SD(L)=SR(L)-ST(L)
      VP(L)=VM(L)
  630 CONTINUE
      VP(3)=H(6)+VP(3)
      ANG=2.*SCATA
      TI=H(7)*H(6)*H(6)
      V1=SCALP(VT,ST)
      V2=SCALP(VR,SR)
      V3=SCALP(VP,SD)
      VS=V1-V2+V3
      DF=DFO
      DO 640 L=1,NFP
      PDQ=PDF(DF,VS,TI,ANG,BFREQ)
      VOLTH(L)=VOLTH(L)+PDQ*VOLTHT
      DF=DF+DELDF
  640 CONTINUE
      VOLZA=VOLZA+VOLTHT

  100 CONTINUE

      VOLRT=RRAD(J)*WRAD(J)
```

```
      DO 650 L=1,NFP
      VOLR(L)=VOLR(L)+VOLTH(L)*VOLRT
  650 CONTINUE
      VOLZR=VOLZR+VOLZA*VOLRT

  200 CONTINUE

      VOLZT=PI*ZNORM*CONST*RPZ*RPZ*WZ(I)
      DO 660 L=1,NFP
      VOLZ(L)=VOLZ(L)+VOLR(L)*VOLZT
  660 CONTINUE
      VOLZZ=VOLZZ+VOLZR*VOLZT

  300 CONTINUE
      WRITE(6,730)
  730 FORMAT(1H1,20X,'VOLUME INTEGRATED SCATTERED ENERGY AT DOPPLER-
     1SHIFTED FREQUENCY'//4X,'N',7X,'DF, KHZ',2X,'DF*C/BFREQ',
     2 2X,'SCATTERED POWER, DB/HZ'/)
      DF=DF0
      DO 750 I=1,NFP
      FNORM=DF*C/BFREQ
      DFKHZ=DF/1000.
      FVOLZ(I)=DFKHZ
      K=I+NFP
      IF(VOLZ(I).LE.0.) VOLZ(I)=1.E-38
      FVOLZ(K)=10.*ALOG10(VOLZ(I))
      WRITE(6,740) I,FVOLZ(I),FNORM,FVOLZ(K)
      DF=DF+DELDF
  750 CONTINUE
      VOLTDB=0.
      IF(VOLZZ.GT.0.) VOLTDB=10.*ALOG10(VOLZZ)
      WRITE(6,760) VOLTDB
  760 FORMAT(1H ,///40X,'FREQUENCY INTEGRATED SCATTERED POWER= ',F10.3,
     1 ' DB')
  740 FORMAT(1H ,2X,I3,2X,3(1PE11.4,1X))
C
C     PRINTER PLOT OF DOPPLER SHIFTED SCATTERED POWER
C
      CALL PLOT(1,FVOLZ,NFP,2)


      RETURN
      END
*************************************************************************
```

```
      FUNCTION PDF(DF,VMK,QQ,ANG,BFREQ)
C
C     GAUSSIAN PROBABILITY DENSITY FUNCTION FOR DOPPLER SHIFTED
C     FREQUENCY
C     AVERAGED OVER ALL ANGLES
C
C     DF=(F-BFREQ)
C     VMK=EFFECTIVE COMPONENT OF MEAN RELATIVE VELOVITY
C     QQ=DIMENSIONAL MEAN SQUARE TURBULENCE INTENSITY
C     ANG=MAGNITUDE OF PROJECTION OF SUM OF UNIT VECTORS
C
      DATA PI,C/3.141592653,2.998E+08/

      QQS=2.*QQ*ANG*ANG
      PDF=0.
      IF(QQS.EQ.0.) RETURN
      A=C*DF/BFREQ-VMK
      ARG=A**2/QQS
      CONST=SQRT(2.*PI*QQ)
      AVG=ABS(ANG)
      PDF=EXP(-ARG)*C/(CONST*AVG*BFREQ)
      RETURN
      END
*********************************************************************
      FUNCTION SCAT(AK)
C
C     COMPUTES Q-FUNCTION FOR TOTAL SCATTERING CROSS-SECTION
C
C     X=2.*(A*K)**2
C     A=CORRELATION LENGTH
C     K=WAVE NUMBER
C
      DATA PI,EX1,EX2,EX3/3.141592653,-.83333333,.16666667,1.1666667/

      SCAT=0.
      X=2.*(AK**2)
      XCUBE=X**3
      IF(XCUBE.GT.0.)  GO TO 10
      RETURN
   10 CONTINUE
      X1=1.+2.*X
      SCAT=(2.*X*X+2.*X+1.)*(1.-X1**EX1)/5.-
     1     2.*(1.+X)*(X1**EX2-1.)+(X1**EX3-1.)/7.
      SCAT=SCAT*6.*PI/XCUBE

      RETURN
      END
*********************************************************************
```

```
      FUNCTION SCALP(A,B)
C
C     SCALP=SCALAR PRODUCT OF TWO VECTORS A AND B
C
      DIMENSION A(3),B(3)
      SCALP=0.
      DO 1 I=1,3
      SCALP=SCALP+A(I)*B(I)
    1 CONTINUE
      RETURN
      END
**********************************************************************
```

Appendix C
DERIVATION OF THE RAY TRACE EQUATION

This appendix outlines the derivation of the equation defining the trajectory of the refracted rays through the plume. We include a derivation that starts with Maxwell's equations to show the approximations made in the geometric optics limit of EM wave propagation used in PRFIC.

By combining Maxwell's equation for the electric and magnetic fields $\vec{E}$ and $\vec{H}$, and assuming a time dependence of each component of the form $e^{-i\omega t}$, the vector wave equation (for either $\vec{E}$ or $\vec{H}$) is (Reference 9)

$$\nabla^2\vec{E} + k^2n^2\vec{E} = -2\nabla\vec{E} \cdot \frac{1}{n^2}\nabla n^2 \qquad \text{(C-1)}$$

The lowest order approximation neglects the right hand side for sufficiently small $\nabla n^2/n^2$. The approximate equation satisfied by the electric field is then

$$\nabla^2\vec{E} + k^2n^2\vec{E} = 0. \qquad \text{(C-2)}$$

In this approximation, the components of the electric field vector all obey the same equation, and it is possible to replace the vector by a scalar amplitude, ϕ, such that

$$\nabla^2\phi + k^2n^2\phi = 0. \qquad \text{(C-3)}$$

We seek solutions to this equation in the form

$$\phi = Ae^{ikS}, \qquad \text{(C-4)}$$

where A,S are two real functions of position. A is an amplitude, and S is a phase, called the Eikonel. If we equate real and imaginary parts of Eq. (C-3) for ϕ given by Eq. (C-4), there are two equations for A and S

$$\frac{\nabla^2 A}{k^2 A} - (\nabla S)^2 + n^2 = 0$$

$$2\nabla \frac{A\nabla S}{A} + \nabla^2 S = 0 \qquad \text{(C-5)}$$

For short wavelengths (large k) and propagation paths such that $\nabla^2 A/A$ is small, the first equation reduces to the Eikonel equation

$$\nabla S = n, \qquad \text{(C-6)}$$

which is the one we solve to determine the ray trajectory. The second equation gives the effect of ray focusing and is not solved in this first version of PRFIC. It reduces to[11]

$$\frac{1}{n^2 A}\frac{d}{ds}(n^2 A) = -\nabla \cdot \hat{t} \qquad \text{(C-7)}$$

and its solution is

$$n^2 A = (n^2 A)_0 \exp -\int_0^s \nabla \cdot \hat{t}\, ds \qquad \text{(C-8)}$$

where $\hat{t}$ is a unit vector in the direction of the ray trajectory, and s is the length along the trajectory. A is essentially the area of a ray bundle propagating along the path, and it can increase or decrease according to the integrated divergence of the unit vector $\hat{t}$ along the path. Since $\hat{t}$ is a unit vector, it has no divergence except that due to change in direction. There is no focusing for a straight line-of-sight.

[11] Molmud, P., "Raybend, a Ray Tracing Program for Microwave Propagation Through Rocket Plumes," JANNAF 12th Plume Trajectory Meeting, U.S. Air Force Academy, Colorado Springs, Nov. 18-20, 1980. (paper, UNCLASSIFIED.) also (CPIA Publication 332, December 1980, pp. 273-312, publication, UNCLASSIFIED.)

Using the geometry of the wave front and its normal, the Eikonel equation can be manipulated into an equation for the ray trajectory[12]

$$\frac{d}{ds}(n\vec{t}) = \nabla n \quad . \tag{C-9}$$

This is the form of the equation solved in PRFIC. The solution proceeds in the following stepwise manner (Reference 7). The position vector of the trajectory is $\vec{r} = \{x(s), y(s), z(s)\}$, and

$$\vec{t} = \frac{d\vec{r}}{ds} = r'(s) \tag{C-10}$$

The solution at $\vec{r}\ (s + \Delta s)$ is obtained from that at $\vec{r}(s)$ by a series expansion

$$\vec{r}(s + \Delta s) = \vec{r}(s) + r'(s)\Delta s + \frac{1}{2} r''(s)\Delta s^2 \tag{C-11}$$

and

$$r'(s + \Delta s) = r'(s) + r''(s)\ \Delta s \tag{C-12}$$

By geometry we obtain (Reference 7)

$$r''(s) = \frac{1}{n}\ \nabla n - \vec{t}(\vec{t} \cdot \nabla n) \tag{C-13}$$

Each term in the expansion (Eq. (C-11)) as now defined at s, and the values at $s + \Delta s$, can be obtained. For completeness, Table C-1 provides the components of each vector in the rectangular cartesian coordinate system used in the calculation.

[12]Kerr, D.E., Propagation of Short Radio Waves, McGraw Hill, New York, 1951, pp. 41-44.

Table C-1. Components of Vectors Used in Ray Trace Solution

Components	$\vec{r}$	$\vec{r}'$	$\vec{r}''$
x	x	$\frac{dx}{as}$	$\frac{1}{n}\left[\frac{\partial n}{\partial r}\cos\theta - \frac{dx}{ds}\left(\frac{\partial n}{\partial r}\cos\theta\,\frac{dx}{ds} + \frac{\partial n}{\partial r}\sin\theta\,\frac{dy}{ds} + \frac{\partial n}{\partial z}\,\frac{dz}{ds}\right)\right]$
y	y	$\frac{dy}{ds}$	$\frac{1}{n}\left[\frac{\partial n}{\partial r}\sin\theta - \frac{dy}{ds}\left(\frac{\partial n}{\partial r}\cos\theta\,\frac{dx}{ds} + \frac{\partial n}{\partial r}\sin\theta\,\frac{dy}{ds} + \frac{\partial n}{\partial z}\,\frac{dz}{ds}\right)\right]$
z	z	$\frac{dz}{ds}$	$\frac{1}{n}\left[\frac{\partial n}{\partial z} - \frac{dz}{ds}\left(\frac{\partial n}{\partial r}\cos\theta\,\frac{dx}{ds} + \frac{\partial n}{\partial r}\sin\theta\,\frac{dy}{ds} + \frac{\partial n}{\partial z}\,\frac{dz}{ds}\right)\right]$

Appendix D
INDEX OF REFRACTION FLUCTUATIONS

The purpose of this appendix is to outline the contribution of the fluctuating plume properties to the index of refraction structure constant

$$C_n^2 = 1.6 \frac{\overline{n'^2}}{\Lambda^{2/3}} \tag{D-1}$$

$\overline{n_e'^2}$ is the ensemble average of the index of refraction fluctuation. The functional dependence of n is

$$n = n\,(\omega_p(n_e),\ \nu_{en}(x_i,T)). \tag{D-2}$$

A Taylor series for n' can be written, giving

$$n' = \frac{\partial n}{\partial \omega_p}\frac{\partial \omega_p}{\partial n_e} n_e' + \frac{\partial n}{\partial \nu_{en}}\frac{\partial \nu_{en}}{\partial x_i} x_i' + \frac{\partial n}{\partial \nu_{en}}\frac{\partial \nu_{en}}{\partial T} T'. \tag{D-3}$$

An ensemble average of n' yields

$$\begin{aligned}\overline{n'^2} = {} & \left(\frac{\partial n}{\partial \omega_p}\right)^2 \left(\frac{\partial \omega_p}{\partial n_e}\right)^2 \overline{n_e'^2} + 2\left(\frac{\partial n}{\partial \omega_p}\right)\left(\frac{\partial \omega_p}{\partial n_e}\right) \sum_{i=1}^{N} \frac{\partial n}{\partial \nu_{en}}\frac{\partial \nu_{en}}{\partial x_i}\overline{x_i' n_e'} \\ & + \left(\frac{\partial n}{\partial \omega_p}\right)\left(\frac{\partial \omega_p}{\partial n_e}\right)\left(\frac{\partial n}{\partial \nu_{en}}\right)\left(\frac{\partial \nu_{en}}{\partial T}\right)\overline{n_e' T'} + \sum_{i=1}^{N}\sum_{j=1}^{N}\left(\frac{\partial n}{\partial \nu_{en}}\right)^2\left(\frac{\partial \nu_{en}}{\partial x_i}\right)^2 \overline{x_i x_j} \\ & + 2\left(\frac{\partial n}{\partial \nu_{en}}\right)^2 \frac{\partial \nu_{en}}{\partial T} \sum_{i=1}^{N} \frac{\partial \nu_{en}}{\partial x_i}\overline{x_i' T'} + \left(\frac{\partial n}{\partial \nu_{en}}\right)^2\left(\frac{\partial \nu_{en}}{\partial T}\right)^2 \overline{T'^2}\end{aligned} \tag{D-4}$$

In principle, the mean square index of refraction fluctuation depends on the cross-correlation of the electron number density, temperature, and chemical species fluctuations.

This degree of detail is not generally available in current exhaust plume flowfield models. The g-equation formulation does give estimates of these quantities, although its accuracy in afterburning, ionized flows has not been established. Moreover, a systematic examination of the importance of each term in Eq. (D-4) is warranted before the effort to include all these contributions is undertaken.

In the verification of PRFIC, we have used only the first term which gives

$$\overline{n'^2} = \overline{n_e'^2} \; \frac{\left(\frac{\omega_p}{\omega}\right)^4}{4n_e^2 \left[1 + \left(\frac{\nu_{en}}{\omega}\right)^2\right]^2} \tag{D-5}$$

or, using $\omega_p^2 = n_e e^2/\varepsilon_o m_e$, $\omega/c = 2\pi/\lambda = k$, and the Thompson radius of the electron $r_t = e^2/4\pi\varepsilon_o m_e c^2$

$$\overline{n'^2} = \frac{4\pi^2}{k^4} \; \frac{\overline{n_e'^2}\, r_t^2}{\left[1 + \left(\frac{\nu_{en}}{\omega}\right)^2\right]^2} \tag{D-6}$$

We have used an additional assumption for this study, that the fluctuations in n_e' depend only on T', through the equilibrium (Saha) equation. We have used this approach for the purpose of verification, because there was no other estimate available within the SPF code at the time. We do have a g-equation formulation for $\overline{T'^2}$, based on the major afterburning species, but no similar results for $\overline{n_e'^2}$ itself were available at this time.

The Saha equation for the electron number density is

$$\frac{n_e^2}{n} = 2\left(\frac{2\pi m_e kT}{h^2}\right)^{3/2} \exp - \frac{I}{kT} \quad . \tag{D-7}$$

(We have used the approximation $n \simeq n - n_e$ in the denominator because

$n_e/n \ll 1$.) With this relationship,

$$n_e' = \frac{\partial n_e}{\partial T} T' \tag{D-8}$$

and

$$\overline{n_e'^2} = \left(\frac{\partial n_e}{\partial T}\right)^2 \overline{T'^2} \tag{D-9}$$

$$\overline{n_e'^2} = n_e^2 \left(\frac{I}{2kT} + \frac{3}{4}\right)^2 \frac{\overline{T'^2}}{\overline{T}^2} \tag{D-10}$$

We obtained $\overline{T'^2}$ from our SPF modified with the g-equation. The ionization potential, I, was taken to be that of potassium (I/k = 50,354 K). The actual number density of electrons, n_e, is given by the kinetics solution in SPF.

Appendix E
DOPPLER SPECTRUM OF SCATTERED POWER

Radiation scattered by the turbulent fluctuations has a frequency spectrum because of the distribution of velocities of the mean and fluctuating velocity. The frequency shift for a particular velocity can be derived by a sequential application of the Doppler shift to the incident and scattered wave. At the scattering volume, the apparent frequency is (see Figure E-1).

$$\nu' = \nu_o + \nu_o \vec{V}_{T/S} \cdot \frac{\hat{s}}{c} \tag{E-1}$$

and at the receiver, the apparent frequency of the scattered wave is

$$\nu'' = \nu' + \nu' \vec{V}_{S/R} \frac{\hat{t}}{c} \tag{E-2}$$

If $\overline{w}$ is the local mean axial velocity of the plume, and $\vec{q}'$ the random turbulent fluctuation, then

$$\vec{V}_{T/S} = \vec{V}_T - (\overline{w}\hat{k} + \vec{V}_m + \vec{q}') \tag{E-3}$$

$$\vec{V}_{S/R} = (\overline{w}\hat{k} + \vec{V}_m + \vec{q}') - \vec{V}_R \tag{E-4}$$

The total frequency shift between the transmitter and receiver is then

$$\nu'' = \nu_o + \frac{\nu_o}{c} (\vec{V}_T \cdot \hat{s} - \vec{V}_R \cdot \hat{t}) + (\overline{w}\hat{k} + \vec{V}_m) \cdot (\hat{t} - \hat{s}) + \vec{q}' \cdot (\hat{t} - \hat{s}) \tag{E-5}$$

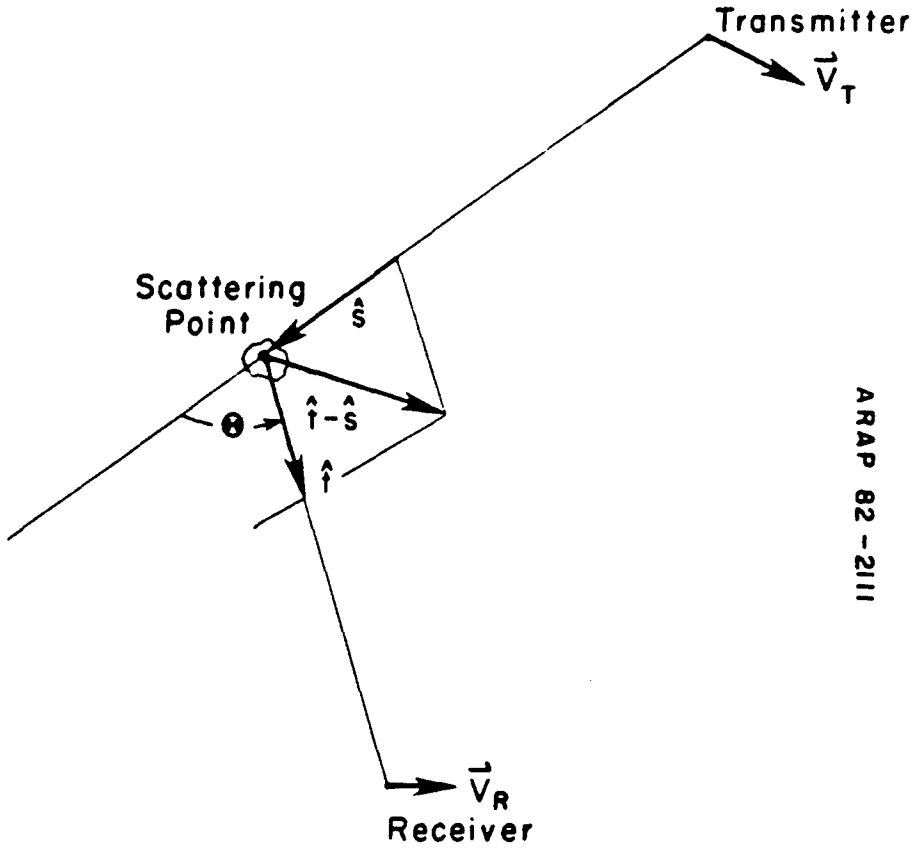

ARAP 82-2111

FIGURE E-1. Coordinate System for Scattering.

or

$$\frac{c(\nu'' - \nu_o)}{\nu_o} = \frac{c\Delta\nu}{\nu_o} = (\vec{V}_T \cdot \vec{s} - \vec{V}_R \cdot \hat{t}) + (\overline{w}\hat{k} + \vec{V}_m) \cdot (\hat{s} - \hat{t}) + \vec{q}' \cdot (\hat{s} - \hat{t}) \tag{E-6}$$

Let the component of the fluctuating velocity that contributes a Doppler shift be written as

$$\vec{q}' \cdot (\hat{s} - \hat{t}) = 2u' \sin \frac{\theta}{2} \tag{E-7}$$

where u' is the component of the turbulent fluctuating velocity in the direction $(\hat{s} - \hat{t})$. At each point in the plume, there will be a probability distribution of frequencies about the shift due to the mean velocities. The frequency shift due only to the mean velocities is

$$\frac{c\Delta\nu}{\nu_o} = (\vec{V}_T \cdot \vec{s} - \vec{V}_R \cdot \hat{t}) + (\overline{w}\hat{k} + \vec{V}_m) \cdot (\hat{s} - \hat{t}) \tag{E-8}$$

For the first version of PRFIC, we have taken the probability density function of the velocity fluctuations to be Gaussian.

$$P(u', v', w') = \frac{1}{\left(2\pi\ \overline{q'^2}\right)^{3/2}} \exp - \frac{u'^2 + v'^2 + w'^2}{2\ \overline{q'^2}} \tag{E-9}$$

Furthermore, we assume that the fluctuations are isotropic. That is, the magnitude of the total fluctuating velocity is independent of direction. With the assumption of isotropy, we can choose a coordinate system at each scattering point with one coordinate direction aligned with the direction of the velocity fluctuation u' in Eq. (E-7). Fluctuations in the other two directions do not contribute to the Doppler shift, so we can integrate over them to find the probability distribution for u', alone.

$$P(u') = \int_{-\infty}^{\infty}\int_{-\infty}^{\infty} P(u',v',w')dv'dw' \qquad \text{(E-10)}$$

$$= \frac{1}{\sqrt{2\pi\overline{q'^2}}} \exp - \frac{u'^2}{2\overline{q'^2}} \qquad \text{(E-11)}$$

With the relation between u' and $\Delta\nu$ (Eq. (E-6)), we can use P(u') to determine $P(\Delta\nu)$

$$u' = \frac{c\Delta\nu}{\nu_o} - (\vec{v}_T \cdot \hat{s} - \vec{v}_R \cdot \hat{t}) - (\overline{w}\hat{k} + \vec{v}_m) \cdot (\hat{s} - \hat{t}) \qquad \text{(E-12)}$$

and

$$du' = \frac{\dfrac{cd(\Delta\nu)}{\nu_o}}{2\sin^2\dfrac{\Theta}{2}} \qquad \text{(E-13)}$$

using

$$\int_{-\infty}^{\infty} P(u')du' = \int_{-\infty}^{\infty} P(\Delta\nu)d\Delta\nu, \qquad \text{(E-14)}$$

the probability density for the Doppler shifted scattered power is

$$P(\Delta\nu) = \frac{1}{\sqrt{(2\pi\ \overline{q'^2})}} \quad \frac{c}{2\nu_o \sin\dfrac{\Theta}{2}} \exp\left[-\frac{\left(\dfrac{c\Delta\nu}{\nu_o} - V_s\right)^2}{8\ \overline{q'^2}\ \sin^2\dfrac{\Theta}{2}}\right] \qquad \text{(E-15)}$$

with

$$V_s = (\vec{V}_T \cdot \hat{S} - \vec{V}_R \cdot \hat{t}) + (\overline{w}\hat{k} + \vec{V}_m) \cdot (\hat{s} - \hat{t}) \qquad \text{(E-16)}$$

the effective component of mean velocities contributing to a Doppler shift. All the individual velocities are known from the velocities of the transmitter, receiver, missile, and exhaust plume flowfield.

NOMENCLATURE

A	Coefficient in scalar wave equation
C_n	Index of refraction structure constant
c	Speed of light
E	Electric field strength
e	Electron charge
G_T, G_R	Transmitter and receiver antenna gains, respectively
h	Planck's constant
I	Ionization potential
$\hat{i}, \hat{j}, \hat{k}$	Unit vector in x,y,z directions, respectively
K, K_R, K_I	Magnitude, real, and imaginary components of complex dielectric constant
M_∞	Missile flight Mach number
m_e	Mass of electron
n	Index of refraction, or total particle number density
n_e	Electron number density
P	Power; P_o is incident power
$P(\Delta\nu)$	Probability density distribution
p	Pressure, or $2k^2\Lambda^2$
q	Root mean square turbulent velocity fluctuation
Q	Total scattering function
r	Radius, or range
r_t	Thompson electron radius
S	Eikonel
s	Distance along ray trajectory
$\hat{s}$	Unit vector from scatterer to receiver
T	Temperature
$\hat{t}$	Unit vector between transmitter and scattering point
u, v, w	Velocity components of exhaust plume
V	Velocity of missile, transmitter, or receiver
x, y, z	Coordinate directions
x_i	Plume species mole fractions
α	Attenuation constant, aspect angle, or direction of ray
β	Phase constant, or angle
γ	Angle
ω_p	Plasma frequency, rad/s
ω	Transmitter frequency rad/s

ν	Frequency, Hz ($\nu = \omega/2\pi$)
ν_{en}	Collision frequency
ν_p	Plasma frequency, Hz
ε_o	Permittivity of free space
χ	Angle between electric vector and scattering direction
Θ	Scattering angle
ϕ	Polar coordinate
Φ	Spectrum function
σ	Scattering cross section
Ω	Solid angle
λ	Wavelength
Λ	Turbulence macroscale
ε	Turbulence energy dissipation

Subscripts

T, R	Transmitter, receiver
i	Chemical species
e	Electron
n	Neutral

Superscripts

'	Fluctuating quantity
-	Ensemble average

INITIAL DISTRIBUTION

12 Naval Air Systems Command
- AIR-00D4 (2)
- AIR-03A (1)
- AIR-03P23, A. R. Habayeb (1)
- AIR-330 (1)
- AIR-340C (1)
- AIR-370D, E. Hooper (1)
- AIR-533 (1)
- AIR-536 (2)
- AIR-53634F, D. Caldwell (1)
- AIR-54922B, W. Whiting (1)

2 Chief of Naval Operations
- OP-35E, L. Triggs (1)
- OP-982F3, Capt. L. F. Pellock (1)

7 Chief of Naval Material
- MAT-08 (1)
- NSP-00 (1)
- NSP-01 (2)
- NSP-10 (1)
- NSP-20 (1)
- PM-22, High Energy Laser (HELI) Project Office (1)

3 Naval Electronic Systems Command
- NAVELEX-03G, R. Golding (1)
- NAVELEX-PME-107-52, A. Ritter (1)
- NAVELEX-PME-107, J. O'Brian (1)

9 Naval Sea Systems Command
- SEA-03D (1)
- SEA-62 (1)
- SEA-62R (1)
- SEA-62R1, T. Tasaka (1)
- SEA-62R2 (1)
- SEA-99612 (4)

1 Chief of Naval Research, Arlington (ONR-473)

1 Assistant Secretary of the Navy (Research, Engineering and Systems, Dr. Hubert Wang)

1 Assistant Navy Deputy, SAM-D ASMS Joint Project, Redstone Arsenal

1 Commander-in-Chief, U.S. Pacific Fleet (Code 325)

1 Commander, Third Fleet, Pearl Harbor

1 Commander, Seventh Fleet, San Francisco

1 David W. Taylor Naval Ship Research and Development Center Detachment, Bethesda (Code 2833, R. Burns)

2 Naval Intelligence Support Center
- NISC-40, Perry Roberts (1)
- NISC-50, Hank Bowers (1)

2 Naval Ocean Systems Center, San Diego
- Code 133 (1)
- Code 532, Dr. J. H. Richter (1)

3 Naval Ordnance Station, Indian Head
- Code 5252, G. A. Buckle (1)
- Code DGS (1)
- Technical Library (1)

4 Naval Research Laboratory
- Code 1409, Dr. Kirshenstein (1)
- Code 5754, Dr. F. M. Alexander (1)
- Code 8320, L. Ruhnke (1)
- Technical Library (1)

3 Naval Ship Weapon Systems Engineering Station, Port Hueneme
- Code 5711, Repository (2)
- Code 5712 (1)

2 Naval Surface Weapons Center, Dahlgren
- Dr. G. Moore (1)
- Technical Library (1)

2 Naval Surface Weapons Center, White Oak Laboratory, Silver Spring
Code 213, A. Hirshman (1)
Code KEM (1)
1 Naval War College, Newport
3 Pacific Missile Test Center, Point Mugu
Code 0141.2, C. Elliott (1)
Code 1232, D. Stowell (1)
Code 1233, Dr. N. Van Slyke (1)
1 Naval Plant Representative Office, Sunnyvale (Code SPL-3124)
1 Army Armament Materiel Readiness Command, Rock Island (DRSAR-LEM)
1 Army Armament Research and Development Command, Dover
1 Army Ballistic Research Laboratory, Aberdeen Proving Ground (DRDAR-TSB-S (STINFO))
1 Army Missile Research & Laboratory Advanced Sensors Directorate, Redstone Arsenal (DRDMI-TEI, H. T. Jackson)
1 Night Vision Laboratory, Fort Belvoir (DRSEL-NV-VI, R. Moulton)
3 Redstone Arsenal
AMCPM-MDER (1)
AMSMI-RDD (1)
AMSMI-RDK, Dr. B. Walker (1)
1 White Sands Missile Range (ERADCOM, DELAS-EO-MO, Atmospheric Sciences Laboratory, T. Hall)
1 Air Force Armament Laboratory, Eglin Air Force Base (AFATL/DLMT-3, Mack Gay)
3 Air Force Geophysics Laboratory, Hanscom Air Force Base
OPA, R. Fenn (1)
OPI, R. McClatchey, Stop 30 (1)
OPR, B. Sanford, Stop 30 (1)
1 Air Force Rocket Propulsion Laboratory, Edwards Air Force Base (DACP, Dr. Andrepoint)
4 Air Force Rocket Propulsion Laboratory, Edwards Air Force Base (Plans and Programs Office)
2 Air Force Rocket Propulsion Laboratory, Edwards Air Force Base (Technical Library)
2 Air Force Wright Aeronautical Laboratories, Wright-Patterson Air Force Base
AFWAL/AAWP, Dr. Richard Sanderson (1)
AFWAL/PORA-1, J. Fultz (1)
2 Arnold Air Force Station
Research Branch, Dr. W. K. McGregor (1)
Special Projects, ETF-PO, C. R. Darlington (1)
1 Arnold Engineering Development Center, Arnold Air Force Station (Dr. Herman Scott)
1 Deputy Under Secretary of Devense, Research and Advanced Technology (Electronics and Physical Sciences, J. MacCallum, Room 3D1079)
2 Defense Advanced Research Projects Agency, Arlington
S. Zakanycz (1)
12 Defense Technical Information Center
1 Department of Defense Explosives Safety Board, Alexandria (6-A-145)
1 George C. Marshall Space Flight Center (S&E, Dr. T. Greenwood)
1 National Aeronautics and Space Administration (Code RP)
1 Aerodyne Research, Inc., Bedford, MA (Dr. Draper)
1 Aerojet Tactical Systems, Sacramento, CA (J. Coughlin), via AFPRO
2 Aeronautical Research Associates of Princeton, Inc., Princeton, NJ
B. Pearce (1)
Technical Library (1)
1 Arvin Calspan, Advanced Technology Center, Buffalo, NY (W. J. Sheeran)
1 Atlantic Research Corporation, Alexandria, VA

2 Brigham Young University, Provo, UT
Dr. D. L. Smoot (1)
Dr. Lane Compton (1)
1 California Institute of Technology, Jet Propulsion Laboratory, Pasadena, CA
1 Environmental Research Institute of Michigan, Ann Arbor (R. Legault)
1 General Applied Sciences Laboratory, Westbury, NY
1 General Dynamics Corporation, Pomona Division, Pomona, CA (E. Piesik)
1 General Research Corporation, McLean, VA (SWL Division, Russ Rollins)
2 Grumman Aerospace Corporation, Bethpage, NY
Experimental Dynamics Research Group (1)
Research Department, J. Selby (1)
1 Hercules Incorporated, Allegany Ballistics Laboratory, Cumberland, MD (G. Williams)
1 Hercules Incorporated, Magna, UT (R. J. Zeamer)
1 Hercules Incorporated, McGregor, TX
1 Hughes Aircraft Company, El Segundo, CA
4 Institute for Defense Analyses, Alexandria, VA
L. Biberman (1)
W. Holzer (1)
Dr. R. Oliver (1)
Dr. H. Wolfhardt (1)
1 Johns Hopkins University, Applied Physics Laboratory, Laurel, MD (H. Hall)
1 Lockheed Missiles and Space Company, Sunnyvale, CA (R. LeCount)
1 Martin Marietta Aerospace, Orlando, FL (J. W. Fisher)
1 Martin Marietta Corporation, Denver, CO (R. E. Compton, Jr.)
2 McDonnell Douglas Corporation, Hungtington Beach, CA
Advanced Propulsion Department A-833, Group P-BBFO (1)
D. Chow (1)
1 Northrop Corporation, Aircraft Division, Hawthorne, CA (Lloyd Tanabe)
1 Raytheon Manufacturing Company, Missile Systems Division, Bedford, MA (B. DeRosa)
1 Rockwell International Corporation, Canoga Park, CA (R. A. Smith)
1 Science Applications, Inc., Princeton, NJ (H. Pergament)
1 Science Applications, Inc., Santa Ana, CA (Gas Dynamics and Energy Division, R. J. Hoffman)
1 Scientific Technology Associates, Inc., Princeton, NJ (CN 5203, Stokes Fishburn)
1 Spectral Science, Inc., Burlington, MA (Dr. D. C. Robertson)
1 System Planning Corporation, Arlington, VA (D. Friedman)
1 TRW, Inc., Redondo Beach, CA (G. J. MacLeod)
1 The Aerospace Corporation, Los Angeles, CA (R. Lee, Mail Stop M4-967)
1 The Boeing Company, Seattle, WA (Dr. J. M. Barton)
1 Thiokol Corporation, Huntsville Division, Huntsville, AL
2 Thiokol Corporation, Wasatch Division, Brigham City, UT
N. Anderson (1)
Webb (1)
1 United Technologies Corporation, Chemical Systems Division, Sunnyvale, CA (C. A. LaFebvre)
1 University of Tennessee Space Institute, Tullahoma, TN (Division of Gas Diagnostics, Dr. K. Harwell)
110 Chemical Propulsion Mailing List dated December 1981, including Categories 1, 2, 3, 4, 5